



**HAL**  
open science

# Organically-modified ceramic membranes for solvent nanofiltration : fabrication and transport studies

Cheryl Raditya Tanardi

► **To cite this version:**

Cheryl Raditya Tanardi. Organically-modified ceramic membranes for solvent nanofiltration : fabrication and transport studies. Material chemistry. Université Montpellier; Universiteit Twente (Enschede, Nederland); KU Leuven (1970-..), 2015. English. NNT : 2015MONT5259 . tel-02289027

**HAL Id: tel-02289027**

**<https://theses.hal.science/tel-02289027>**

Submitted on 16 Sep 2019

**HAL** is a multi-disciplinary open access archive for the deposit and dissemination of scientific research documents, whether they are published or not. The documents may come from teaching and research institutions in France or abroad, or from public or private research centers.

L'archive ouverte pluridisciplinaire **HAL**, est destinée au dépôt et à la diffusion de documents scientifiques de niveau recherche, publiés ou non, émanant des établissements d'enseignement et de recherche français ou étrangers, des laboratoires publics ou privés.

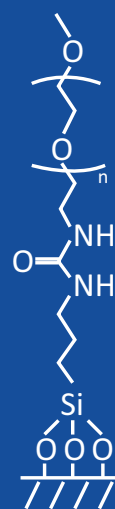
UNIVERSITY OF TWENTE.

KU LEUVEN



# Organically-modified Ceramic Membranes for Solvent Nanofiltration: Fabrication and Transport Studies

Cheryl Raditya Tanardi



ORGANICALLY-MODIFIED CERAMIC MEMBRANES FOR  
SOLVENT NANOFILTRATION:  
FABRICATION AND TRANSPORT STUDIES

Cheryl Raditya Tanardi

## Promotion Committee at University of Twente

Prof. Dr. Ir. J.W.M. Hilgenkamp (chairman)	University of Twente
Prof. Dr. Ir. A. Nijmeijer (promotor)	University of Twente
Prof. Dr. A.J.A. Winnubst (promotor)	University of Science and Technology of China / University of Twente
Prof. Dr. I. F. J. Vankelecom	KU Leuven, Belgium
Prof. Dr. A. Ayral	University of Montpellier, France
Prof. Dr. Ir. J.E. ten Elshof	University of Twente
Prof. Dr. G. Mul	University of Twente
Prof. Dr. V. Hulea	Ecole Nationale Supérieure de Chimie de Montpellier, France
Prof. Dr. E.J.R. Sudhölter	Delft University of Technology

This research was performed in the framework of Erasmus Mundus Doctorate in Membrane Engineering (EUDIME) (<http://eudime.unical.it/>). The EUDIME is one of the nine selected proposals among 151 applications submitted to EACEA in 2010.

The work described in this thesis was performed at the Inorganic Membranes Group, MESA+ Institute for Nanotechnology, University of Twente together with KU Leuven and IEM at University of Montpellier.

Cover designed by Vania Kristi Linaya

## **Organically-modified ceramic membranes for solvent nanofiltration: Fabrication and transport studies**

ISBN: 978-94-6233-135-8

Doctoraatsproefschrift nr. 1319 aan de faculteit Bio-ingenieurswetenschappen van de KU Leuven.

ORGANICALLY-MODIFIED CERAMIC MEMBRANES FOR  
SOLVENT NANOFILTRATION:  
FABRICATION AND TRANSPORT STUDIES

**DISSERTATION**

to obtain  
the degree of doctor at the University of Twente,  
on the authority of the rector magnificus,  
Prof. Dr. H. Brinksma,  
on account of the decision of the graduation committee,  
to be publicly defended  
on Thursday 12<sup>th</sup> of November 2015 at 12h45

by

**Cheryl Raditya Tanardi**

born on 3<sup>rd</sup> of December 1984

in Surabaya, Indonesia

For the University of Twente this dissertation has been approved by the promotor:

Prof. Dr. Ir. A. Nijmeijer

Prof. Dr. A.J.A. Winnubst

ORGANICALLY-MODIFIED CERAMIC MEMBRANES FOR  
SOLVENT NANOFILTRATION:  
FABRICATION AND TRANSPORT STUDIES

**DISSERTATION**

prepared in the framework of

Erasmus Mundus Doctorate in Membrane Engineering (EUDIME)

to obtain multiple Doctorate degrees issued by

**University of Twente (Faculty of Science and Technology)**

**KU Leuven (Faculty of Bioscience Engineering)**

**University of Montpellier (Graduate School of Chemical Sciences)**

to be publicly defended

on Thursday 12<sup>th</sup> of November 2015 at 12h45

by

**Cheryl Raditya Tanardi**

born on 3<sup>rd</sup> of December 1984

in Surabaya, Indonesia

## EUDIME Doctorate Board

### Promotors:

Prof. Dr. Ir. A. Nijmeijer

University of Twente

Prof. Dr. A.J.A. Winnubst

University of Science and Technology of China /

University of Twente

Prof. Dr. I. F. J. Vankelecom

KU Leuven, Belgium

Prof. Dr. A. Ayrál

IEM/ University of Montpellier, France

Dr. Mihai Barboiu

IEM/ University of Montpellier, France

### External Reviewers:

Prof. Joe da Costa

University of Queensland, Australia

Prof. Dr. E.J.R. Sudhölter

Delft University of Technology

Dr. Rob Ameloot

KU Leuven, Belgium

### Other Members:

Prof. Dr. Ir. J.E. ten Elshof

University of Twente

Prof. Dr. G. Mul

University of Twente

Prof. Dr. V. Hulea

Ecole Nationale Supérieure de Chimie de Montpellier,  
France



UNIVERSITY OF TWENTE.





## Table of Contents

<b>Chapter 1: Introduction</b>	<b>1</b>
<b>Chapter 2: PDMS Grafting of Mesoporous <math>\gamma</math>-Alumina Membranes for Nanofiltration of Organic Solvents</b>	<b>25</b>
<b>Chapter 3: Solvent Permeation Behavior of PDMS Grafted <math>\gamma</math>-Alumina Membranes</b>	<b>47</b>
<b>Chapter 4: Solute Rejection in SRNF using PDMS Grafted <math>\gamma</math>-Alumina Membranes</b>	<b>79</b>
<b>Chapter 5: Coupled-PDMS Grafted Mesoporous <math>\gamma</math>-Alumina Membranes for Solvent Nanofiltration</b>	<b>101</b>
<b>Chapter 6: Polyethyleneglycol Grafting of <math>\gamma</math>-Alumina Membranes for Solvent Resistant Nanofiltration</b>	<b>123</b>
<b>Chapter 7: Reflections and Outlook</b>	<b>155</b>
<b>Summary</b>	<b>165</b>
<b>Samenvatting</b>	<b>169</b>
<b>Résumé</b>	<b>173</b>
<b>Résumé Général</b>	<b>175</b>
<b>Acknowledgement</b>	<b>177</b>
<b>About the Author</b>	<b>179</b>
<b>List of Publications</b>	<b>181</b>



# **Chapter 1**

## **Introduction**

Nanofiltration, one type of the pressure-driven membrane separation processes, has become very important during the past decade. In regard to separation performance, nanofiltration lies between reverse osmosis (RO) and ultrafiltration (UF) with nominal molecular weight cutoffs ranging from 200 to 1000 Da (neutral solutes) with estimated pore sizes of around 0.5–2 nm(1). Nanofiltration has been used for liquid-phase separation of a wide range of aqueous mixtures and solutions.

Potential application of nanofiltration membranes include separation of non-aqueous liquids, such as removal of impurities from used organic solvents in solvent recycle processes. Growing environmental concerns, increased public awareness and stricter environmental regulations have resulted in a more sustainable practice in various industries, such as solvent recovery to reduce the amount of solvent waste in the chemical, pharmaceutical, and petrochemical industries. Up to now, solvent waste is recovered by distillation, which is not energy-efficient, or directly sent to burners or incinerators, resulting in global warming due to increased emissions of CO<sub>2</sub>. Solvent Resistant Nanofiltration (SRNF) or Organic Solvent Nanofiltration (OSN) has great potential for better sustainable processes in industry. By applying SRNF, the used solvent can be recycled and the solvent waste can be minimized. SRNF is more environmentally friendly due to its lower chemicals and energy consumption compared to other separation technologies such as evaporation, extraction, and distillation. Potential industrial applications for SRNF in the pharmaceutical, biochemical, and petrochemical industries for recovery of valuable compounds are identified. Examples are separations in the lube oil dewaxing process, homogeneous catalyst recycling and recovery, ionic liquids recovery, solvent exchange in chemical synthesis, edible oil production (2-3), concentration of reaction products (4), removal of solvent from mother liquor crystals (5), removal of toxins from pharmaceutical compounds (6), or as a membrane reactor to perform organic reactions, i.e. biotransformations of hydrophobic molecules (7). However, industrial application of this technology demands a robust membrane that is able to endure aggressive environments such as a continuous exposure towards organic solvents.

### **1.1. Membrane materials for solvent resistant nanofiltration**

Membranes have been developed for several decades using polymers as a main ingredient (1). Polymers are relatively inexpensive materials and are available with a wide variety of functional groups. They are frequently used as a material for SRNF membranes (3, 8).

However, currently investigated SRNF polymeric membranes, such as those made from PDMS (polydimethylsiloxane) (9), PPSU (polyphenylsulfone) (10), and chitosan (11), were reported to swell significantly in organic solvents, like toluene, diethylether, acetone, methylene chloride, hexane, ethyl acetate, methanol, ethanol, isopropanol, or methyl ethyl ketone (9-14).

Ceramic membranes, on the other hand, exhibit a high chemical stability towards organic solvents (15-16). Despite these superior characteristics, ceramic membranes are not suitable for nanofiltration of nonpolar solvents, because the pore surface of these membranes is always covered with the surface OH-groups when the membranes are not well dried and are stored at ambient conditions [21]. As a consequence, pore blockage, due to the adsorbed water bonded on the ceramic pore wall, hinders the permeation of nonpolar organic solvents in the nanofiltration regime, causing negligible permeation of nonpolar organic solvent (17-19). Significant decline in nonpolar solvent flux after water permeation has been observed with hydrophilic tight UF ceramic membranes (20-21). It is also reported that a serious decrease in flux was observed for nonpolar feed contaminated with water due to the adsorption of this water on the hydrophilic pore walls (22). For these reasons, the functionalization of porous ceramics by hydrophobic organic moieties for nonpolar solvent filtration was proposed (19). On the other hand, for polar solvents, functionalization of porous ceramic is interesting for pore size tuning or introducing special functions to the ceramic membranes.

### **1.2. Functionalization of ceramic membranes**

Functionalization of ceramic membranes is viable through grafting. Grafting is a process in which a specific organic substance is chemically bonded to an inorganic substrate. The OH-groups of the oxide ceramic surface will react with the hydrolysable groups of the to-be-

grafted organic moiety to produce a stable covalent bond, resulting in a permanent modification of ceramic membranes.

Modification of porous inorganic membranes by grafting has been used to prepare membranes for various applications (23-30). Leger et al. (23) used silicone oil (viscosity 545 mPa) to graft the surface of alumina membranes with a pore size of 5 nm used for gas permeation and pervaporation. The membrane was shown to be chemically stable in toluene, acetone and THF. Faibish et al. (24) grafted polyvinylpyrrolidone on zirconia membranes for oil-in-water emulsion treatment. Here free-radical graft polymerization was applied by using a vinyl silane as linker to the zirconia membranes. The authors claim a reduction in pore size of around 25 % after grafting but no pore size values are given in this paper. Yoshida et al. (25) grafted  $\gamma$ -alumina (pore size 5 nm) by using vinyl acetate or vinyl pyrrolidone monomers and made a layer of terminally bonded polymer on the surface of a  $\gamma$ -alumina tubular support. In another paper Yoshida et al. (26) grafted vinyl acetate or vinyl pyrrolidone to silica membranes (pore size of 20 nm) by free radical graft polymerization for pervaporation of methyl-tert-butyl ether from water. Popat et al. (27) grafted polyethylene glycol to straight pore alumina membranes ("anodisc") using a silane coupling agent. Lee et al. (28) used polyethylene glycol to graft straight pore alumina membranes for the application as anti-fouling membrane for biomolecules. The pore size of the bare alumina, used in (27) and (28), are of the order of 25 - 80 nm, while the grafted membranes are still in the ultra-filtration range. These studies showed that permanent membrane modification by grafting is possible. Moreover, these studies demonstrate that grafting can reduce the membrane pore size due to the presence of the grafted moiety. The possibility that by means of grafting the membrane pore size can be reduced is interesting for the development of new types solvent resistant nanofiltration (SRNF) membranes, meaning that existing UF ceramic membranes can be modified and turned into NF membranes. This approach was used in Chapter 2, 5 and 6 of this thesis, in which mesoporous  $\gamma$ -alumina UF membranes were grafted by different natures of organic moieties to decrease the membrane pore diameter of the existing  $\gamma$ -alumina UF down to the nanofiltration range.

The hydroxyl groups on the membrane surface can be exploited as reactive sites for introduction of organic moieties. Figure 1.1 shows different possible -OH configurations on

the surface of  $\gamma$ -alumina: the isolated hydroxyl groups (Figure 1.1a) and the non-isolated hydroxyl groups forming hydrogen bonding with the adjacent hydroxyl (Figure 1.1b to d) (31-32). The non-isolated hydroxyl groups are those that can form hydrogen bridges with the adjacent hydroxyl while the isolated hydroxyl groups refer to the hydroxyl groups where the separation distance between each oxygen atom of the two surface hydroxyl is larger than 0.3 nm(33). All these surface -OH configurations were identified as potentially reactive on  $\gamma$ -alumina (31-32).

The surface concentration of hydroxyl groups on the  $\gamma$ -alumina has been reported to be between 3 to 9 -OH groups per  $\text{nm}^2$  (31-32). For comparison, an average concentration of 3 to 4.6 -OH groups per  $\text{nm}^2$  were reported for silica (34). The  $\alpha$ -alumina layer being sintered at high temperatures (1000°C or more), on the other hand, has a low concentration of surface hydroxyl groups (35). In this thesis, a mesoporous layer of  $\gamma$ -alumina, supported on a macroporous  $\alpha$ -alumina macroporous, was chosen as the inorganic substrate to be grafted.

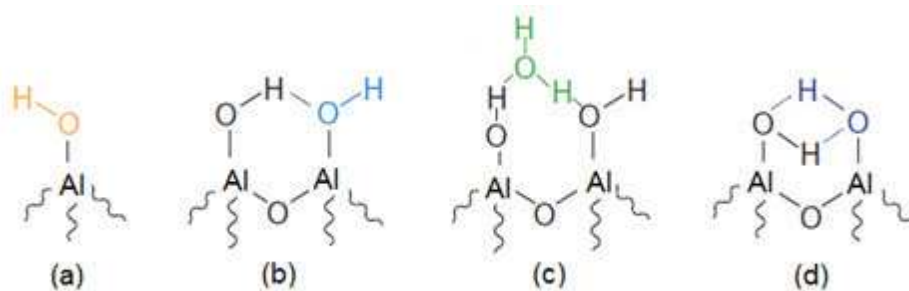


Figure 1.1. Different possible -OH configurations on the surface of  $\gamma$ -alumina as described in (31-32) : a) isolated -OH groups, b-d) the non-isolated hydroxyl groups forming hydrogen bonding with the adjacent -OH or water molecules. Figure adapted from (36).

Organosilanes compounds such as chloroalkylsilanes and fluoroalkylsilanes have hydrolysable groups on one end and an organic moiety on the other end. These organosilanes can be utilized to graft an organic moiety to the pore wall of the inorganic substrate. The hydrolysable groups of these organosilanes can react with the hydroxyl groups on the inorganic substrates such as ceramics to form stable covalent bonds. The grafting reaction between the organoalkoxysilanes and the surface hydroxyls proceeds by hydrolysis of the alkoxy groups, followed by a condensation reaction upon meeting the hydroxyl groups on the membrane surface, resulting in a stable covalent Al-O-Si bond

between the oxide surfaces and the grafting agent (37-38). In this reaction, moisture from the substrate acts as a catalyst for the hydrolysis (37-38). For the silanes to access the hydroxyl groups on the membrane surface, no more than 2 or 3 monolayers of water should exist on the substrate surface (37).

The nature of the grafting agents such as the number of the hydrolyzable groups can affect the grafting result. Fadeev et al. (39) found that the number of the hydrolyzable groups, such as mono-, di-, or trifunctional organosilanes, affect the layer thickness, homogeneity, and wettability degree of the modified substrate. Organosilanes with more functional groups promote thicker layers, better homogeneity and higher water contact angle than organosilanes with less functional groups. Two possibilities of binding routes were identified for organosilanes with two or more functional groups. First, the hydrolyzable group of the organosilanes may condense with the hydroxyl groups on the inorganic substrate and a stable covalent bond was formed between the organosilyl and the inorganic surface. Secondly, the hydrolyzable group of the organosilanes may react with other organosilanes and form a polymeric layer in the presence of water. Several possible structures that can result from the grafting reaction between organosilanes and metal oxide surfaces are given in Figure 1.2.



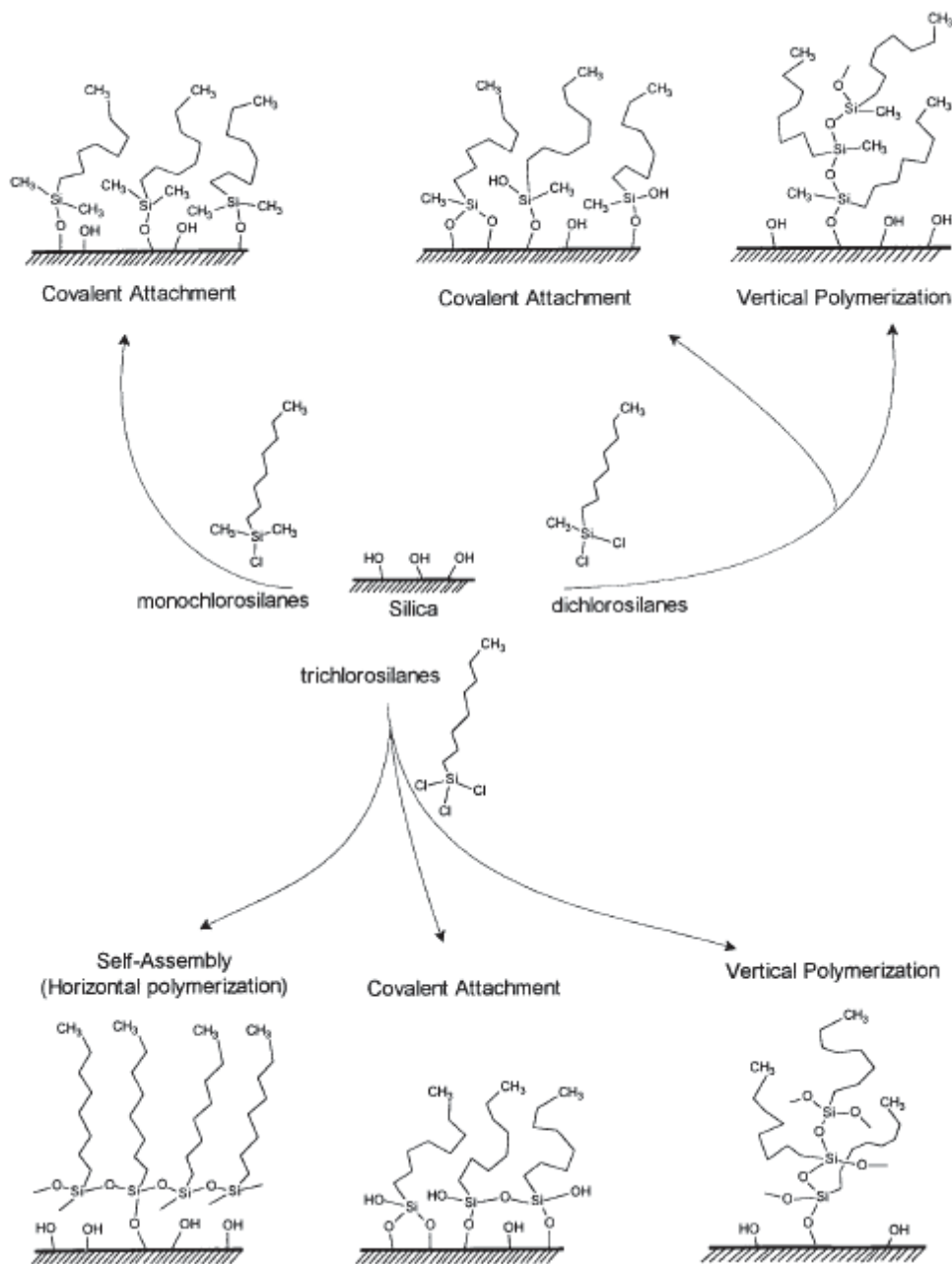


Figure 1.2. Possible structures resulting from the grafting reaction between organosilanes and metal oxide surfaces (39)

*Sah et al.* (40) hydrophobized a mesoporous metal oxide membrane using organosilanes with different bulkiness of the alkyl/aromatic chain and different numbers of hydrolysable groups. For the membrane modified with less bulky silanes and more hydrolysable groups, a higher density of grafting was found.

*Picard et al.* (41) modified a mesoporous metal oxide membrane using fluorinated silanes. The effect of grafting time on the degree of modification was studied. It was found that

longer grafting time results in a higher water contact angle of the modified membranes, possibly due to longer time allowed to complete the grafting reaction.

*Alami Younsi et al. (42-43)* modified a mesoporous metal oxide membrane using organosilanes with different types of hydrolyzable groups. The effect of different chemical nature of the functional groups like chloro-, methoxy-, and ethoxy-groups on the surface modification result studied. It was found that among the three, chlorosilanes results in the highest grafting density as concluded from TGA measurements, followed by the methoxysilanes, and finally the ethoxysilanes.

*Belyavskii et al. (44)* studied the effect of several factors on the grafting of  $\gamma\text{-Al}_2\text{O}_3$  substrate by aryl silanes, such as the nature of the grafting agents as well as the presence of water. The amount of grafted moieties, as studied by FTIR and elemental analysis, largely depends on the number of functional groups of the organosilanes. Organosilanes with more functional groups achieve higher surface coverage. Moreover, water was found to play an important role in the grafting process. It was observed that the hydrolysis step is the rate limiting step in the silanization process which caused silanization to progress very slowly without the presence of water.

All these studies showed that the nature of the grafting agents can affect the grafting results. In chapter 6 of this thesis, the grafting performance of  $\gamma$ -alumina with different grafting agents having different number of hydrolyzable groups, different number of ureido functionality groups and different molecular weights, were assessed further by means of FTIR, TGA,  $^{29}\text{Si-NMR}$ , and BET in order to study the effect of different properties on the grafting result.

Grafting with silylated low MW polymers was found to be an effective way to prepare an SRNF membrane(29). Pinheiro et al. (29) developed nanofiltration membranes by grafting PDMS in the pores of porous  $\gamma$ -alumina supports (pore size 5 nm) using aminopropylethoxysilane (APTES) as the linker and (mono(2,3-epoxy) polyetherterminated polydimethylsiloxane with an average number of repeating monomers (n) of 10 and a viscosity of 10-50 mPa. This two-step grafting procedure is schematically given in Figure 1.3. It was demonstrated that polymer grafting can result in a chemically stable membrane with

a permselectivity in the nanofiltration regime. In (29), grafting of silanes with the surface hydroxyl groups of the ceramic substrate was done by a vapor phase deposition method (VPD). Depending on the reactivity of the silylated grafting agents solvent phase deposition (SPD) or VPD will be used. VPD is used for relatively reactive silanes as it results in a monolayer or near-monolayer silane coverage on the pore wall (45). The strategy as shown in Figure 1.3 was adopted in Chapter 2.

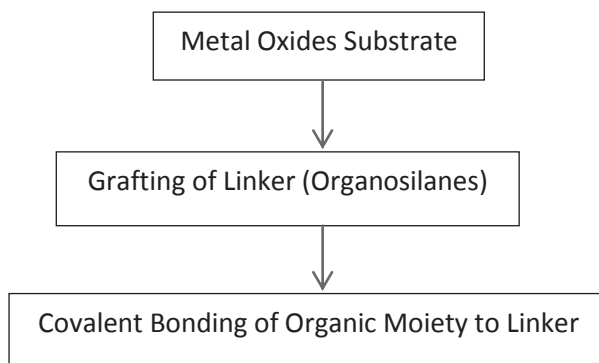


Figure 1.3. Schematic description of a two-step chemical grafting process

Another grafting route involves preparation of an organic group, where the low MW organic moiety was silylated prior to grafting. This strategy was adopted in Chapter 6.

The small-chain organic polymer can be grown from monomers both in-situ during grafting or ex-situ (46-47). In the “grafting-to” approach the organic moiety is grown ex-situ from the monomers before the functional groups of the organic moiety are reacted with the reactive sites of the solid substrate. The “grafting-to” mechanism is interesting due to several advantages, i.e. the grafted polymer can be thoroughly synthesized and characterized by traditional methods in solution.

In the “grafting from” approach, the organic moiety is grown from the monomers in-situ during grafting. Theoretically, any possible polymerization mechanisms can be employed to grow the polymeric chain from the monomers (46). An example is the free radical polymerization by vinyl monomers as performed by the group of Cohen et. al. (24-26). In this approach the immobilization of the initiator near the reactive sites of the substrate is an important step. Since the grafting from mechanism involves a polymerization at high local concentration of monomers, side reactions could occur and polydispersity might be difficult

to control. Another way to grow the organic moiety from the pore wall is by covalent coupling. This covalent coupling technique can be used to extend the length of the grafted moiety by means of reactions between organic molecules and a coupling agent. Popat et al. (27) and Lee et al. (28) employed a catalyzed covalent reaction between low MW poly(ethylene glycol) and a coupling agent (in this case silicon tetrachloride) so that the organic chain was grown from the surface of the pore wall. In covalent coupling the structure of the monomer and the coupling agent can be chosen in such a way that grafting results in a not too dense membrane, so pore size can be controlled in this way. This strategy is adopted in Chapter 5 in order to form a grafted network on the membrane pore wall.

Figure 1.4 gave an illustration of different grafting methods, i.e. the “grafting to” method (Figure 1.4a) and the “grafting from” method (Figure 1.4b).

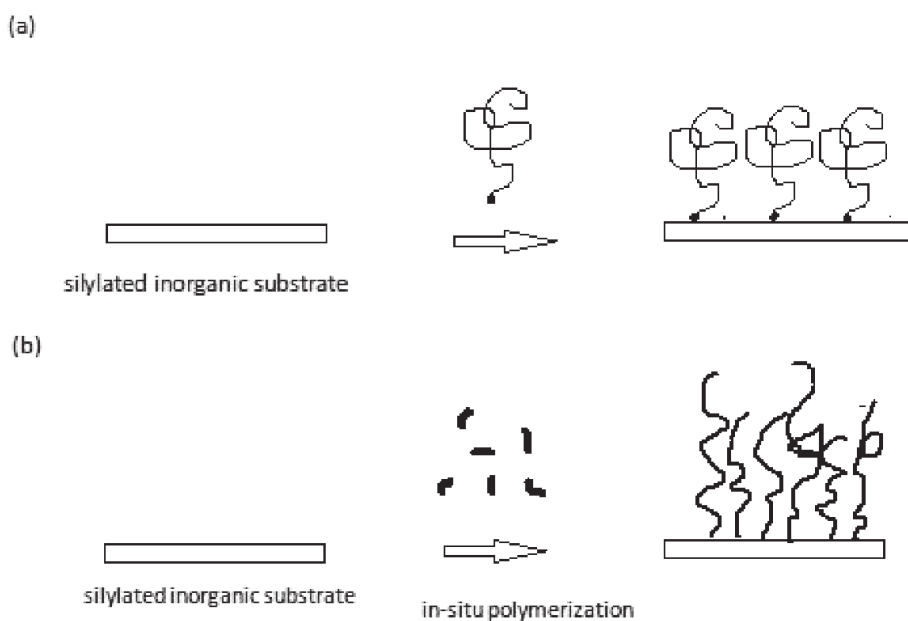


Figure 1.4. Grafting methods, i.e. a) “grafting to” b) “grafting from” method

Porous ceramic material as a non-swelling material is considered suitable to be used as a cylindrical frame for the organic moieties to be grafted on. For the development of the grafted ceramic membranes, it is important to have a good quality support in terms of pore size distribution, porosity, and chemical stability. A  $\gamma$ -alumina mesoporous layer with an average pore diameter of 5 nm supported on an  $\alpha$ -alumina membrane with an average pore diameter of 80 nm (Pervatech) were chosen. A ceramic support having a pore size as small as

possible but sufficiently large to graft a (small) polymer on the pore walls was chosen in order to have the largest benefit of the rigid character of a ceramic membrane system. The membrane with a porosity of 40-50% can stand pressures up to 30 bars (48).

### **1.3. Transport Behavior of SRNF Membranes**

More attention on how these membranes perform in different solvents is important. *Yang et al.* (49) observed that the solute retention in nanofiltration of organic solvents are specific for each solvent due to the different membrane-solvent-solute interaction for each specific solvent, governing the solvent and solute transport through the membranes. In aqueous applications, the membrane selectivity can be defined by a rejection of a certain solute in water. For the non-aqueous application, especially for polymeric membranes, it was found that different types of solvents can lead to different membrane permeability and selectivity.

Variables such as membrane process parameters, membrane material properties, as well as the type of solvents and solutes influence the nanofiltration performances (50). The type of modules as well as the process parameters of the membrane (e.g. feed concentrations, applied pressures and temperatures) can be important parameters influencing the membrane performance. The membrane material properties such as pore size, swelling resistance, and surface chemistry can also affect the membrane performance. The types of solvent (e.g. viscosity, polarity, molecular size, and/or surface tension) and the types of solute (e.g. size, shape, and/or charges of the solute) is another factor influencing nanofiltration performance. In summary solvent nanofiltration is affected by the interactions between membrane, solvents and solutes (3). Figure 1.5 summarizes possible governing factors affecting solvent and solute transport in SRNF membranes.

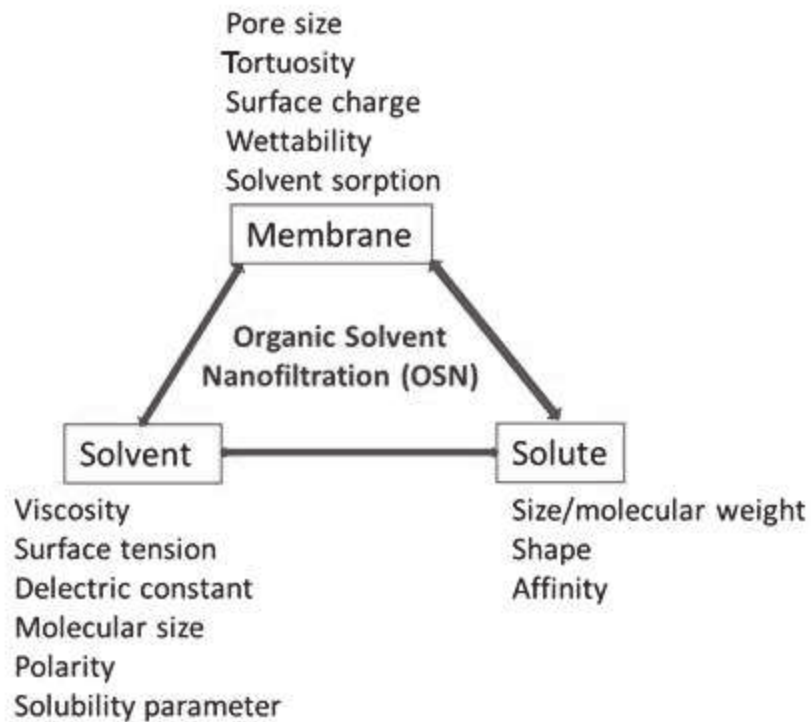


Figure 1.5. Several possible governing factors affecting solvent and solute transport in SRNF membranes

Castro et al. (51) studied the effect of different types of solvents on the permeability of an ultrafiltration membrane, prepared by grafting of PVP inside the pores of a macroporous silica support with a native pore diameter of 410 nm. It was found that for the hydrophilic PVP grafted membranes, the permeability of nonpolar solvents, like cyclohexane and toluene, was higher than the permeability of polar solvents, like propanol, water, and ethanol contrary to what was expected. Further on, Castro et al. (52) observed a shear-rate flow induced behavior of a PVP grafted macroporous ceramic substrate with an average pore size of 410 nm due to the mobility of the grafted polymeric chains. The effect of shear rate on the permeability of the grafted membrane was described as a condition that at increasing trans-membrane pressure, the membrane is experiencing a more open membrane structure due to the movement of the grafted moieties in the direction of the feed flow, resulting in an exponential increase in the membrane permeability towards the trans-membrane pressure. These findings signify that the grafted ceramic membranes may possess a unique set of transport behaviour that is worth further investigation.

As many parameters can affect the nanofiltration performance in non-aqueous applications, quantification of each factor contributing to the nanofiltration performance as well as

modelling of transport can be difficult. A general strategy on quantifying the transport mechanism of a membrane (despite the many possible contributing factors) is by looking whether the transport models previously applied for aqueous systems can be used to describe membrane transport in solvent nanofiltration.

Two models are generally used to describe solvent transport through membranes, i. e. the pore flow model and the solution diffusion model (1). In the pore-flow model, the membrane is regarded to have defined open pores from the feed side to the permeate side. Darcy's Law, often referred to as the pore-flow or viscous-flow model, describes liquid permeation through porous media as a function of the trans-membrane pressure (TMP):

$$J = \frac{k \Delta P}{\mu l} \quad (1.1)$$

where  $J$  is the solvent flux,  $k$  the permeability constant,  $\mu$  the fluid viscosity,  $\Delta P$  the trans-membrane pressure, and  $l$  the membrane thickness.

For viscous flow, the Darcy's law can be combined with the Hagen–Poiseuille equation:

$$J = k \frac{\Delta P}{\mu} \quad (1.2)$$

with

$$k = \frac{\epsilon r_p^2}{8\tau l} \quad (1.3)$$

where  $J$  is the solvent flux,  $\Delta P$  the trans-membrane pressure,  $\mu$  the solvent viscosity, and  $k$  the membrane permeability constant representing the structural properties of the membrane with  $\epsilon$  the membrane porosity,  $r_p$  the membrane average pore diameter,  $\tau$  the membrane tortuosity, and  $l$  the membrane thickness. Pore tortuosity,  $\tau$ , is defined as the true length of the flow path relative to the straight-line distance between the feed and permeate side of the membrane. The solvent viscosity ( $\mu$ ) is a parameter identifying the characteristics of different solvents.

If there are no pores identified in the membrane, the solution-diffusion model is generally used (1). This means that the transport of liquids occurs via free volume elements between polymeric chains, which can appear and disappear as a function of time and place according to the movement of the solvent (53). This model assumes that the pressure is constant throughout the membrane and the driving force of solvent transport is the chemical activity

difference between the feed and permeate side of the dense membrane. The solution-diffusion equation is as follows:

$$J_i = \frac{D_i K_i}{l} \left[ a_{if} - a_{ip} \exp\left(\frac{-v_i(P_f - P_p)}{R_g T}\right) \right] \quad (1.4)$$

where  $J_i$  represents the solvent flux,  $l$  the membrane thickness,  $D_i$  the diffusion coefficient of the solvent or solute  $i$  through the membrane,  $K_i$  the partition coefficient,  $a_{if}$  and  $a_{ip}$  are the activities of species  $i$  in respectively feed and permeate,  $v_i$  the partial molar volume of specimen  $i$ ,  $P_f$  and  $P_p$  the pressures at feed and permeate side,  $R_g$  the gas constant and  $T$  the temperature. If a pure solvent is used, then  $a_{if}$  is 1 and  $v_i$  is 1, while  $a_{ip}$  is 0. Thus, the equation becomes:

$$J_i = \frac{D_i K_i}{l} \left[ 1 - \exp\left(\frac{-(\Delta P - \Delta \pi)}{R_g T}\right) \right] \quad (1.5)$$

where  $\Delta \pi$  stands for the osmotic pressure (54).

When the difference between the applied and osmotic pressure is small, the equation can be written as:

$$J_i = \frac{D_i K_i}{R_g l T} (\Delta P - \Delta \pi) \quad (1.6)$$

$$J_i = A(\Delta P - \Delta \pi) \quad (1.7)$$

where  $A$  is a solvent permeability constant.

For a PDMS-based solvent resistant NF membrane, both pore-flow and solution-diffusion models have been used to describe the membrane transport. Vankelecom et al. (53) suggested that a viscous flow model can be used to describe the permeation of pure solvents through non-supported PDMS polymeric membranes by taking into account membrane swelling. This finding was later confirmed by Robinson et al. (55), who successfully used a pore-flow model to describe the solvent transport through PAN-supported PDMS membranes for nonpolar solvents based on the reasoning that the dense selective PDMS layer may form a pore-like structure in the presence of nonpolar solvents. Meanwhile, Zeidler et al. (56) observed negative rejections of dye solutes in ethanol through PDMS membranes. It was confirmed that in the presence of swelling solvents like n-heptane



and THF, a viscous flow behavior was observed for PDMS membranes. On the other hand, in the presence of non-swelling solvents like ethanol, it was proposed that the rejection of PDMS might be closer to that of the solution-diffusion mechanism. Postel et al. (57) examined this phenomenon and successfully used the solution-diffusion model to describe the negative rejections of dye solutes using ethanol as a solvent through dense PDMS polymeric membranes. These studies show that the existing transport model for aqueous applications can be used as a starting point to investigate the transport behavior of solvent-resistant nanofiltration membranes. Once the identification of the major parameters is carried out in this way, the identification of the more subtle factors influencing the membrane transport may be progressed further by studying whether there are any differences between the experimental data and the existing transport models. In chapter 3, this strategy is followed to identify major parameters governing the solvent and solute transport through the grafted ceramic membranes.

A general model to describe solute transport for both porous and nonporous membranes is given by Kedem-Katchalsky (58). In this model membranes are considered as a black box comprising feed and permeate as the input and output, respectively. The flux of the solute through the membrane is described as:

$$J_c = P_c \Delta x \frac{dc}{dx} + (1 - \sigma)J_v \quad (1.8)$$

with  $J_c$  is the solute flux,  $P_c$  the solute permeability,  $\Delta x$  the membrane thickness,  $\frac{dc}{dx}$  the concentration gradient over the membrane,  $\sigma$  the reflection coefficient, which is a measure for the rejection of a solute,  $J_c$  the solute flux, and  $J_v$  the solvent flux.

In Equation 1.8, the first term describes the transport of solutes by a diffusion mechanism, while the second term describes the transport of solutes by a convection mechanism. If the contribution of solute flux by diffusion is negligible, Equation 1.8 can be simplified to Equation 1.9 as follows

$$\sigma = 1 - \frac{J_c}{J_v} \quad (1.9)$$

Ferry et al. (59) proposed a solute transport model, which relates the reflection coefficient with the ratio of solute diameter versus pore diameter. In this model it is assumed that

solute, having similar or larger diameter than the membrane pore diameter, are completely rejected and solutes with smaller diameter than the effective diameter of the membrane pores completely permeate. The membrane pore diameter, as well as the diameter of the solute, are defined as average values rather than nominal values. Besides, no interaction between the membrane, solvent, and solute is taken into account in this model of Ferry. Here, the reflection coefficient will develop from 0 to 1 as the ratio of  $d_c$  (the average solute diameter) versus  $d_p$  (the mean pore diameter) increases. This means  $\sigma = 0$  for  $d_c/d_p \geq 1$  and  $\sigma=1$  for  $d_c/d_p \leq 1$ . The model of Ferry describes  $\sigma$  in the following way:

$$\sigma = \left(\frac{d_c}{d_p} \left(\frac{d_c}{d_p} - 2\right)\right)^2 \quad (1.10)$$

The Verniory model (60) considers that solutes with particle diameter smaller than the pore diameter of the membranes are partially rejected due to drag forces, caused by wall friction. The Verniory model can be written as:

$$\sigma = 1 - \left(\frac{1 - \frac{2d_c^2}{3d_p} - 0.2\frac{d_c^5}{d_p}}{1 - 0.76\frac{d_c^5}{d_p}}\right) \left(1 - \frac{d_c}{d_p}\right)^2 \left(2 - \left(1 - \frac{d_c}{d_p}\right)^2\right) \quad (1.11)$$

The Verniory model accounts for the wall friction occurring between the solute and membrane wall while attractive forces between the solute and membrane are not taken into account. The steric hindrance pore model (61), instead, accounts for a rejection case in which the wall friction effect is negligible due to attractive forces between membrane and solute. As a consequence, solutes having a particle diameter larger than the pore diameter of the membranes were assumed to be partially permeated. The steric hindrance pore model is presented as:

$$\sigma = 1 - \left(1 + \frac{16}{9} \frac{d_c^2}{d_p}\right) \left(1 - \frac{d_c}{d_p}\right)^2 \left(2 - \left(1 - \frac{d_c}{d_p}\right)^2\right) \quad (1.12)$$

When the solute transports by a diffusion mechanism, the solute flux proceeds by

$$J_c = P_c \Delta x \frac{dc}{dx} \quad (1.13)$$

With

$$P_c = D_{sm} K_s \quad (1.14)$$

with  $J_c$  is the solute flux,  $P_c$  the solute permeability,  $\Delta x$  the membrane thickness,  $\frac{dc}{dx}$  the concentration gradient over the membrane,  $D_{sm}$  the diffusivity of the solute, and  $K_s$  the solute distribution coefficient.

In Chapter 4, the applicability of the existing rejection models to predict the rejection behavior of PDMS-grafted ceramic membranes is described.

#### 1.4. Dissertation overview

This thesis deals with the grafting of ceramic membranes with organic moieties for solvent resistant nanofiltration and studying of their solvent and solute transport properties.

In **Chapter 2**, the grafting of a mesoporous (pore size 5 nm)  $\gamma$ -alumina layer, supported on macro porous  $\alpha$ -alumina, with 3-mercaptopropyltriethoxysilane (MPTES) as linking agent is described. Subsequently, the system is grafted with monovinyl-terminated polydimethylsiloxane (PDMS) in order to generate a membrane suitable for solvent nanofiltration. PDMS was selected as it has been proven to be an excellent material for SRNF applications (29-30, 62-64).  $\gamma$ -alumina with a pore size as small as possible but sufficiently large to graft a (small) polymer on the pore walls was chosen in order to have the largest benefit of the rigid character of a ceramic membrane system, while changing the hydrophilic nature of the inorganic membrane to hydrophobic. The grafting behaviour of the organic moieties on the  $\gamma$ -alumina was studied by Fourier Transform Infrared spectroscopy (FTIR). Contact angle measurements and solvent permeability tests were used to study the membrane properties. Chemical stability tests in toluene at elevated temperatures were performed as well.

In **Chapter 3**, major parameters influencing solvent transport were investigated for two types of grafted membranes with a relatively short or long chain of PDMS (n=10 and n=39). The permeability was studied by means of permeation tests at operating pressures between 1 to 20 bar to investigate the effect of trans-membrane pressure on the membrane

permeability. Various solvents were used to study the effect of different solvent types on the membrane permeation behavior. Permeation tests at elevated temperature were conducted to study the effect of temperature on the membrane permeability. A model is proposed to describe the permeation of pure solvents through these membranes.

In **Chapter 4**, rejection behavior of PDMS grafted membranes for different types of solutes in nonpolar and polar solvents were studied. The applicability of existing solute rejection models, based on a size-exclusion mechanism, to describe the solute rejection of the PDMS-grafted ceramic membranes is discussed and were assessed. Three rejection models based on size-exclusion, namely the Ferry, Verniory, and SHP models were used to predict the rejection of several solutes using pore diameter information from the N<sub>2</sub> physisorption measurement when no solvent is present. Important parameters which control the transport mechanism through PDMS grafted ceramic membranes were identified.

In **Chapter 5**, grafting of mesoporous  $\gamma$ -alumina membranes with hydride terminated polydimethylsiloxanes, using vinyltriethoxysilanes as linking agent and tetrakis (vinyl dimethylsiloxy)silane as the coupling agent, in order to generate a membrane suitable for solvent nanofiltration is described. In this work, a coupling agent was used via a covalent coupling technique to couple the grafted moiety inside the ceramic pores to further decrease the pore size of the grafted membranes. Different from the material as described in Chapter 2, in which a low MW PDMS was grafted to the ceramic pore wall without an additional growing of the organic chain from the pore wall, in this Chapter 5 a covalent coupling technique was used to couple the grafted moiety forming a polymer network inside the ceramic pores via a covalent reaction between PDMS molecules and a coupling agent. It is expected that this method results in a smaller membrane pore diameter compared to the results given in Chapter 2 to accommodate the need for removing very small size impurities during solvent recycling. Grafting performance of the organic moieties on  $\gamma$ -alumina powders was analyzed by FTIR, TGA, contact angle, SEM-EDX, permeation and solute rejection tests.

In **Chapter 6**, grafting of a mesoporous  $\gamma$ -alumina layer, supported on a macro porous  $\alpha$ -alumina, with several types of silane terminated polyethylene glycol as to result in a

chemically and thermally stable membrane with hydrophilic characteristic for solvent nanofiltration is described. The grafting performance of each grafting agent, having different molecular weights, number of alkoxy groups, and number of ureido functionalities, was analysed by means of thermogravimetric analysis, FTIR, Si-NMR and BET. The grafting agent having the highest grafting density according to the TGA analysis was selected to be grafted on ceramic membranes. Contact angle measurements, solvent permeability tests, and rejection tests were used to assess the membrane performance. The permeability behavior with respect to different types of permeating solvent (polar and nonpolar) was also investigated.

Finally, the general conclusions and future work are presented in **Chapter 7**.

## References

1. Mulder, M. (1996) *Basic principles of membrane technology*, 2nd ed., Kluwer Academic Publisher, Netherlands.
2. Volkov, A. V., Korneeva, G. A., and Tereshchenko, G. F. (2008) Organic solvent nanofiltration: Prospects and application, *Russian Chemical Reviews* 77, 983-993.
3. Vandezande, P., Gevers, L. E. M., and Vankelecom, I. F. J. (2008) Solvent resistant nanofiltration: Separating on a molecular level, *Chemical Society Reviews* 37, 365-405.
4. Peshev, D., Peeva, L. G., Peev, G., Baptista, I. I. R., and Boam, A. T. (2011) Application of organic solvent nanofiltration for concentration of antioxidant extracts of rosemary (*Rosmarinus officinalis* L.), *Chemical Engineering Research and Design* 89, 318-327.
5. Rundquist, E. M., Pink, C. J., and Livingston, A. G. (2012) Organic solvent nanofiltration: a potential alternative to distillation for solvent recovery from crystallisation mother liquors, *Green Chemistry*.
6. Székely, G., Bandarra, J., Heggie, W., Selligren, B., and Ferreira, F. C. (2011) Organic solvent nanofiltration: A platform for removal of genotoxins from active pharmaceutical ingredients, *Journal of Membrane Science* 381, 21-33.
7. Valadez-Blanco, R., Ferreira, F. C., Jorge, R. F., and Livingston, A. G. (2008) A membrane bioreactor for biotransformations of hydrophobic molecules using organic solvent nanofiltration (OSN) membranes, *Journal of Membrane Science* 317, 50-64.

8. Bhanushali, D., Kloos, S., Kurth, C., and Bhattacharyya, D. (2001) Performance of solvent-resistant membranes for non-aqueous systems: Solvent permeation results and modeling, *Journal of Membrane Science* 189, 1-21.
9. Van der Bruggen, B., Geens, J., and Vandecasteele, C. (2002) Influence of organic solvents on the performance of polymeric nanofiltration membranes, *Separation Science and Technology* 37, 783-797.
10. Darvishmanesh, S., Jansen, J. C., Tasselli, F., Tocci, E., Luis, P., Degrève, J., Drioli, E., and Van der Bruggen, B. (2011) Novel polyphenylsulfone membrane for potential use in solvent nanofiltration, *Journal of Membrane Science* 379, 60-68.
11. Musale, D. A., and Kumar, A. (2000) Solvent and pH resistance of surface crosslinked chitosan/poly(acrylonitrile) composite nanofiltration membranes, *Journal of Applied Polymer Science* 77, 1782-1793.
12. Tarleton, E. S., Robinson, J. P., and Salman, M. (2006) Solvent-induced swelling of membranes - Measurements and influence in nanofiltration, *Journal of Membrane Science* 280, 442-451.
13. Darvishmanesh, S., Degrè, J., and Bruggen, B. V. D. (2010) Performance of solvent-pretreated polyimide nanofiltration membranes for separation of dissolved dyes from toluene, *Industrial and Engineering Chemistry Research* 49, 9330-9338.
14. Van der Bruggen, B., Geens, J., and Vandecasteele, C. (2002) Fluxes and rejections for nanofiltration with solvent stable polymeric membranes in water, ethanol and n-hexane, *Chemical Engineering Science* 57, 2511-2518.
15. Buekenhoudt, A. (2008) *Stability of Porous Ceramic Membranes*, Vol. 13, Elsevier B.V., Belgium.
16. Van Gestel, T., Vandecasteele, C., Buekenhoudt, A., Dotremont, C., Luyten, J., Van Der Bruggen, B., and Maes, G. (2003) Corrosion properties of alumina and titania NF membranes, *Journal of Membrane Science* 214, 21-29.
17. Tsuru, T., Sudou, T., Kawahara, S. I., Yoshioka, T., and Asaeda, M. (2000) Permeation of liquids through inorganic nanofiltration membranes, *Journal of Colloid and Interface Science* 228, 292-296.
18. Buekenhoudt, A., Bisignano, F., De Luca, G., Vandezande, P., Wouters, M., and Verhulst, K. (2013) Unravelling the solvent flux behaviour of ceramic nanofiltration and ultrafiltration membranes, *Journal of Membrane Science* 439, 36-47.
19. Verrecht, B., Leysen, R., Buekenhoudt, A., Vandecasteele, C., and Van der Bruggen, B. (2006) Chemical surface modification of  $\gamma$ -Al<sub>2</sub>O<sub>3</sub> and TiO<sub>2</sub> toplayer membranes for increased hydrophobicity, *Desalination* 200, 385-386.
20. Chowdhury, S. R., Schmuhl, R., Keizer, K., Ten Elshof, J. E., and Blank, D. H. A. (2003) Pore size and surface chemistry effects on the transport of hydrophobic and

- hydrophilic solvents through mesoporous  $\gamma$ -alumina and silica MCM-48, *Journal of Membrane Science* 225, 177-186.
21. Chowdhury, S. R., Keizer, K., Ten Elshof, J. E., and Blank, D. H. A. (2004) Effect of trace amounts of water on organic solvent transport through  $\gamma$ -Alumina membranes with varying pore sizes, *Langmuir* 20, 4548-4552.
  22. Tsuru, T., Narita, M., Shinagawa, R., and Yoshioka, T. (2008) Nanoporous titania membranes for permeation and filtration of organic solutions, *Desalination* 233, 1-9.
  23. Leger, C., De Lira, H. L., and Paterson, R. (1996) Preparation and properties of surface modified ceramic membranes. Part II. Gas and liquid permeabilities of 5 nm alumina membranes modified by a monolayer of bound polydimethylsiloxane (PDMS) silicone oil, *Journal of Membrane Science* 120, 135-146.
  24. Faibish, R. S., and Cohen, Y. (2001) Fouling-resistant ceramic-supported polymer membranes for ultrafiltration of oil-in-water microemulsions, *Journal of Membrane Science* 185, 129-143.
  25. Yoshida, W., and Cohen, Y. (2003) Ceramic-supported polymer membranes for pervaporation of binary organic/organic mixtures, *Journal of Membrane Science* 213, 145-157.
  26. Yoshida, W., and Cohen, Y. (2004) Removal of methyl tert-butyl ether from water by pervaporation using ceramic-supported polymer membranes, *Journal of Membrane Science* 229, 27-32.
  27. Popat, K. C., Mor, G., Grimes, C. A., and Desai, T. A. (2004) Surface Modification of Nanoporous Alumina Surfaces with Poly(ethylene glycol), *Langmuir* 20, 8035-8041.
  28. Sang Won, L., Hao, S., Richard, T. H., Vania, P., and Gil, U. L. (2005) Transport and functional behaviour of poly(ethylene glycol)-modified nanoporous alumina membranes, *Nanotechnology* 16, 1335.
  29. Pinheiro, A. F. M., Hoogendoorn, D., Nijmeijer, A., and Winnubst, L. (2014) Development of a PDMS-grafted alumina membrane and its evaluation as solvent resistant nanofiltration membrane, *Journal of Membrane Science* 463, 24-32.
  30. Tanardi, C. R., Pinheiro, A. F. M., Nijmeijer, A., and Winnubst, L. (2014) PDMS grafting of mesoporous  $\gamma$ -alumina membranes for nanofiltration of organic solvents, *Journal of Membrane Science* 469, 471-477.
  31. Hart, L. D., (Ed.) (1990) *Alumina Chemicals: Science and Technology Handbook*, America Ceramic Society, Westerville.
  32. Nortier, P., Fourre, P., Saad, A. B. M., Saur, O., and Lavalley, J. C. (1990) Effects of crystallinity and morphology on the surface properties of alumina, *Applied Catalysis* 61, 141-160.

33. Zhuravlev, L. T. (1987) Concentration of hydroxyl groups on the surface of amorphous silicas, *Langmuir* 3, 316-318.
34. Rajagopal, S., Marini, H. J., Marzari, J. A., and Miranda, R. (1994) Silica-Alumina-Supported Acidic Molybdenum Catalysts - TPR and XRD Characterization, *Journal of Catalysis* 147, 417-428.
35. Koonaphapdeelert, S., and Li, K. (2007) Preparation and characterization of hydrophobic ceramic hollow fibre membrane, *Journal of Membrane Science* 291, 70-76.
36. Kappert, E. J. (2015) Firing membranes, Universiteit Twente.
37. Yoshida, W., Castro, R. P., Jou, J.-D., and Cohen, Y. (2001) Multilayer Alkoxysilane Silylation of Oxide Surfaces, *Langmuir* 17, 5882-5888.
38. Pinheiro, A. F. M. (2013) Development and Characterization of Polymer-grafted Ceramic Membranes for Solvent Nanofiltration, In *PhD Thesis*, University of Twente, Enschede.
39. Fadeev, A. Y., and McCarthy, T. J. (2000) Self-assembly is not the only reaction possible between alkyltrichlorosilanes and surfaces: monomolecular and oligomeric covalently attached layers of dichloro- and trichloroalkylsilanes on silicon, *Langmuir* 16, 7268-7274.
40. Sah, A., Castricum, H. L., Blik, A., Blank, D. H. A., and Ten Elshof, J. E. (2004) Hydrophobic modification of  $\gamma$ -alumina membranes with organochlorosilanes, *Journal of Membrane Science* 243, 125-132.
41. Picard, C., Larbot, A., Guida-Pietrasanta, F., Boutevin, B., and Ratsimihety, A. (2001) Grafting of ceramic membranes by fluorinated silanes: Hydrophobic features, *Separation and Purification Technology* 25, 65-69.
42. Alami Younssi, S., Iraqi, A., Rafiq, M., Persin, M., Larbot, A., and Sarrazin, J. (2003)  $\gamma$  Alumina membranes grafting by organosilanes and its application to the separation of solvent mixtures by pervaporation, *Separation and Purification Technology* 32, 175-179.
43. Alami-Younssi, S., Kiefer, C., Larbot, A., Persin, M., and Sarrazin, J. (1998) Grafting  $\gamma$  alumina microporous membranes by organosilanes: Characterisation by pervaporation, *J. Membr. Sci.* 143, 27-36.
44. Belyavskii, S. G., Mingalev, P. G., and Lisichkin, G. V. (2004) Chemical modification of  $\gamma$ -Al<sub>2</sub>O<sub>3</sub> surface with aryl silanes, *Colloid Journal* 66, 128-136.
45. Sripathi, V. G. P., Mojet, B. L., Nijmeijer, A., and Benes, N. E. (2013) Vapor phase versus liquid phase grafting of meso-porous alumina, *Microporous and Mesoporous Materials* 172, 1-6.



46. Bhattacharya, A., and Misra, B. N. (2004) Grafting: a versatile means to modify polymers: Techniques, factors and applications, *Progress in Polymer Science* 29, 767-814.
47. Zdyrko, B., and Luzinov, I. (2011) Polymer brushes by the "grafting to" method, *Macromolecular rapid communications* 32, 859-869.
48. Leenaars, A., Keizer, K., and Burggraaf, A. (1984) The preparation and characterization of alumina membranes with ultra-fine pores, *Journal of Materials Science* 19, 1077-1088.
49. Yang, X. J., Livingston, A. G., and Freitas Dos Santos, L. (2001) Experimental observations of nanofiltration with organic solvents, *Journal of Membrane Science* 190, 45-55.
50. Darvishmanesh, S., Degreève, J., and Van Der Bruggen, B. (2010) Mechanisms of solute rejection in solvent resistant nanofiltration: The effect of solvent on solute rejection, *Physical Chemistry Chemical Physics* 12, 13333-13342.
51. Castro, R. P., Cohen, Y., and Monbouquette, H. G. (1993) The permeability behavior of polyvinylpyrrolidone-modified porous silica membranes, *Journal of Membrane Science* 84, 151-160.
52. Castro, R. P., Monbouquette, H. G., and Cohen, Y. (2000) Shear-induced permeability changes in a polymer grafted silica membrane, *Journal of Membrane Science* 179, 207-220.
53. Vankelecom, I. F. J., De Smet, K., Gevers, L. E. M., Livingston, A., Nair, D., Aerts, S., Kuypers, S., and Jacobs, P. A. (2004) Physico-chemical interpretation of the SRNF transport mechanism for solvents through dense silicone membranes, *Journal of Membrane Science* 231, 99-108.
54. Wijmans, J. G., and Baker, R. W. (1995) The solution-diffusion model: a review, *Journal of Membrane Science* 107, 1-21.
55. Robinson, J. P., Tarleton, E. S., Millington, C. R., and Nijmeijer, A. (2004) Solvent flux through dense polymeric nanofiltration membranes, *Journal of Membrane Science* 230, 29-37.
56. Zeidler, S., Kätzel, U., and Kreis, P. (2013) Systematic investigation on the influence of solutes on the separation behavior of a PDMS membrane in organic solvent nanofiltration, *Journal of Membrane Science* 429, 295-303.
57. Postel, S., Spalding, G., Chirnside, M., and Wessling, M. (2013) On negative retentions in organic solvent nanofiltration, *Journal of Membrane Science* 447, 57-65.
58. Kedem, O., and Katchalsky, A. (1958) Thermodynamic analysis of the permeability of biological membranes to non-electrolytes, *Biochimica et Biophysica Acta* 27, 229-246.

59. Ferry, J. D. (1936) Ultrafilter membranes and ultrafiltration, *Chemical Reviews* 18, 373-455.
60. Verniory, A., du Bois, R., Decoodt, P., Gasee, J. P., and Lambert, P. P. (1973) Measurement of the permeability of biological membranes. Application to the glomerular wall, *Journal of General Physiology* 62, 489-507.
61. Nakao, S.-I., and Kimura, S. (1982) Models of membrane transport phenomena and their applications for ultrafiltration data, *Journal of Chemical Engineering of Japan* 15, 200-205.
62. Aerts, S., Vanhulsel, A., Buekenhoudt, A., Weyten, H., Kuypers, S., Chen, H., Bryjak, M., Gevers, L. E. M., Vankelecom, I. F. J., and Jacobs, P. A. (2006) Plasma-treated PDMS-membranes in solvent resistant nanofiltration: Characterization and study of transport mechanism, *Journal of Membrane Science* 275, 212-219.
63. Gevers, L. E. M., Vankelecom, I. F. J., and Jacobs, P. A. (2006) Solvent-resistant nanofiltration with filled polydimethylsiloxane (PDMS) membranes, *Journal of Membrane Science* 278, 199-204.
64. Gevers, L. E. M., Vankelecom, I. F. J., and Jacobs, P. A. (2005) Zeolite filled polydimethylsiloxane (PDMS) as an improved membrane for solvent-resistant nanofiltration (SRNF), *Chemical Communications*, 2500-2502.

# Chapter 2

## PDMS Grafting of Mesoporous $\gamma$ -Alumina Membranes for Nanofiltration of Organic Solvents

This chapter has been published as:

Tanardi, C. R., Pinheiro, A. F. M., Nijmeijer, A., and Winnubst, L. (2014) PDMS grafting of mesoporous  $\gamma$ -alumina membranes for nanofiltration of organic solvents, *Journal of Membrane Science* 469, 471-477.

## Abstract

Grafting of mesoporous  $\gamma$ -alumina membranes with monovinyl terminated polydimethylsiloxane (PDMS), using 3-mercaptopropyltriethoxysilane (MPTES) as a linking agent, is described. The grafting performance of the organic moieties on  $\gamma$ -alumina powders was studied by FTIR. Contact angle measurements and solvent permeability tests were used to characterize the membrane properties. The results indicated that grafting reactions were successfully carried out. The toluene permeability of the membrane was reduced from 5.3 to 2.1 L/m<sup>2</sup>.h.bar after grafting with the polymer. No degradation of the membrane material was observed after chemical stability tests in toluene for 6 days at room temperature and at elevated temperatures (up to 90°C).

## 2.1. Introduction

Nanofiltration of organic solvents for solvent recovery is an ideal solution in the quest for more sustainable processes in the pharmaceutical, biochemical, and petrochemical industry. The main driver for applying nanofiltration is that it consumes less energy compared to other separation technologies, such as evaporation and distillation. However, industrial application of this technology demands a robust membrane that is able to endure an aggressive environment such as a continuous exposure towards organic solvents. In order to make the application of solvent nanofiltration technically feasible, a hydrophobic and chemically stable membrane with nanofiltration properties is required.

Membranes have been developed for several decades using polymers as a main ingredient (1). Polymers are relatively inexpensive materials and are available with a wide variety of functional groups. They are frequently used as Solvent Resistance Nanofiltration (SRNF) membranes (2-3). However, currently used SRNF polymeric membranes, such as those made from PDMS (polydimethylsiloxane) (4), PPSU (polyphenylsulfone) (5), and chitosan (6), were reported to swell significantly in organic solvents, like toluene, diethylether, acetone, methylene chloride, hexane, ethyl acetate, methanol, ethanol, isopropanol, or methyl ethyl ketone (4-6). A loss in nanofiltration performance of these membranes due to swelling was observed after several hours in contact with these organic solvents (3, 7-9). A need for nanofiltration membranes with less swelling towards organic solvents therefore emerged.

Ceramic membranes exhibit a high chemical stability towards organic solvents (10-11). In addition to this ceramic membranes are also mechanically stable under operational pressures of up to at least 20 bars (10), in which most polymers will severely suffer from compaction. Despite these superior characteristics, ceramic membranes are not suitable for the nanofiltration of nonpolar solvents, because the hydroxyl (OH-) groups on the ceramic pore walls hinder the permeation of organic solvents in the nanofiltration regime (12).

A new type of membrane showing 1) high chemical stability, 2) suitable wettability properties, 3) high permeability and selectivity, and 4) non-swelling and non-compressible, is expected to be interesting for organic solvent nanofiltration applications. To achieve this aim, a method is proposed, in which applying a polymer inside the pores of a ceramic

material can provide a win-win solution to obtain in this way a hydrophobic and chemically stable membrane. A mesoporous ceramic, as non-swelling and non-compressible porous material, is rendered suitable to provide a rigid support for polymeric materials grafted inside their pores. If the polymer is confined in the perimeter of the ceramic pores, swelling can be brought to a minimum (being the space left inside the pores as the maximum swelling limit). Besides, the ceramic pore will act as a rigid cylindrical spine which will restrain the movement of the grafted polymers from compaction when high pressures are introduced to the membrane system.

A suitable polymeric material grafted on the ceramic pore walls can give a hydrophobic character to the porous ceramic support, thus allowing better wettability for organic solvents. The effective pore size of the ceramic membrane is reduced, thus increasing the selectivity of the membrane. In this way a porous UF ceramic membrane can be changed into a NF membrane we intended. In the work, as described in this paper, a ceramic membrane is used with a pore size as small as possible but sufficiently large to graft a (small) polymer on the pore walls in order to have the largest benefit of the rigid character of a ceramic membrane system, while changing the hydrophilic property of the inorganic membrane in a hydrophobic structure. Polymer grafting is a process in which a specific organic substance is chemically bonded to an inorganic substrate. The OH- groups of the oxide ceramic surface will react with the hydrolysable groups of the to-be-grafted organic moiety to produce a stable covalent bond.

In literature several examples are given on modification of porous inorganic membranes by grafting for various applications. Leger et al. (13) used silicone oil (viscosity 545 mPa) to graft the surface of alumina membranes with a pore size of 5 nm used for gas permeation and pervaporation. The membrane was shown to be chemically stable in toluene, acetone and THF. Faibish et al.(14) grafted polyvinylpyrrolidone on zirconia membranes for oil-in-water emulsion treatment. Free-radical graft polymerization was used by using a vinyl silane as linker to the zirconia membranes. The authors claim a reduction in pore size of around 25 % after grafting but no pore size values are given in this paper. Yoshida et al. (15) grafted  $\gamma$ -alumina (pore size 5 nm) by using vinyl acetate or vinyl pyrrolidone monomers and made a layer of terminally bonded polymer on the surface of the gamma alumina tubular support. In

another paper Yoshida et al. (16) grafted vinyl acetate or vinyl pyrrolidone to silica membranes (pore size of 20 nm) by free radical graft polymerization for pervaporation of methyl-tert-butyl ether from water. Popat et al. (17) grafted polyethylene glycol to straight pore alumina membranes (“anodisc”) using a silane coupling agent. Lee et al. (18) used polyethylene glycol to graft straight pore alumina membranes for the application of anti-fouling membrane for biomolecules. The pore size of the bare alumina, used in (17) and (18), are in the order of 25 - 80 nm, while the grafted membranes are in the ultra-filtration range. Pinheiro et al. (19) developed nanofiltration membranes by grafting PDMS in  $\gamma$ -alumina porous supports (pore size 5 nm) using aminopropylethoxysilane (APTES) as the linker and (mono(2,3-epoxy) polyetherterminated polydimethylsiloxane with an average number of repeating monomers (n) of 10 and a viscosity of 10-50 mPa.

The work described in this paper is on grafting a mesoporous (pore size 5 nm)  $\gamma$ -alumina layer, supported on macro porous  $\alpha$ -alumina, with 3-mercaptopropyltriethoxysilane (MPTES) as linking agent. Subsequently, the system is grafted with monovinyl-terminated polydimethylsiloxane (PDMS) in order to generate a membrane for solvent nanofiltration. The grafting behaviour of the organic moieties on the  $\gamma$ -alumina was studied by Fourier Transform Infrared spectroscopy (FTIR). Contact angle measurements and solvent permeability tests were used to determine the membrane properties. Chemical stability tests in toluene at elevated temperatures were performed as well.

## 2.2. Experimental procedure

Anhydrous toluene was obtained from Sigma-Aldrich. 3-mercaptopropyltriethoxysilane (MPTES) was purchased from Fluka. Monovinyl terminated polydimethylsiloxane (PDMS) was purchased from ABCR with an average number of repeating monomers (n) of 39 and a viscosity of 80-100 mPa.s. An azobisisobutyronitrile catalyst was purchased from Sigma Aldrich. All chemicals were used as received. Flat  $\alpha$ -Al<sub>2</sub>O<sub>3</sub> supported  $\gamma$ -Al<sub>2</sub>O<sub>3</sub> membranes with a diameter of 39 mm were purchased from Pervatech. The mean pore diameter of the 3  $\mu$ m thick  $\gamma$ -Al<sub>2</sub>O<sub>3</sub> layer and the 1.7 mm thick  $\alpha$ -Al<sub>2</sub>O<sub>3</sub> support were 5 nm and 80 nm, respectively (20-21).

The unmodified  $\gamma$ -Al<sub>2</sub>O<sub>3</sub> membranes were soaked in an ethanol/water (2:1) solution for 24 hours at ambient temperature to remove dust and provide suitable hydroxylation. The membranes were then dried at 100°C for 24 hours under vacuum and stored at room temperature under nitrogen atmosphere until further use.

Inside a glove box, under nitrogen atmosphere, a 100 ml solution of 12.5 mM MPTES in anhydrous toluene was prepared in a 500 ml five-necked round flask. A soaked and dried  $\gamma$ -Al<sub>2</sub>O<sub>3</sub> membrane was placed in a sample holder located a few centimetres above the MPTES solution. The solution was stirred and heated to perform the grafting reaction between MPTES vapour and  $\gamma$ -Al<sub>2</sub>O<sub>3</sub> at 80°C for 4 hours under nitrogen flow. Details on this Vapour Phase Deposition (VPD) method are given elsewhere (22-23). After 4 hours the reaction mixture was allowed to cool down. Immediately after the cooling down, the membrane was retrieved from the sample holder and rinsed with toluene and dried under vacuum at 100°C for 24 hours.

PDMS was grafted on the MPTES linker by a Solution Phase Deposition (SPD) method. A 100 ml solution of 12.5 mM PDMS in toluene was prepared in a 500 ml five-necked round flask. The MPTES-grafted  $\gamma$ -Al<sub>2</sub>O<sub>3</sub> membrane was then immersed into the PDMS /toluene solution on a sample holder and kept in the solution throughout the reaction. As catalyst, 5% (n/n) Azobisisobutyronitrile (ABN) was added. The grafting reaction between monovinyl terminated PDMS and the MPTES-grafted  $\gamma$ -Al<sub>2</sub>O<sub>3</sub> was carried out under continuous stirring at 70°C for 24 hours under nitrogen flow. After 24 hours the reaction mixture was allowed to cool down. The membrane was then retrieved from the mixture and soaked overnight in toluene to remove any physically adsorbed PDMS. The membrane was further rinsed by isopropanol and ethanol before drying under vacuum at 100°C for 24 hours.

In order to study the grafting performance of  $\gamma$ -Al<sub>2</sub>O<sub>3</sub> by means of FTIR, porous  $\gamma$ -Al<sub>2</sub>O<sub>3</sub> flakes were used as starting inorganic material. The  $\gamma$ -Al<sub>2</sub>O<sub>3</sub> flakes were prepared from a boehmite sol which was dried and calcined at 650°C for 3 hours at a heating rate of 1°C/min. To remove dust and provide suitable hydroxylation, the  $\gamma$ -Al<sub>2</sub>O<sub>3</sub> flakes were soaked in an ethanol/water (2:1) solution for 24 hours at ambient temperature. The flakes were then dried at 100°C for 24 hours under vacuum and stored under nitrogen atmosphere prior to



grafting. Grafting of the  $\gamma$ -Al<sub>2</sub>O<sub>3</sub> flakes was performed as follows. Inside a glove box, under nitrogen atmosphere, a 100 ml solution of 12.5 mM MPTES in anhydrous toluene was prepared in a 250 ml two-necked round flask. The round flask was removed from the glove box and connected with a glass tube to another 250 ml round flask where 600 mg of  $\gamma$ -Al<sub>2</sub>O<sub>3</sub> flakes were placed. Both flasks were heated at 80°C for 4 hours under nitrogen flow to allow the grafting reaction between MPTES vapor and  $\gamma$ -Al<sub>2</sub>O<sub>3</sub>. Details on this vapor phase deposition (VPD) method are given elsewhere (22-23). After 4 hours, both flasks were cooled to ambient temperature. Immediately after, the modified flakes were retrieved and rinsed 3 times in toluene to remove any physically absorbed MPTES. The flakes were further dried for 24 hours at 100°C under vacuum.

PDMS was grafted on the MPTES linker by a solution phase deposition (SPD) method. A 100 ml solution of 12.5 mM PDMS in toluene was prepared in a 250 ml two-necked round flask. The MPTES-grafted  $\gamma$ -Al<sub>2</sub>O<sub>3</sub> flakes were then immersed into the PDMS/toluene solution and kept stirred in the solution throughout the reaction. 5% of ABN catalyst was added. The grafting reaction between monovinyl terminated PDMS and the MPTES-grafted  $\gamma$ -Al<sub>2</sub>O<sub>3</sub> was carried out at 70°C for 24 hours under nitrogen flow. After 24 hours the reaction mixture was allowed to cool down. Immediately after, the flakes were retrieved from the mixture and centrifuged 3 times in toluene to remove any physically adsorbed MVPDMS. The flakes were further dried at 100°C for 24 hours under vacuum.

### *Characterization*

FTIR analysis was performed using a Bruker Optik GmbH Tensor 27 TGA-IR spectrometer equipped with a universal ATR polarization accessory. The FTIR spectra were recorded at room temperature over a scanning range of 600-4000 cm<sup>-1</sup> with a resolution of 4.0 cm<sup>-1</sup>. The grafted  $\gamma$ -Al<sub>2</sub>O<sub>3</sub> powder sample is considered to have the same chemical characteristics as the actual  $\gamma$ -Al<sub>2</sub>O<sub>3</sub> membrane and therefore can be used to describe the chemical reactions that occur between ceramic membrane and grafting agent.

Contact angles were measured by the sessile drop method to evaluate the hydrophobicity of the membrane after the modification was carried out. 5  $\mu$ L *Millipore Q2* water was dropped at a speed of 2  $\mu$ L s<sup>-1</sup> on a membrane surface using a *Hamilton Microliter* syringe. The water

contact angle data were collected by a Data Physics Optical Contact Angle instrument (OCA 20).

Toluene permeation tests were carried out at room temperature using a dead-end pressure cell made from stainless steel. Three different membrane samples were analysed to ensure reproducibility. Prior to the solvent permeation test the membranes were soaked for preconditioning in the organic solvent for 12 hours. The cell was filled with the solvent and helium was used to pressurize the cell. Permeate fluxes were obtained by measuring the weight of the collected permeate as a function of time. The membrane permeability was calculated in  $\text{L}\cdot\text{m}^{-2}\cdot\text{hr}^{-1}\cdot\text{bar}^{-1}$  unit according to the equation below:

Permeability =  $J/\Delta P$  where  $J = V/A\cdot t$ ,

$J$  is the flux in  $\text{L}\cdot\text{m}^{-2}\cdot\text{hr}^{-1}$ ,  $V$  is the permeate volume in L,  $A$  is the effective membrane surface area in  $\text{m}^2$ ,  $t$  is the permeation period in hr, and  $\Delta P$  is the trans-membrane pressure in bar.

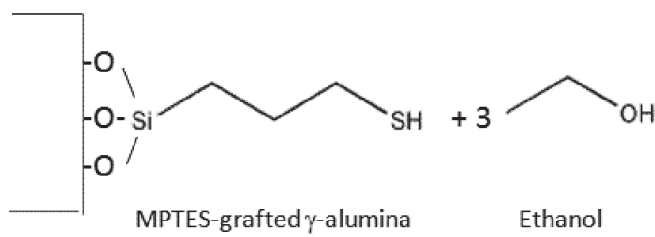
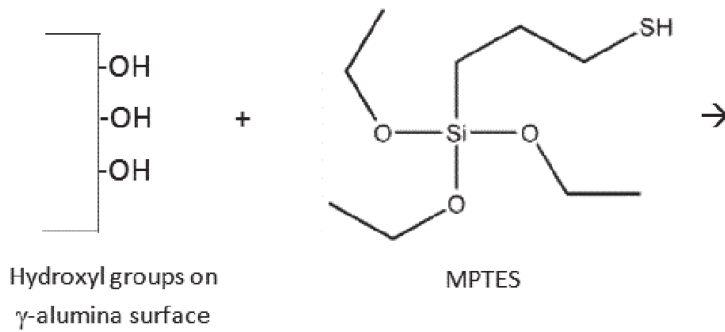
Chemical stability tests were done by immersing 0.1 gr of grafted  $\gamma\text{-Al}_2\text{O}_3$  powders into 40 ml of toluene for 6 days at 30, 60, 80 or 90°C under continuous stirring. After immersion, the system was cooled down to room temperature and retrieved from the solvent by centrifuge. The retrieved powder was three times washed by centrifuging with respectively ethanol and water and subsequently dried in the vacuum oven. Afterwards FTIR analysis were done to check whether there is any degradation of membrane material, marked by appearance of new bands or absence of characteristic absorption bands as compared to the FTIR spectra of freshly-grafted powders.

## **2.3. Results and Discussion**

### **2.3.1. Chemical Reaction Background**

In this work chemical grafting was carried out using two consecutive steps. The first step was the attachment of 3-mercaptopropyl-triethoxysilane (MPTES) onto the pore wall of the gamma-alumina. The grafting reaction between the  $\gamma\text{-Al}_2\text{O}_3$  pore surface and MPTES is depicted in step 1 of Figure 2.1.

Step 1:



Step 2:

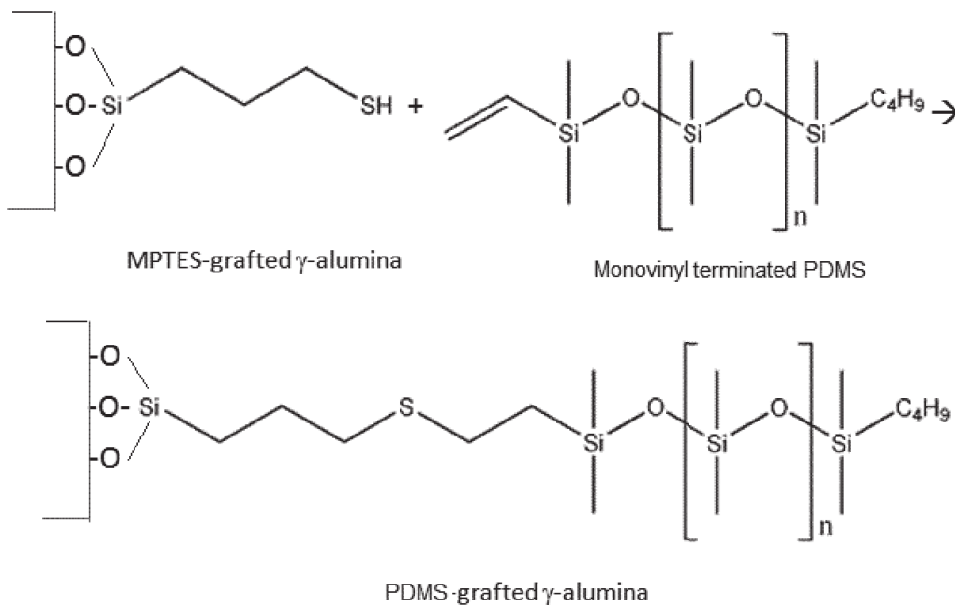


Figure 2.1. Proposed grafting reactions; step 1 grafting of the linker MPTES; step 2: grafting of MVPDMS

The hydroxyl groups on the  $\gamma$ -alumina surface act as the active sites for the grafting reaction. The silylation of the porous ceramic substrate by Vapor Phase Deposition (VPD) provides a

more uniform and homogeneous distribution of products as compared to a Solution Phase Deposition (SPD) method and results in a monolayer or near-monolayer silane coverage on the pore wall (22-23). The grafting reaction proceeds by hydrolysis of the alkoxy groups of the MPTES followed by a condensation reaction upon meeting the hydroxyl groups on the membrane surface, resulting in a stable covalent Al-O-Si bond between the oxide surfaces and the MPTES. In this reaction, moisture from the substrate acts as a catalyst for the hydrolysis (23-24). For the silanes to access the hydroxyl groups on the membrane surface, no more than 2 or 3 monolayers of water should exist on the substrate surface (24). In order to limit the amount of moisture present on the substrate to be grafted, the substrate was kept in nitrogen atmosphere before grafting. To limit the amount of moisture present in the grafting process, the reaction was performed in a dry atmosphere and anhydrous solvents are used.

After this first reaction step, the S-H group from the linker will react with the vinyl group from the Monovinyl terminated polydimethylsiloxane to form a stable S-C bond. PDMS was chosen due to its highly hydrophobic character and good chemical stability towards organic solvents (25). Upon successful grafting, the grafted polydimethylsiloxane will act as a hydrophobic pillow that will enhance the permeation of nonpolar organic solvents through the membrane pores. The reaction between the MPTES-grafted  $\gamma$ -Al<sub>2</sub>O<sub>3</sub> membrane and monovinyl terminated PDMS is represented in step 2 of Figure 2.1. It is a thiol-ene reaction which involves the reaction of a S-H with a double bond. Thiol-ene reactions are efficient since it produces high yields and the resulting chemical bond is stable in various solvents (26).

### 2.3.2. FTIR

Figure 2.2 shows the FTIR absorbance spectra of unmodified, silane-grafted and polymer-grafted  $\gamma$ -Al<sub>2</sub>O<sub>3</sub> powders. Figure 2.2a shows the spectrum of the unmodified  $\gamma$ -Al<sub>2</sub>O<sub>3</sub> powder. For the silane-grafted powder spectrum (Figure 2.2b), the characteristic absorption peaks at 1060 and 700 cm<sup>-1</sup> are attributed to the covalent Si-O-Al bonds (27-28) confirming that grafting of the linker, MPTES, on the  $\gamma$ -Al<sub>2</sub>O<sub>3</sub> powder has occurred.

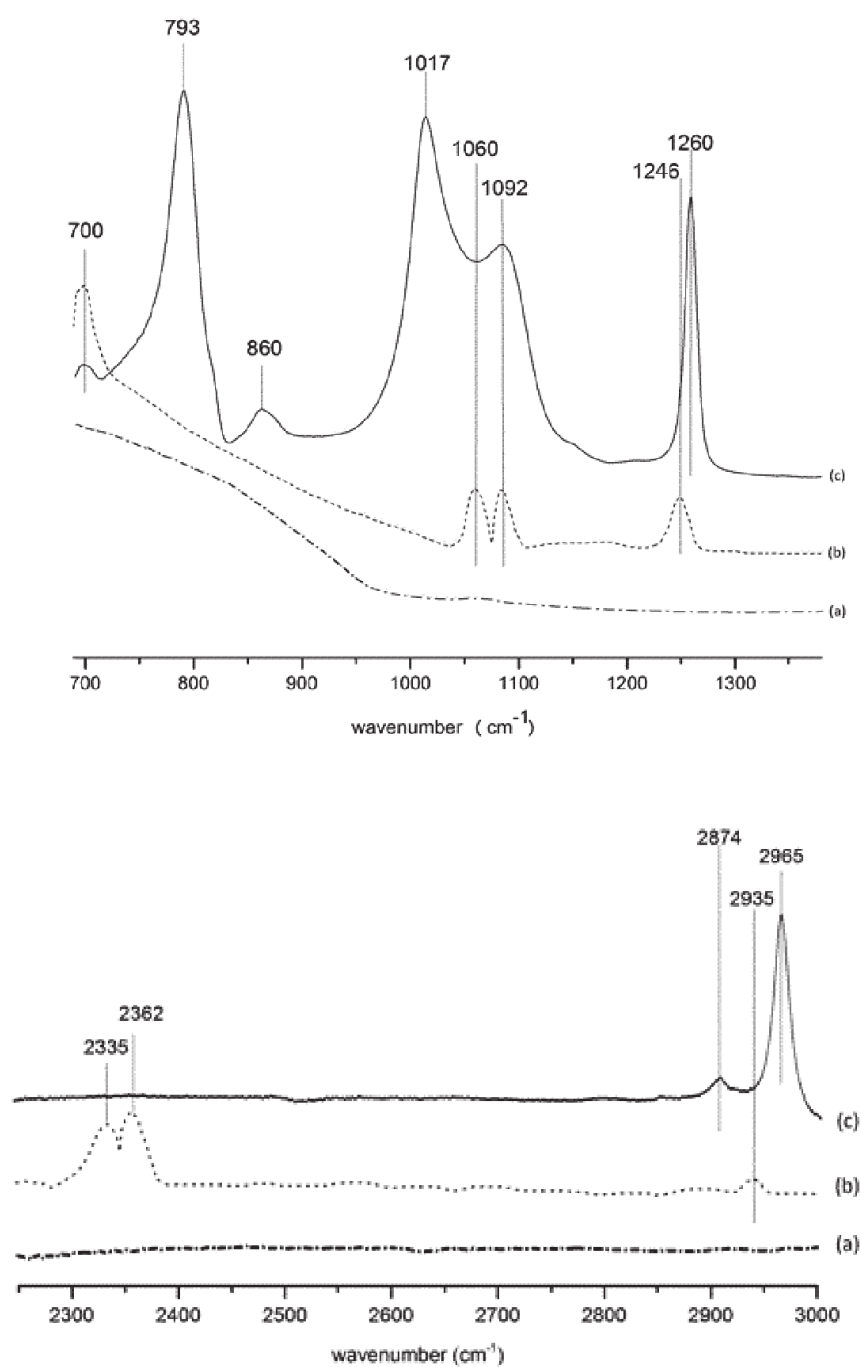


Figure 2.2. FTIR absorbance spectra of a) unmodified  $\gamma$ - $\text{Al}_2\text{O}_3$  powder b) MPTES-grafted  $\gamma$ - $\text{Al}_2\text{O}_3$  powder and c) MVPDMS-MPTES-grafted  $\gamma$ - $\text{Al}_2\text{O}_3$  powder

The peaks at 2335 and 2362  $\text{cm}^{-1}$  in Figure 2.2b are ascribed to S-H stretching of the thiol (SH-) groups from the MPTES-grafted  $\gamma$ - $\text{Al}_2\text{O}_3$  powder (29). During the grafting reaction, not all three functional alkoxy groups from the MPTES might react with the surface -OH groups. One or more hydrolysable groups out of total three functional alkoxy groups that are present

at MPTES may also react with one of the silanols from the adjacent MPTES forming a siloxane network. The reaction of silanols with the surface hydroxyl groups on the ceramic surface and the adjacent silanols can happen at the same time, creating Si-O-Si bonds that are apparent by the peak at  $1092\text{ cm}^{-1}$  (30). The polycondensation reaction between two silanols occurs through the reaction:



The peak at  $2935\text{ cm}^{-1}$  is ascribed to the asymmetric stretching of  $\text{CH}_2$  from the propyl groups of the grafted silanes (31). The peak at  $1246\text{ cm}^{-1}$  is assigned to the  $\text{CH}_2$  wagging of the  $\text{Si}(\text{CH}_2)$  groups of the grafted silanes (31). During the grafting reaction between the MPTES-grafted  $\gamma\text{-Al}_2\text{O}_3$  powder and the MVPDMS polymer, the S-H bond should be broken by forming a covalent S-C bond through a thiol-ene reaction. Clearly the S-H bands at  $2335$  and  $2362\text{ cm}^{-1}$  disappeared after reaction of the linker with MVPDMS as can be seen from Figure 2.2c, confirming the thiol-ene reaction between MPTES and MVPDMS. In the FTIR spectrum of polymer-grafted  $\gamma\text{-Al}_2\text{O}_3$  powder (Figure 2.2c), the peaks at  $2965\text{ cm}^{-1}$  and  $2874\text{ cm}^{-1}$  are ascribed to C-H asymmetric stretching and symmetric stretching of methyl ( $\text{CH}_3$ -) groups of PDMS (31). A strong peak at  $1260\text{ cm}^{-1}$  is caused by symmetric C-H bending and peaks at  $860$  and  $793\text{ cm}^{-1}$  are caused by Si-C vibration and  $\text{CH}_3$  rocking from the  $\text{SiCH}_3$  group (30). The two peaks at  $1092$  and  $1017\text{ cm}^{-1}$  are ascribed to the Si-O-Si bond (30-31). These peaks at  $793$ ,  $1017$ ,  $1092$ ,  $1260\text{ cm}^{-1}$  and  $2965\text{ cm}^{-1}$  confirm the presence of polydimethylsiloxane groups on the PDMS-grafted  $\gamma\text{-Al}_2\text{O}_3$  powder (23, 30-31). Figure 2.3 shows a schematic illustration of the possible structure resulted from the overall reaction between linker and alumina and respectively between linker and PDMS.

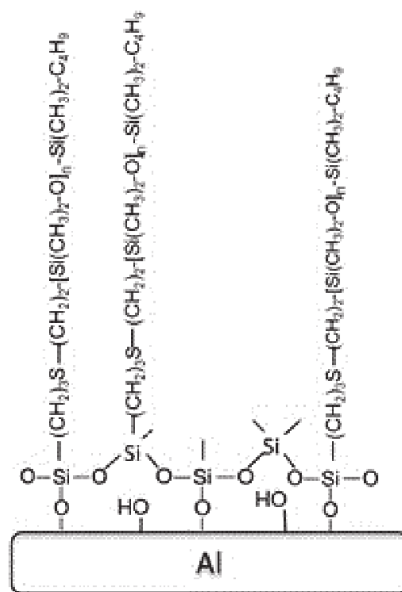


Figure 2.3. Schematic illustration of the possible structure resulted from the overall reaction between linker and alumina and respectively between linker and PDMS.

It can be concluded from these FTIR analysis that the grafting reaction between  $\gamma$ -alumina and MPTES and subsequently with a monovinyl terminated PDMS is successfully performed.

### 2.3.3. Contact Angle

Table 2.1 shows the measured contact angles of the unmodified, silane-grafted, and PDMS-grafted  $\gamma$ -Al<sub>2</sub>O<sub>3</sub> membranes. The observed change in the contact angles represents the change of the surface properties of the modified membrane relative to those of the unmodified substrate. The contact angle measurements were taken from 5 different points on the flat membrane surface and averaged. The negligible standard deviation shows that grafting reaction has occurred homogeneously over the membrane surface.

Table 2.1. Water contact angles (°) of unmodified, MPTES and MPTES-PDMS grafted  $\gamma$ -Al<sub>2</sub>O<sub>3</sub> membranes

	Unmodified ( $\gamma$ -Al <sub>2</sub> O <sub>3</sub> membrane)	After silylation with MPTES	After PDMS Grafting
Contact Angle (°)	0	44 ± 2	95 ± 1

For the unmodified gamma-alumina membrane, the water droplet immediately wetted the membrane surface. A corresponding water contact angle of 0° is therefore assumed, indicating the hydrophilic characteristic of the  $\gamma\text{-Al}_2\text{O}_3$  membrane due to natural presence of hydroxyl (OH-) groups on the ceramic surface. In general, an increase in contact angle was observed after modification of  $\gamma\text{-Al}_2\text{O}_3$  membranes with MPTES and PDMS.

A higher contact angle observed after modification with MPTES might be attributed to the presence of the thiol group and the hydrophobic propyl group after modification of  $\gamma\text{-Al}_2\text{O}_3$  with MPTES. Thiol (SH-) groups are less polar than hydroxyl (OH-) groups, causing a weaker attraction between the water droplet and the MPTES-grafted  $\gamma\text{-Al}_2\text{O}_3$  membrane, and thus a comparatively higher contact angle.

A further increase in contact angle was observed after modification with PDMS. The higher contact angle might be attributed to the nonpolarity of the dimethylsiloxane groups. There are more potential sources contributing to the actual contact angle value measured, such as the nanotextures of the grafted moieties depending on the molecule orientation and grafting density of the grafted moieties, in combination with the presence of the pores. For a comparison, the modification of  $\gamma$ -alumina membranes with a mono-epoxy-terminated PDMS (n=10), using an aminosilane as the linker, resulted in contact angle values ranging from 91 to 97 degrees (23).

#### 2.3.4. Permeation

Permeation tests were conducted on the unmodified and modified membranes, using toluene as a probe solvent to assess the membrane permeability after grafting with PDMS. The toluene permeability of the unmodified and modified  $\gamma$ -alumina membranes are shown in Table 2.2.

Table 2.2. Toluene permeability of unmodified, MPTES and MPTES-PDMS grafted  $\gamma\text{-Al}_2\text{O}_3$  membranes. Average values and standard deviations are given for measurements on three different membranes.

	Unmodified	After PDMS Grafting
Toluene permeability, $\text{L}\cdot\text{m}^{-2}\cdot\text{h}^{-1}\cdot\text{bar}^{-1}$	5.80±0.11	2.09±0.13



From Table 2.2, it can be seen that the toluene permeability is lower after grafting with PDMS. The improvement of wettability properties should have led to higher fluxes of toluene if we assumed that the membrane pore size is constant before and after grafting. However, lower toluene permeability was observed after grafting with PDMS. The lower permeability observed is attributed to the membrane pore size reduction due to the presence of the grafted molecules. In such cases, overall reduction of fluxes may be the result when the flux decrease due to the pore size reduction is more significant than the flux improvements due to better surface wettability. In this work, three membranes were grafted separately using the same grafting procedure. The standard deviations, given in Table 2.2, were calculated from the average values of the toluene permeability of three membranes. It was demonstrated that this method of grafting results in membranes with high reproducibility.

In order to examine whether the way of applying subsequent trans membrane pressures (TMP) affects the flux, permeation tests were performed in two different orders, starting from the lowest and going to the highest TMP and subsequently from the highest to the lowest TMP (see Figure 2.4). No significant differences in fluxes were observed for ascending or descending TMP permeation tests. Thus no irreversible effects towards pressure are present in the tested trans-membrane pressure range.

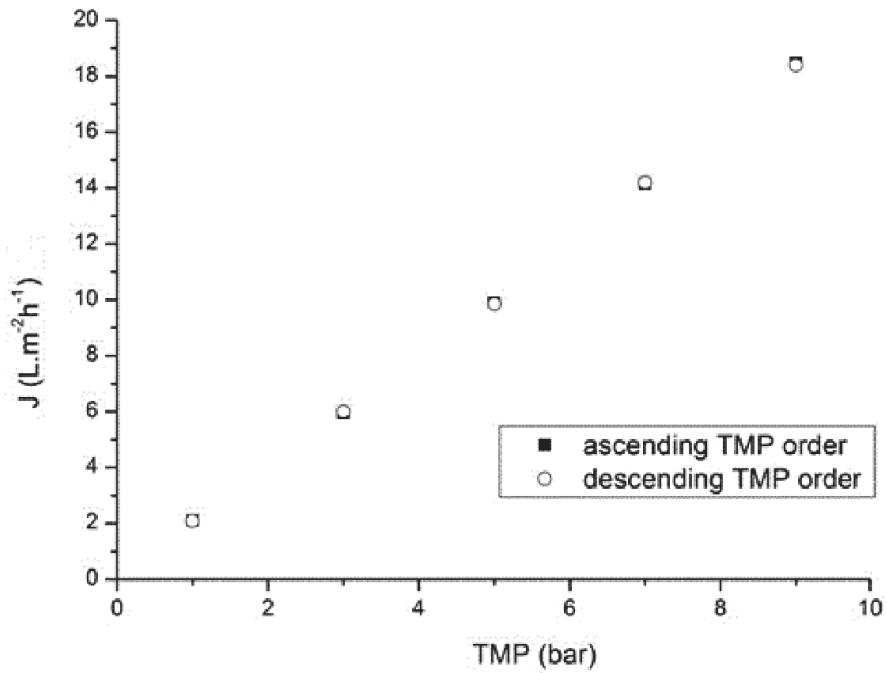


Figure 2.4. Flux (J) as a function of Trans Membrane Pressure (TMP) at room temperature

An estimation of the pore radius of the modified membrane can be obtained by using the simple pore capillary model (32). For a steady-state system, where the solvent is incompressible, a simple capillary model for the pore geometry can be derived:

$$\frac{r_{\text{modified}}}{r_{\text{unmodified}}} = \sqrt{\frac{(L\eta)_{\text{modified}}}{(L\eta)_{\text{unmodified}}}} \quad (1)$$

where  $r_{\text{modified}}$  and  $r_{\text{unmodified}}$  are the mean pore radii of the modified and unmodified  $\gamma\text{-Al}_2\text{O}_3$  membranes,  $L_{\text{modified}}$  and  $L_{\text{unmodified}}$  are the permeabilities of toluene for the modified and unmodified membranes in  $\text{L.m}^{-2}.\text{hr}^{-1}.\text{bar}^{-1}$ , and  $\eta_{\text{modified}}$  and  $\eta_{\text{unmodified}}$  are the toluene viscosity.

The mean pore radius of the unmodified  $\gamma\text{-Al}_2\text{O}_3$  membrane is 2.5 nm, as determined by permoporometry [13]. The values of  $L_{\text{modified}}$  and  $L_{\text{unmodified}}$  are respectively 2.1 and 5.8  $\text{L.m}^{-2}.\text{hr}^{-1}.\text{bar}^{-1}$ . By applying these data in equation (1) a pore radius of 1.5 nm is calculated for the PDMS modified membrane. In this model any possible interactions between solvent and the respective membranes are not taken into account. This implies that in the case of negligible interfacial tension differences between the reference and the system in question, the estimated pore radius value of 1.5 nm might hold. However, the PDMS-modified

membrane is much more hydrophobic than the pure  $\gamma\text{-Al}_2\text{O}_3$  and it is therefore expected that there is less interfacial tension between the toluene and the grafted PDMS. So, the estimation method as used over here is expected to give a maximum value of the pore radius for the PDMS-modified membrane. The same calculation for the  $\gamma$ -alumina membranes grafted with a mono-epoxy-terminated PDMS ( $n=10$ ), using an aminosilane as the linker from Pinheiro et al. work (23) gave a maximum pore radius of 1.83 nm, with  $L_{\text{modified}}$  and  $L_{\text{unmodified}}$  of 3.1 and 5.9  $\text{L}\cdot\text{m}^{-2}\cdot\text{hr}^{-1}\cdot\text{bar}^{-1}$ .

### 2.3.5. Chemical stability

The chemical stability of the membrane material in toluene was analyzed on  $\gamma\text{-Al}_2\text{O}_3$  flakes grafted with only MPTES and flakes grafted with MPTES and PDMS. If the chemical bond between the grafting agents and the  $\gamma\text{-Al}_2\text{O}_3$ , was not stable then toluene, used as solvent for grafting the membranes, would likely wash away the grafting agents. The FTIR spectra of the MPTES grafted  $\gamma\text{-Al}_2\text{O}_3$  powder immersed in toluene at different temperatures (30 - 90°C) are shown in Figure 2.5.

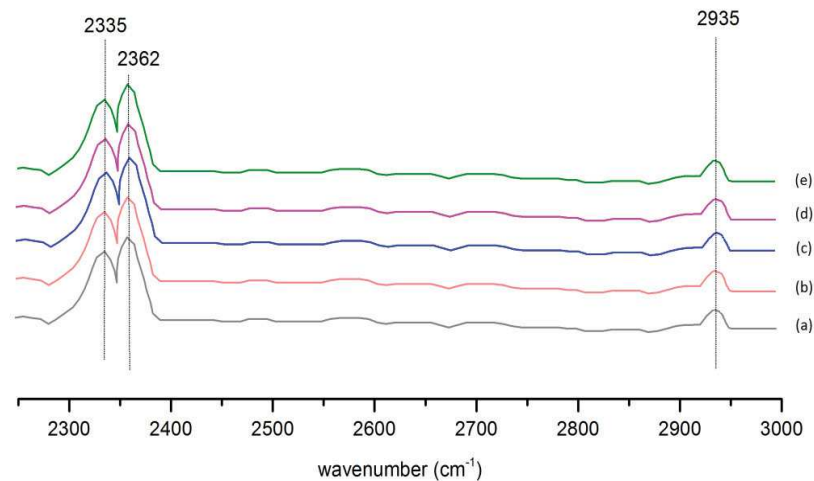


Figure 2.5. FTIR Absorbance Spectra of MPTES-grafted  $\gamma\text{-Al}_2\text{O}_3$  powders soaked in toluene at different temperatures for 6 days: a) no immersion, b)30°C, c)60°C, d)80°C, e)90°C

From these chemical stability tests, it was observed that the MPTES grafted  $\gamma\text{-Al}_2\text{O}_3$  powder immersed in toluene at all temperatures showed no changes in FTIR spectra. The characteristic bands of S-H at 2335 and 2362  $\text{cm}^{-1}$  were still present with no change in

intensity. It was demonstrated that continuous stirring for 6 days cannot dissolve the MPTES that has been grafted onto the  $\gamma$ -Al<sub>2</sub>O<sub>3</sub> powder. This is only possible if a stable covalent bond is present between the grafted moiety and the  $\gamma$ -Al<sub>2</sub>O<sub>3</sub> surface.

Figure 2.6 shows the FTIR Spectra of the PDMS-grafted  $\gamma$ -Al<sub>2</sub>O<sub>3</sub> powder after being immersed in toluene at different temperatures (30 - 90°C) for 6 days.

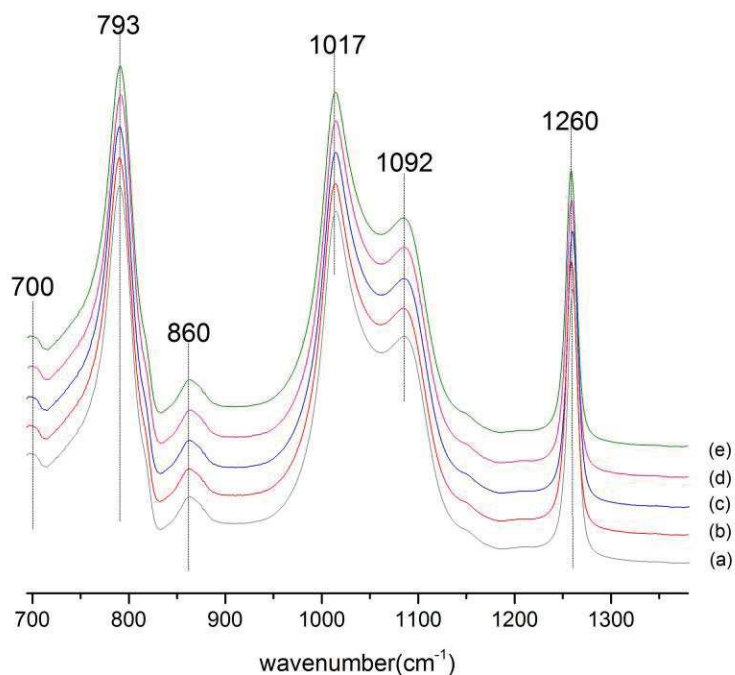


Figure 2.6. FTIR Absorbance Spectra of MVPDMS-grafted  $\gamma$ -Al<sub>2</sub>O<sub>3</sub> powders immersed in toluene at different temperatures for 6 days: a) no immersion, b)30°C, c)60°C, d)80°C, e)90°C

Pure PDMS easily dissolves in toluene (33). If PDMS is only physically adsorbed on the ceramic powder, the grafted material will easily be washed away by toluene. The characteristic absorption peaks at 793, 1092, 1017, 1260 cm<sup>-1</sup> of the PDMS-grafted  $\gamma$ -Al<sub>2</sub>O<sub>3</sub> powders were still present without any decrease in intensity, demonstrating that the grafted material can maintain its integrity even after long term exposure of toluene at elevated temperatures. From the chemical stability tests it can be concluded, that no degradation of the membrane material was found, demonstrating the potential use of these membranes in solvents like toluene at elevated temperatures.

## 2.4. Conclusion

A method of grafting a mesoporous  $\gamma$ -alumina layer, supported on macro porous  $\alpha$ -alumina, with 3-mercaptopropyltriethoxysilane (MPTES) as linking agent and subsequently with Monovinyl terminated polydimethylsiloxane (PDMS) as polymer grafted to this linker was presented. It was shown that this method of grafting resulted in stable covalent bonds between the PDMS, MPTES, and  $\gamma$ -alumina. Contact angle measurements have shown that this method of grafting renders the  $\gamma$ -Al<sub>2</sub>O<sub>3</sub> substrate into hydrophobic properties. The grafting method described in this paper resulted in a hydrophobic and chemically stable membrane for potential use as chemical and thermal stable organic solvent nanofiltration membranes.

## Acknowledgement

The authors would like to thank the European Union – The Education, Audiovisual and Culture Executive Agency (EACEA) under the Program “ Erasmus Mundus Doctorate in Membrane Engineering” – EUDIME (FPA 2011-2014) for funding this research.

## References

1. Mulder, M. (1996) *Basic principles of membrane technology*, 2nd ed., Kluwer Academic Publisher, Netherlands.
2. Bhanushali, D., Kloos, S., Kurth, C., and Bhattacharyya, D. (2001) Performance of solvent-resistant membranes for non-aqueous systems: Solvent permeation results and modeling, *Journal of Membrane Science* 189, 1-21.
3. Vandezande, P., Gevers, L. E. M., and Vankelecom, I. F. J. (2008) Solvent resistant nanofiltration: Separating on a molecular level, *Chemical Society Reviews* 37, 365-405.
4. Van der Bruggen, B., Geens, J., and Vandecasteele, C. (2002) Influence of organic solvents on the performance of polymeric nanofiltration membranes, *Separation Science and Technology* 37, 783-797.
5. Darvishmanesh, S., Jansen, J. C., Tasselli, F., Tocci, E., Luis, P., Degrève, J., Drioli, E., and Van der Bruggen, B. (2011) Novel polyphenylsulfone membrane for potential use in solvent nanofiltration, *Journal of Membrane Science* 379, 60-68.

6. Musale, D. A., and Kumar, A. (2000) Solvent and pH resistance of surface crosslinked chitosan/poly(acrylonitrile) composite nanofiltration membranes, *Journal of Applied Polymer Science* 77, 1782-1793.
7. Darvishmanesh, S., Degrè, J., and Bruggen, B. V. D. (2010) Performance of solvent-pretreated polyimide nanofiltration membranes for separation of dissolved dyes from toluene, *Industrial and Engineering Chemistry Research* 49, 9330-9338.
8. Tarleton, E. S., Robinson, J. P., and Salman, M. (2006) Solvent-induced swelling of membranes - Measurements and influence in nanofiltration, *Journal of Membrane Science* 280, 442-451.
9. Van der Bruggen, B., Geens, J., and Vandecasteele, C. (2002) Fluxes and rejections for nanofiltration with solvent stable polymeric membranes in water, ethanol and n-hexane, *Chemical Engineering Science* 57, 2511-2518.
10. Buekenhoudt, A. (2008) *Stability of Porous Ceramic Membranes*, Vol. 13, Elsevier B.V., Belgium.
11. Van Gestel, T., Vandecasteele, C., Buekenhoudt, A., Dotremont, C., Luyten, J., Van Der Bruggen, B., and Maes, G. (2003) Corrosion properties of alumina and titania NF membranes, *Journal of Membrane Science* 214, 21-29.
12. Tsuru, T., Sudou, T., Kawahara, S. I., Yoshioka, T., and Asaeda, M. (2000) Permeation of liquids through inorganic nanofiltration membranes, *Journal of Colloid and Interface Science* 228, 292-296.
13. Leger, C., De Lira, H. L., and Paterson, R. (1996) Preparation and properties of surface modified ceramic membranes. Part II. Gas and liquid permeabilities of 5 nm alumina membranes modified by a monolayer of bound polydimethylsiloxane (PDMS) silicone oil, *Journal of Membrane Science* 120, 135-146.
14. Faibish, R. S., and Cohen, Y. (2001) Fouling-resistant ceramic-supported polymer membranes for ultrafiltration of oil-in-water microemulsions, *Journal of Membrane Science* 185, 129-143.
15. Yoshida, W., and Cohen, Y. (2003) Ceramic-supported polymer membranes for pervaporation of binary organic/organic mixtures, *Journal of Membrane Science* 213, 145-157.
16. Yoshida, W., and Cohen, Y. (2004) Removal of methyl tert-butyl ether from water by pervaporation using ceramic-supported polymer membranes, *Journal of Membrane Science* 229, 27-32.
17. Papat, K. C., Mor, G., Grimes, C. A., and Desai, T. A. (2004) Surface Modification of Nanoporous Alumina Surfaces with Poly(ethylene glycol), *Langmuir* 20, 8035-8041.
18. Sang Won, L., Hao, S., Richard, T. H., Vania, P., and Gil, U. L. (2005) Transport and functional behaviour of poly(ethylene glycol)-modified nanoporous alumina membranes, *Nanotechnology* 16, 1335.

19. Pinheiro, A. F. M., Hoogendoorn, D., Nijmeijer, A., and Winnubst, L. (2014) Development of a PDMS-grafted alumina membrane and its evaluation as solvent resistant nanofiltration membrane, *Journal of Membrane Science* 463, 24-32.
20. Nijmeijer, A., Bladergroen, B. J., and Verweij, H. (1998) Low-temperature CVI modification of  $\gamma$ -alumina membranes, *Microporous and Mesoporous Materials* 25, 179-184.
21. Cuperus, F. P., Bargeman, D., and Smolders, C. A. (1992) Permporometry: the determination of the size distribution of active pores in UF membranes, *Journal of Membrane Science* 71, 57-67.
22. Sripathi, V. G. P., Mojet, B. L., Nijmeijer, A., and Benes, N. E. (2013) Vapor phase versus liquid phase grafting of meso-porous alumina, *Microporous and Mesoporous Materials* 172, 1-6.
23. Pinheiro, A. F. M. (2013) Development and Characterization of Polymer-grafted Ceramic Membranes for Solvent Nanofiltration, In *PhD Thesis*, University of Twente, Enschede.
24. Yoshida, W., Castro, R. P., Jou, J.-D., and Cohen, Y. (2001) Multilayer Alkoxysilane Silylation of Oxide Surfaces, *Langmuir* 17, 5882-5888.
25. Volkov, A. V., Korneeva, G. A., and Tereshchenko, G. F. (2008) Organic solvent nanofiltration: Prospects and application, *Russian Chemical Reviews* 77, 983-993.
26. Rissing, C., and Son, D. Y. (2008) Thiol-ene reaction for the synthesis of multifunctional branched organosilanes, *Organometallics* 27, 5394-5397.
27. Jakobsson, S. (2002) Determination of Si/Al Ratios in Semicrystalline Aluminosilicates by FT-IR Spectroscopy, *Spectroscopy Techniques* 56, 797-799.
28. Sinko K., M. R., Rohonczy, J., Frazl P. (1999) Gel Structures Containing Al(III), *Langmuir* 15, 6631-6636.
29. Patai, S. (1974) *The chemistry of the thiol group*, Ed. Wiley, London.
30. Anderson, D. R. (1974) *Analysis of Silicones*, Wiley-Interscience, New York.
31. Bellamy, L. J. (1975) *The Infra-red Spectra of Complex Molecules*, 3rd ed., Chapman and Hall, London.
32. Dullien, F. A. L. (1992) *Porous Media: Fluid Transport and Pore Structure*, 8-9, Academic Press, New York.
33. Barton, A. F. M. (1990) *CRC Handbook of Polymer-Liquid Interaction Parameters and Solubility Parameters*, CRC Press, US.





# Chapter 3

## Solvent Permeation Behavior of PDMS Grafted $\gamma$ -Alumina Membranes

This chapter has been published as:

Tanardi, C. R., Vankelecom, I. F., Pinheiro, A. F., Tetala, K. K., Nijmeijer, A., & Winnubst, L. (2015). Solvent permeation behavior of PDMS grafted  $\gamma$ -alumina membranes. *Journal of Membrane Science*, 495, 216-225.

## Abstract

Solvent permeability in PDMS grafted ceramic membranes was described by incorporating solvent sorption terms into the Hagen-Poiseuille equation. Two types of ceramic membranes grafted with a relative short or long PDMS chain ( $n=10$  and  $n=39$ ), which differed in pore size, were examined. Sorption was measured "ex situ" using a pure PDMS phase. The results show that the flux differences can be described by incorporating sorption and viscosity differences between the solvents. It is suggested that the membrane permeable volume reduces if a solvent is strongly swelling. This provides an initial way to predict the performance of grafted ceramic membranes for solvent nanofiltration.

### 3.1. Introduction

Solvent resistant nanofiltration (SRNF) or organic solvent nanofiltration (OSN) is a potential separation technology for e.g. the recycling of solvents and the recovery of products from reaction solvents (1). For SRNF, a chemically stable membrane is required to endure the rather aggressive operation environment. Modification of mesoporous ceramic membranes by means of grafting is an interesting way to prepare a chemically stable nanofiltration membrane. In the grafting process, the macromolecules are linked to the membrane surface by a covalent bond, resulting in a chemically stable modified ceramic membrane. The surface wettability of the membrane can be tuned by grafting a suitable polymer with the desired hydrophobicity. In the same time, pore size tuning can be realized by grafting macromolecules inside the ceramic pores.

In literature, several examples are given on modification of porous inorganic membranes by grafting for various applications. Leger et al. (2) used silicone oil (viscosity 545 mPa) to graft the surface of alumina membranes with a pore size of 5 nm for gas permeation and pervaporation. Faibish et al. (3) grafted polyvinylpyrrolidone on zirconia membranes for oil-in-water emulsion treatment. Free-radical graft polymerization was performed by using a vinyl silane as linker to the zirconia membranes. A reduction in pore size of around 25 % after grafting was claimed. Yoshida et al. (4) grafted  $\gamma$ -alumina membranes (pore size 5 nm) by using vinyl acetate or vinyl pyrrolidone monomers. Yoshida et al. (5) grafted vinyl acetate or vinyl pyrrolidone to silica membranes (pore size of 20 nm) by free radical graft polymerization for pervaporation of methyl-tertiary-butyl ether from water. Popat et al. (6) grafted polyethylene glycol to straight pore alumina membranes ("anodisc") using a silane coupling agent. Lee et al. (7) grafted polyethylene glycol to render straight pore alumina membranes for anti-fouling properties. The pore sizes of the bare alumina, used in (6) and (7), are in the order of 25 - 80 nm, while the grafted membranes are still in the ultrafiltration range.

Pinheiro et al. (8) developed nanofiltration membranes by grafting PDMS in the pores of  $\gamma$ -alumina membranes (pore size 5 nm) using aminopropylethoxysilane as the linker and (mono(2,3-epoxy) polyetherterminated polydimethylsiloxane with an average number of repeating monomers (n) of 10 and a viscosity of 10-50 mPa. Tanardi et al. (9) grafted PDMS

with an average number of repeating monomers ( $n$ ) of 39 on the same type of mesoporous (pore size 5 nm)  $\gamma$ -alumina layer, supported on macro porous  $\alpha$ -alumina, with 3-mercaptopropyltriethoxysilane as linker.

Detailed knowledge of major parameters influencing the solvent transport of grafted ceramic membranes is very important in order to predict their permeation behavior for various solvents. Castro et al. (10) studied the effect of different types of solvents on the permeability of an ultrafiltration membrane, prepared by grafting of PVP inside the pores of a macroporous silica support with a native pore diameter of 410 nm. It was found that the permeability of nonpolar solvents, like cyclohexane and toluene, was higher than the permeability of polar solvents, like propanol, water, and ethanol, for the hydrophilic PVP grafted membranes, as opposite to what was expected.

An interesting behavior of modified ceramic membranes prepared via grafting of macromolecules inside the pores is their response towards the applied pressure. Castro et al. (11) observed a shear-rate flow induced behavior of the PVP grafted macroporous ceramic substrate with  $d_{avg}$  of 410 nm due to the mobility of the grafted polymeric chain. The effect of shear rate on the permeability of the grafted membrane was described as a condition in which the membrane is experiencing a more open membrane structure due to the movement of the grafted moieties in the direction of the feed flow, resulting in an exponential increase in the membrane permeability towards the trans-membrane pressure.

In this study, the effect of viscosity, as well as sorption of solvent, on the transport behavior were investigated for two types of grafted membranes with a relative short or long chain of PDMS ( $n=10$  and  $n=39$ ). PDMS was selected as it has been proven to be an excellent material for SRNF applications (8-9, 12-14). The permeability was studied by means of permeation tests at operating pressures between 1 to 20 bar to investigate the effect of trans-membrane pressure on the membrane permeability. Various solvents were used to study the effect of different solvent types on the membrane permeation behavior. Permeation tests at elevated temperature were conducted to study the effect of temperature on the membrane permeability. A model is proposed to describe the permeation of pure solvents through these membranes.

### 3.2. Existing transport models for porous and dense membranes

Two models are generally used to describe solvent transport through membranes (15). The first one is the pore-flow model, in which the membrane is regarded to have defined open pores from the feed side to the permeate side. Darcy's Law, often referred to as the pore-flow or viscous-flow model, describes liquid permeation through porous media as a function of the trans-membrane pressure (TMP):

$$J = \frac{k \Delta P}{\mu l} \quad (3.1)$$

where  $J$  is the solvent flux,  $k$  the permeability constant,  $\mu$  the fluid viscosity,  $\Delta P$  the trans-membrane pressure, and  $l$  the membrane thickness.

For viscous flow, the Darcy's law can be combined with the Hagen–Poiseuille equation:

$$J = k \frac{\Delta P}{\mu} \quad (3.2)$$

with

$$k = \frac{\epsilon r_p^2}{8\tau l} \quad (3.3)$$

where  $J$  is the solvent flux,  $\Delta P$  the trans-membrane pressure,  $\mu$  the solvent viscosity, and  $k$  the membrane permeability constant representing the structural properties of the membrane with  $\epsilon$  the membrane porosity,  $r_p$  the membrane average pore diameter,  $\tau$  the membrane tortuosity, and  $l$  the membrane thickness.

If there are no pores identified in the membrane, the solution-diffusion model is generally used (15). This means that the transport of liquids occurs via free volume elements between polymeric chains which can appear and disappear as a function of time and place according to the movement of the solvent (16). The model assumes that pressure is constant through the membrane and the driving force of solvent transport is the chemical activity difference between the feed and permeate side of the dense membrane. The solution-diffusion equation is as follows:

$$J_i = \frac{D_i K_i}{l} \left[ a_{if} - a_{ip} \exp\left(\frac{-v_i(P_f - P_p)}{R_g T}\right) \right] \quad (3.4)$$

where  $J_i$  represents the solvent flux,  $l$  the membrane thickness,  $D_i$  the diffusion coefficient of solvent or solute  $i$  through the membrane,  $K_i$  the partition coefficient,  $a_{if}$  and  $a_{ip}$  are the

activities of species  $i$  in respectively feed and permeate,  $v_i$  the partial molar volume of specimen  $i$ ,  $P_f$  and  $P_p$  the pressures at feed and permeate side,  $R_g$  the gas constant and  $T$  the temperature. If a pure solvent is used, then the  $a_{if}$  is 1 and  $v_i$  is 1, while the  $a_{ip}$  is 0. Thus, the equation becomes:

$$J_i = \frac{D_i K_i}{l} \left[ 1 - \exp\left(\frac{-(\Delta P - \Delta \pi)}{R_g T}\right) \right] \quad (3.5)$$

where  $\Delta \pi$  stands for the osmotic pressure (17).

When the difference between the applied and osmotic pressure is small, the equation can be written as:

$$J_i = \frac{D_i K_i}{R_g l T} (\Delta P - \Delta \pi) = S_i (\Delta P - \Delta \pi) \quad (3.6)$$

where  $S_i$  is a solvent permeability constant of solvent or solute  $i$ .

The pore-flow and the solution-diffusion models are commonly used for aqueous applications (15, 18-19). For SRNF membranes, both pore-flow and solution-diffusion models have been used in literature to describe the transport behavior of PDMS membranes. Vankelecom et al. (16) found that a viscous flow model can be used to describe the permeation of pure solvents through PDMS membranes by taking into account membrane swelling. This finding was later confirmed by Robinson et al. (20), who successfully used a pore-flow model to describe the transport behavior of PDMS membranes for nonpolar solvents based on the reasoning that the swollen PDMS layer may form a pore-like structure in the presence of nonpolar solvents. Meanwhile, Zeidler et al. (21) observed that a viscous flow behavior was observed for PDMS membranes in the presence of swelling solvents like n-heptane and THF. On the other hand, in the presence of non-swelling solvents, like ethanol, it was proposed that the rejection of PDMS might be closer to that of the solution-diffusion mechanism. Postel et al. (22) used the solution-diffusion model to describe the negative rejections of dye solutes in ethanol by dense PDMS membranes. No prior study is found in the literature to investigate the use of these models for modelling of the transport behavior of grafted ceramic membranes.

### 3.3. Experimental procedures

Three types of membranes were investigated. All membranes were in the form of flat discs with a diameter of 20 mm and a total thickness of 2.5 mm. The first series of membranes (M1) consisted of a mesoporous  $\gamma$ -Al<sub>2</sub>O<sub>3</sub> layer with a pore diameter of 5 nm and 3  $\mu$ m thickness, supported on macroporous  $\alpha$ -Al<sub>2</sub>O<sub>3</sub> supports (23-24). The second series (M2) consisted of macroporous  $\alpha$ -Al<sub>2</sub>O<sub>3</sub> supports, coated with a 3  $\mu$ m thick mesoporous (5 nm)  $\gamma$ -Al<sub>2</sub>O<sub>3</sub> layer, which is modified with 3-aminopropyltriethoxysilane followed by mono(2,3-epoxy)polyetherterminated polydimethylsiloxane (n=10). Details of the membrane fabrication procedures for M2 were described in (8). The third series of membranes (M3) consisted of macroporous  $\alpha$ -Al<sub>2</sub>O<sub>3</sub> supports, coated with a 3  $\mu$ m thick mesoporous (5 nm)  $\gamma$ -Al<sub>2</sub>O<sub>3</sub> layer and further modified with 3-mercaptopropyl triethoxysilane followed by monovinyl terminated polydimethylsiloxane (n=39). Details of the membrane fabrication procedures for M3 were described in (9). SEM-EDX analysis by a Thermo-Noran instrument was used to identify the morphology of the grafted membranes.

Pure solvent flux tests were conducted with different solvents. Octane (98 % purity), cyclooctane (> 99 %), p-xylene (> 99 %), and n-hexane (> 99 %) were purchased from Sigma-Aldrich. Toluene (100 %), ethyl acetate (99.9 %), and isopropanol (100 %) were purchased from VWR. Zeolite A (molecular mesh 4-8 nm) was purchased from Sigma-Aldrich to dry all chemicals. Table 3.1 gives some physical characteristics of these solvents.

Table 3.1. Physical properties of the solvents used for permeability tests (26-31)

Name	Molecular Shape	Viscosity (mPa.s at 20°C)	Dipole Moment (D)	Dielectric Constant ( $\epsilon$ )	Surface Tension (mN/m at 20°C)	Molar volume (cm <sup>3</sup> /mol)	Vapor Pressure (mmHg at 20°C)
Hexane	linear	0.31	0.08	1.89	18	130.58	129.1
Octane	linear	0.54	0	1.95	22	162.49	13.9
Cyclooctane	cyclic	2.13	0	2.12	32	107.91	4.4
p-Xylene	aromatic	0.64	0.07	2.27	29	123.31	7.6
Toluene	aromatic	0.59	0.34	2.38	30	105.91	26.3
Ethyl acetate	branched linear	0.45	1.88	6.02	24	97.68	109.1
Isopropanol	branched linear	2.39	1.66	19.92	21	76.90	78.2

Permeability tests were performed using a high pressure dead-end stainless steel permeation set-up at operating pressures between 1 to 20 bar (25). The cell was filled with solvent and nitrogen was used to pressurize the cell. Permeate fluxes ( $J$  in  $\text{L}\cdot\text{m}^{-2}\cdot\text{h}^{-1}$ ) were obtained by measuring the weight of the collected permeate as a function of time.

After each permeation test, the samples were rinsed thoroughly with ethanol 3 times and soaked in fresh ethanol for 24 hours before being dried in a vacuum oven for one hour at  $110^{\circ}\text{C}$ . Membranes were cooled down for 24 hours in a vacuum oven at  $30^{\circ}\text{C}$  prior to soaking for 8 hours in the solvent to be tested before the permeation test was started. All measurements were performed on three samples for each type of membrane and two times for each sample. The influence of temperature was studied by performing permeability tests up to  $70^{\circ}\text{C}$  at 6 bars for octane, toluene, and isopropanol.

Contact angle measurements, hexane flux tests at 10 bar, and molecular weight cut off (MWCO) measurements were used to control the membrane condition before and after the permeation tests with series of solvents.

Contact angles were measured by the static sessile drop method by the Data Physics Optical Contact Angle (OCA 20) instrument.  $5\ \mu\text{L}$  of water was dropped respectively at a speed of  $2\ \mu\text{L}\ \text{s}^{-1}$  on the membranes surface using a *Hamilton Microliter* syringe. Measurements were taken on 5 different spots on the membrane surface.

MWCO measurements were performed with the same dead-end permeation set-up as used for the permeation tests by using polyethylene glycol (PEG, Fluka) with molecular weights of 200, 400, 600, and 1000 g/mol respectively as probe solutes in toluene. The rejection test was performed until an equilibrium retention value was reached. All measurements were performed on three different membrane samples for each type of membrane. The feed solution was stirred at 500 rpm to avoid any concentration polarization. The feed concentration was set at 8000 ppm. Solute concentrations in the permeate and feed solution were analyzed by a Thermo Electron Corporation HPLC with a C8 econosphere column connected to an Evaporative Light Scattering Detector 2000 ES (32). A nebulizer temperature of  $95^{\circ}\text{C}$ , a gas flow of 2.5 L/min, a column temperature of  $40^{\circ}\text{C}$  and a sample volume of  $20\ \mu\text{L}$  were used. Methanol-water (4:1) was used as the eluent for the HPLC. The



feed and permeate solute concentration ( $C_f$  and  $C_p$ ) were determined for different MWs as a function of the total peak area from the electrical potential difference plot against the retention time. The rejection percentage ( $R$ ) was calculated from the following equation:  $R = (1 - C_p/C_f) \times 100\%$ , where  $C_p$  and  $C_f$  are the solute concentrations in the permeate and feed solution, respectively. The MWCO value is determined as a solute molecular weight for which a 90% retention is observed.

It was not possible to directly measure the solvent sorption behavior of PDMS in different solvents using the as-prepared membranes. Thus, to indicate the sorption tendency of PDMS in different solvents, sorption tests were performed on non-grafted PDMS samples and the values were normalized towards the PDMS sorption of one reference solvent. This provides an indication of the affinity between PDMS and different types of solvent. For this sorption study PDMS samples were prepared by dissolving 10 wt% of RTV-615 A in hexane. PDMS RTV-615A and RTV-615B were purchased from Momentive Performance Materials Belgium. 1% of RTV-615B was added into the solution and pre-polymerized at 60°C for 1 hour. The pre-polymerized solution was then poured into a flat petri dish and the solvent was allowed to evaporate overnight. The samples were put into a vacuum oven at 110°C for 8 hours to complete the polymerization. Afterwards, the samples were cooled down and cut into 0.2 mm thick discs with a diameter of 20 mm each. Sorption tests were performed by immersing the PDMS samples into 10 ml of solvents at different temperatures. The mass of the PDMS sample was weighed before and after the immersion, by wiping the solvent quickly from the external surface after immersion. The sorption value ( $S$ ) in  $\text{cm}^3/\text{g}$  was defined as:  $S = ((m_e - m_o)/m_o)/\rho_s$ , with  $m_o$  is the dry mass of PDMS (g),  $m_e$  the mass of swollen PDMS (g), and  $\rho_s$  the density of the solvents ( $\text{g}/\text{cm}^3$ ). Measurements were performed three times for each type of solvent.

### 3.4. Results and Discussion

#### 3.4.1. Membrane structure and stability

In previous work, it was shown that a chemical bond exists between  $\gamma$ -alumina and the grafted organic moieties (8-9). The thickness of the polymer grafted layer was analysed by SEM-EDX which results are given in Figure 3.1.

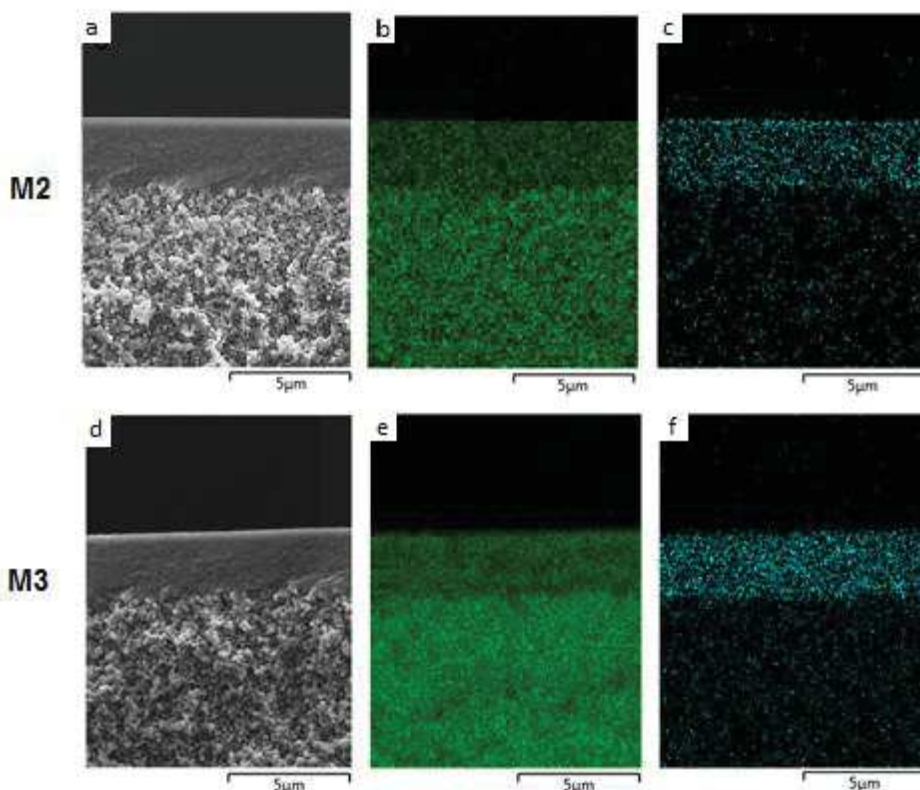


Figure 3.1. SEM and EDX results for M2 membrane (a) SEM picture, (b) Al mapping (green), (c) Si mapping (blue) as well as for M3 membrane (d) SEM picture, (e) Al mapping (green), (f) Si mapping (blue)

The SEM pictures of the M2 and M3 membranes in Figure 3.1a and d show the modified  $\gamma$ - $\text{Al}_2\text{O}_3$  substrate supported on top of  $\alpha$ - $\text{Al}_2\text{O}_3$ . Al and Si EDX mapping of the M2 and M3 membranes are given in Figure 3.1. As can be seen from the EDX picture, the grafting occurs throughout the  $\gamma$ -alumina layer with an observed thickness of about  $3 \mu\text{m}$  for the selective layer for both M2 and M3 membranes.

In order to conduct proper solvent transport studies, it is important that the membranes remain stable and retain their (micro) structure during all tests. Therefore, some membrane

characteristics were analysed before and after these permeation tests: water contact angle, hexane flux and MWCO of PEG in toluene. These results are summarized in Table 3.2.

Table 3.2. Membrane characteristics

Code	Material	Water Contact Angle (°) <sup>a</sup>	Water Contact Angle (°) <sup>b</sup>	MWCO (Da) <sup>a</sup>	MWCO (Da) <sup>b</sup>	Hexane flux at 10 bar (L.m <sup>-2</sup> h <sup>-1</sup> ) <sup>a</sup>	Hexane flux at 10 bar (L.m <sup>-2</sup> h <sup>-1</sup> ) <sup>b</sup>
M1	γ-alumina	~0	~0	7500(33)	N/A	87.1±2.7	87.0±2.5
M2	γ-alumina/ PDMS n=10	94±1	94±1	600	600	48.0±1.9	47.9±1.8
M3	γ-alumina/ PDMS n=39	95±1	95±1	400	400	26.7±1.0	26.6±0.9

<sup>a</sup> Values, measured prior to permeability experiments on the solvents as indicated in Table 3.1

<sup>b</sup> Values, measured after all permeability experiments were performed

As can be seen from this table, water contact angle, MWCO and hexane permeability are similar before and after all permeation tests without any significant differences. All these results showed that all membranes remained stable during the whole testing period.

Both M2 and M3 showed lower MWCO values as compared to the unmodified γ-alumina membranes due to the presence of the grafted PDMS in the pores. M3 showed a lower MWCO than M2. On the other hand, the pure hexane permeability through the M2 membranes is higher than that of M3. This is an indication that M2 membranes have a more open structure than M3 membranes. This will be discussed further in the next section.

### 3.4.2. Permeability performance

Pure solvent flux data at room temperature for M2 and M3 membranes at different trans-membrane pressures (TMP) are given in Figure 3.2. The flux values, as presented in Figure 3.2, are the average equilibrium values of measurements performed on three different membrane samples for each type of membrane and two measurements for each sample. Standard deviations observed for the fluxes were within 4% error.

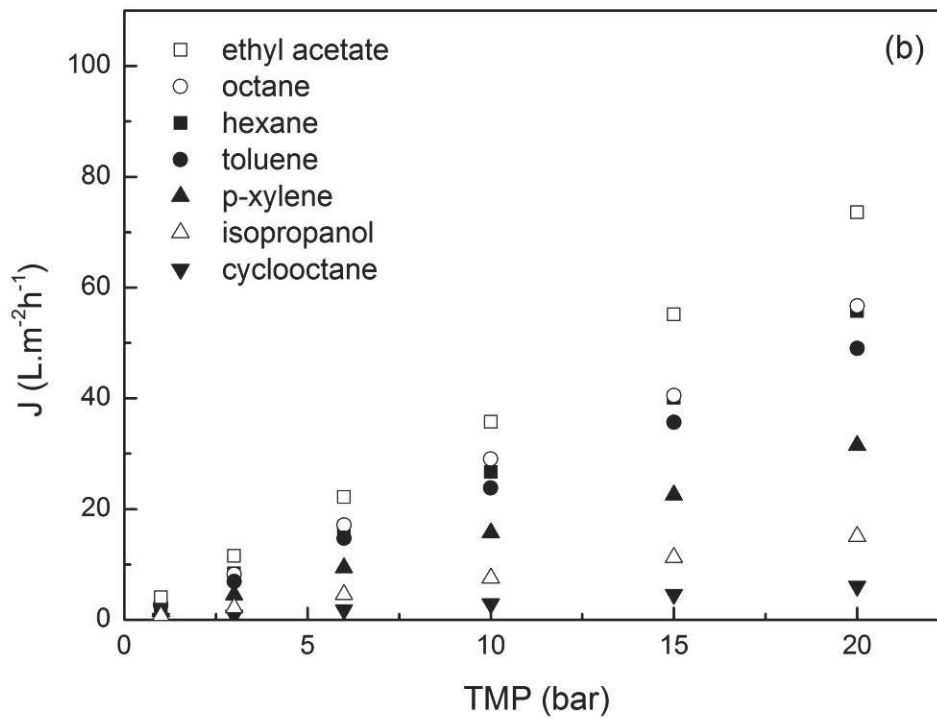
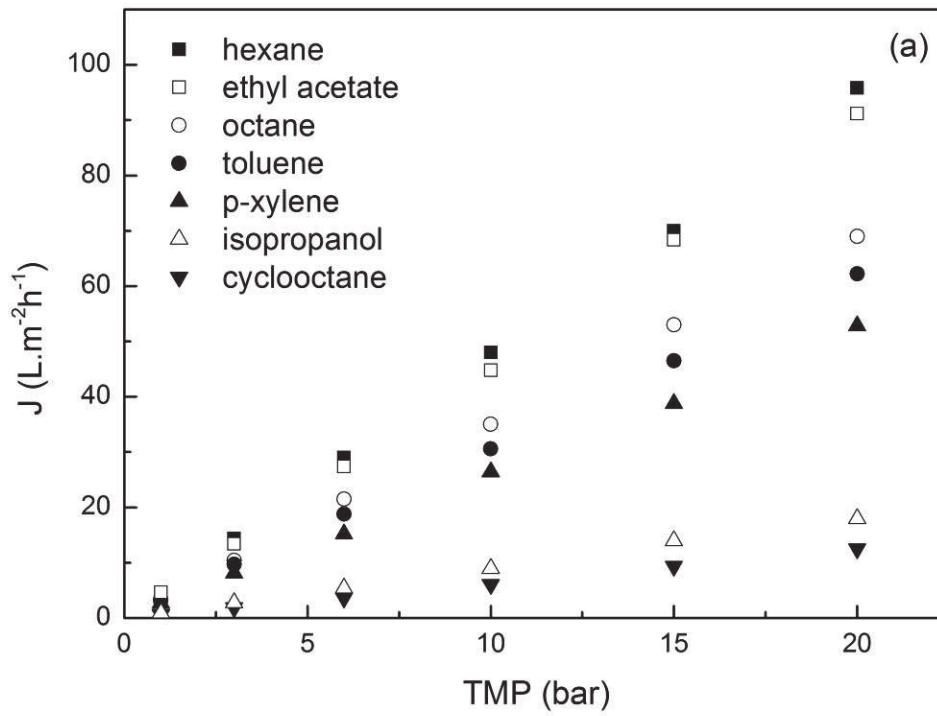


Figure 3.2. Pure solvent flux versus TMP for a) M2 and b) M3 membranes at 20°C

As can be seen in Figure 3.2, a linear relationship of flux versus TMP was observed for both types of membranes for all solvents, suggesting no effect of compaction. This behavior is in contrast with what is mostly found for pure PDMS polymeric membranes where a non-linear behavior in flux versus TMP is observed due to compaction (16, 34). The linear relationship between the flux and TMP, as observed in our work, also indicates the absence of any shear rate flow-induced behavior as described by Castro et al. (11), who studied the permeability for PVP-grafted porous silica membranes with a native pore diameter of 410 nm. In Castro's work, a more than linear increase of flux ( $J$ ) as function of TMP was observed, suggesting deformation of the grafted polymeric chains as a result of the shear rate, which increases the effective membrane pore diameter with increasing operational pressure. This difference between the results as described in (11) and those given in Figure 3.2 can be explained by the smaller pore size of the ceramic porous support (5 nm) used in this work which might provide higher confinement towards the shear rate effect than for macroporous ceramic supports (410 nm).

If solvent transport in these membranes is according to the viscous-flow or pore-flow model (Hagen- Poiseuille law), an identical slope ( $k$ ) must be found for all solvents, when flux is plotted versus  $\text{TMP}/\mu$  ( $\mu$ : solvent viscosity). In that case the membrane permeability constant ( $k$ ) in Equation 3.2 represents the membrane pore geometry, meaning a single value of  $k$  should be identified for all solvents since it is assumed that the membrane pore geometry is identical regardless of the type of the permeating solvent. To validate whether the solvent permeation through the grafted membranes is following the viscous-flow mechanism, fluxes are plotted as function of  $\text{TMP}/\mu$  in Figure 3.3.

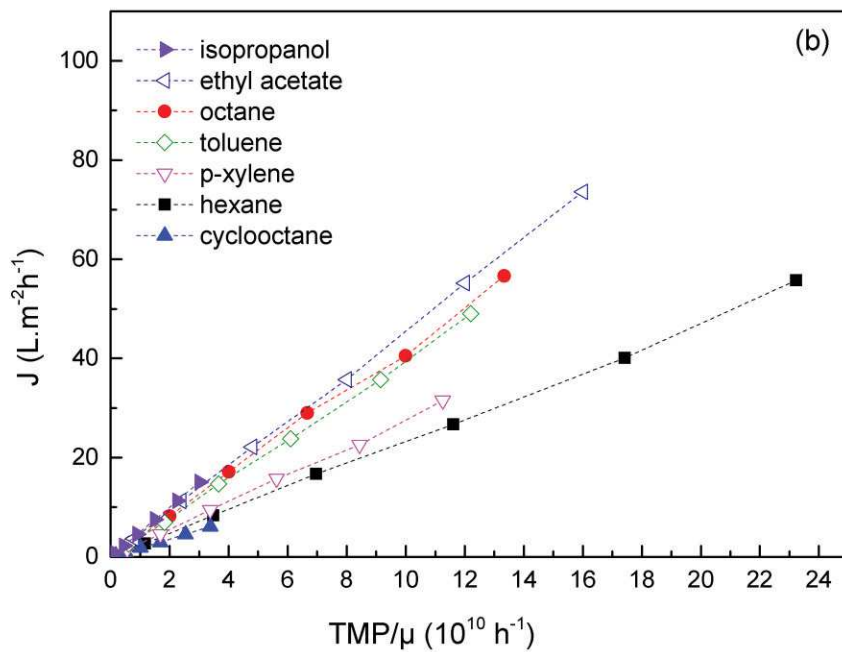
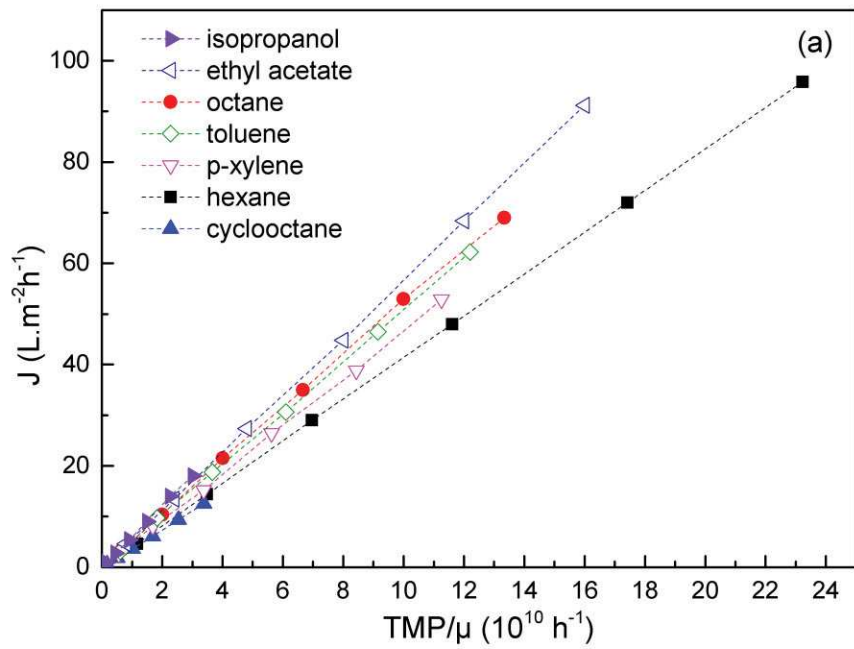


Figure 3.3. Fluxes versus the TMP/ $\mu$  for a) M2 and b) M3 membranes at 20°C

From the different slopes in Figure 3.3, whose values are summarized in Table 3.3, it can be deduced that for both M2 and M3, permeability is not (or not only) dependent on solvent viscosity.

Table 3.3. Slopes ( $k_i$ ) of J versus  $\text{TMP}/\mu$  curves, as given in Figure 3.3 for each solvent

Solvent Types	$k_i$	$k_i$
	M2	M3
Isopropanol	0.60±0.02	0.50±0.02
Ethyl acetate	0.57±0.02	0.46±0.02
Octane	0.52±0.02	0.43±0.02
Toluene	0.51±0.02	0.40±0.02
p-xylene	0.47±0.02	0.28±0.01
Hexane	0.41±0.02	0.24±0.01
Cyclooctane	0.37±0.01	0.18±0.01

The pore-flow model does not take into account the interaction between the membrane and the permeating solvent. It is assumed that the membrane pore geometry is constant regardless the type of the permeating solvent. An adapted pore-flow model is now discussed, assuming that permeation is following the viscous flow mechanism, while the membrane pore geometry is varying in the presence of different types of solvent. It is known that PDMS can swell to a large extent in the presence of nonpolar solvents (14, 35). The degree of swelling depends on the affinity between the PDMS and the solvent. Larger swelling means that more solvent molecules are sorbed by PDMS. Swelling can have an influence on the pore geometry of a grafted membrane, because sorption of the solvent molecules by the grafted moiety can decrease the effective membrane permeation volume (porosity and pore size), i.e. the cylinder-like empty space in the central axis of the pores left by the swollen grafted PDMS. It should be noted that molecules that are responsible for the PDMS swelling are only loosely interacting with the PDMS chains and should surely not be considered as completely immobile.

This hypothesis can be translated into a modified Hagen-Poiseuille law. Assuming that the slope of J versus  $\text{TMP}/\mu$  is different for every solvent due to a change in membrane porosity and pore size when using different solvents, a slope  $k_i$  for each solvent  $i$  can be determined and by using Equation 3.3 we obtain:.

$$k_i = \frac{\varepsilon_i r_{p,i}^2}{8\tau l} \quad (3.7)$$

where  $\varepsilon_i$  and  $r_{p,i}$  are the actual membrane porosity and pore size in the presence of the permeating solvent  $i$ . It is assumed that the membrane porosity and pore size do not have the same value for all solvents, while the other parameters (tortuosity and thickness) do not change significantly with changing solvent.

The permeability constant for each solvent ( $k_i$ ) can be normalized towards the permeability constant of a reference solvent ( $k_{ref}$ ). In combination with Equation 3.7 this normalized permeability constant ( $k_i'$ ) is expressed as:

$$k_i' = \frac{k_i}{k_{ref}} = \frac{\frac{\varepsilon_i r_{p,i}^2}{8\tau l}}{\left(\frac{\varepsilon_i r_{p,i}^2}{8\tau l}\right)_{ref}} = \frac{V_e}{(V_e)_{ref}} \quad (3.8)$$

Here an effective permeable volume of the membrane ( $V_e$ ) is defined ( $\tau$  and  $l$  are identical for all solvents).  $V_e$  can be described as the difference between the membrane permeable volume per unit mass of the grafted moiety when there is no solvent present ( $V_o$  in  $\text{cm}^3/\text{g}$ ) and the volume of sorbed solvent per unit of mass of the grafted moiety ( $V_s$  in  $\text{cm}^3/\text{g}$ ):

$$V_e = V_o - V_s \quad (3.9)$$

Combination of Equation 3.8 and 3.9 gives:

$$k_i' = \frac{k_i}{k_{ref}} = \frac{V_e}{(V_e)_{ref}} = \frac{V_o - V_{s,i}}{V_o - V_{s,ref}} \quad (3.10)$$

The value of  $V_o$  is specific for each type of grafted membrane (M2, M3) and depends on the pore volume of the ceramic substrate and the mass of the grafted moiety. The values of  $V_{s,i}$  in  $\text{cm}^3/\text{g}$  depends on the type of solvent (the affinity of the solvent with the grafted moiety).  $V_{s,ref}$  is the volume of the sorbed solvent per unit mass of the grafted moiety for a reference solvent ( $\text{cm}^3/\text{g}$ ). From here, with a simple mathematical derivation Equation 3.10 becomes:



$$k_i' = \frac{k_i}{k_{ref}} = \frac{V_o - V_{s,i}}{V_o - V_{s,ref}} = \frac{V_o}{V_o - V_{s,ref}} - \frac{V_{s,i}}{V_o - V_{s,ref}} \quad (3.11)$$

If:

$$V_{s,i}' = \frac{V_{s,i}}{V_{s,ref}} \quad (3.12)$$

with  $V_{s,i}'$  the ratio of the sorption tendency in one solvent relative to that of the reference solvent, or so called the normalized sorption value, then Equation 3.11 becomes:

$$k_i' = \frac{k_i}{k_{ref}} = \frac{V_o}{V_o - V_{s,ref}} - \frac{V_{s,ref}}{V_o - V_{s,ref}} V_{s,i}' = A - B V_{s,i}' \quad (3.13)$$

with

$$A = \frac{V_o}{V_o - V_{s,ref}} \quad (3.14)$$

and

$$B = \frac{V_{s,ref}}{V_o - V_{s,ref}} \quad (3.15)$$

where A is the intercept and B the slope of a plot of  $k_i'$  versus  $V_{s,i}'$ .

Incorporating Equation 3.13 in Equation 3.2 results in:

$$J_i = k_i \frac{\Delta P}{\mu} = k_{ref} (A - B V_{s,i}') \frac{\Delta P}{\mu} \quad (3.16)$$

with  $k_i$  is the slope of  $J_i$  versus  $\frac{\Delta P}{\mu}$  for each solvent as a function of  $V_{s,i}'$ . In this work values of  $V_{s,i}$  are obtained through sorption measurements of a PDMS sample in different types of solvent. Crosslinked PDMS samples with a low amount of crosslinker (9 %w/w) is chosen as the sample. Table 3.4 gives the measured sorption values and the sorption values normalized against the sorption of isopropanol, which is chosen as a solvent of reference in

this work. In fact, any solvent can be freely chosen as a reference solvent for the calculation of the normalized sorption value.

Table 3.4. Sorption value of a pure PDMS sample with a 9 w/w% of crosslinker at 20°C and the normalized sorption values against the sorption of isopropanol which is chosen as a solvent of reference

Solvent	Sorption value $V_{s,i}$ (cm <sup>3</sup> /g)	Normalized sorption value $V_{s,i}' = V_{s,i}/V_{s,isopropanol}$ (-)	Dipole Moment (D)	Dielectric Constant ( $\epsilon$ )	Vapor Pressure (mmHg at 20°C)
Isopropanol	0.47	1.00	1.66	19.92	78.2
Ethyl acetate	0.48	1.02	1.88	6.02	109.1
Toluene	0.53	1.12	0.34	2.38	26.3
Octane	0.54	1.15	0.00	1.95	13.9
p-Xylene	0.63	1.34	0.07	2.27	7.6
Hexane	0.66	1.40	0.08	1.89	129.1
Cyclooctane	0.70	1.48	0.00	2.12	4.4

A possible relation between sorption values and solvent polarity (such as dipole moment and dielectric constant) as well as solvent vapor pressure is summarized in Table 3.4. In general a lower sorption value is observed for polar solvents like isopropanol (dielectric constant of 19.92) or ethyl acetate (dielectric constant of 6.02) if compared to sorption values of nonpolar solvents having dielectric constant between 1.5 and 2.5. A lower sorption value was also found for polar solvents with dipole moments of more than 1.5, while higher sorption values were found for nonpolar solvents with dipole moments less than 0.5. No trend was observed between the sorption value and the vapor pressure of the solvents.

In order to use Equation 3.16, the A and B values need to be determined. To solve the A and B, the  $k_i'$  is plotted against  $V_{s,i}'$  according to Equation 3.13. In this way for membrane M2 A and B values of respectively  $1.68 \pm 0.07$  and  $0.68 \pm 0.09$  were calculated while for membrane M3 A and B values were respectively  $2.27 \pm 0.09$  and  $1.27 \pm 0.07$ . Details on  $k_i'$  versus  $V_{s,i}'$  are given in the appendix to this paper. If  $k_i$  is corrected with  $(A - B V_{s,i}')$ , then, according to Equation 3.16, the slopes in the curve of flux versus  $\text{TMP}/\mu$  will unite into a single slope, which is equal to  $k_{ref}$ . The plot of the  $\text{flux}/(A - B V_{s,i}')$  versus  $\text{TMP}/\mu$  for M2 and M3 membranes are given in Figure 3.4.

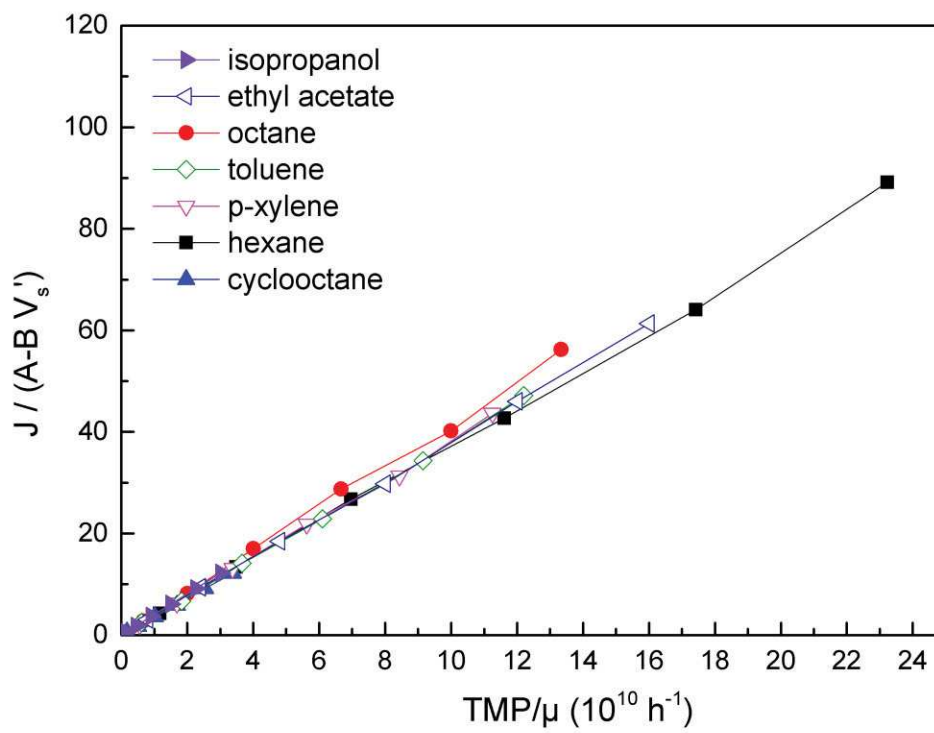
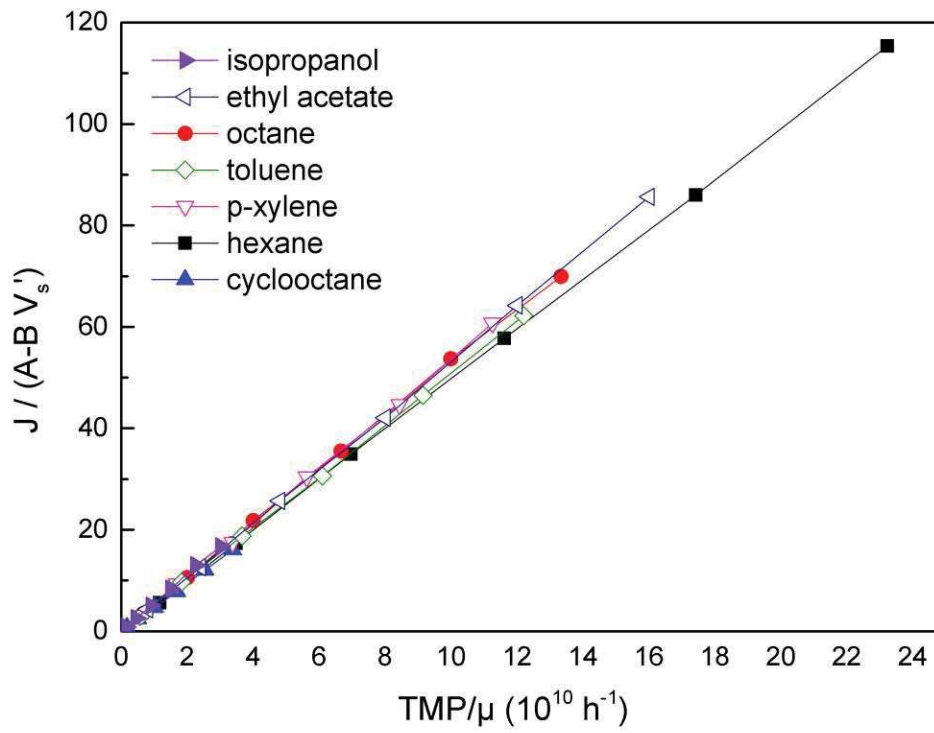


Figure 3.4. Plot of  $J$  corrected with  $(A - B V_{s,i})'$  against  $\text{TMP}/\mu$  at  $20^\circ\text{C}$

From Figure 3.4, it can be seen that almost a single slope is formed when  $J$  corrected with  $(A - B V_{s,i}')$  is plotted against  $\text{TMP}/\mu$  in accordance to Equation 3.13. The applicability of this equation for describing the solvent permeation of these grafted ceramic membranes indicates that the solvent permeability behavior of grafted membranes is governed by the sorption tendency of the grafted moiety aside from the solvent viscosity for porous grafted membranes. The slopes of  $J/(A - B V_{s,i}')$  versus  $\text{TMP}/\mu$  as given in Figure 3.4 for each solvent including the error values are presented in Table 3.5 for M2 and M3 approaching the  $k_{\text{ref}}$ .

Table 3.5. Slopes of  $J/(A - B V_{s,i}')$  versus  $\text{TMP}/\mu$  as given in Figure 3.4 for each solvent indicating the  $k_{\text{ref}}$  values

Solvent Types	Slopes	
	M2	M3
Isopropanol	0.60±0.02	0.50±0.02
Ethyl acetate	0.58±0.02	0.47±0.03
Octane	0.58±0.02	0.53±0.02
Toluene	0.56±0.03	0.47±0.04
p-xylene	0.61±0.03	0.49±0.02
Hexane	0.56±0.03	0.49±0.03
Cyclooctane	0.55±0.03	0.46±0.02

### 3.4.3. Flux as function of temperature

In order to check whether similar major parameters affect membrane permeability at elevated temperatures, permeability tests were done in the temperature range of 20 - 70 °C and given in Figure 3.5.

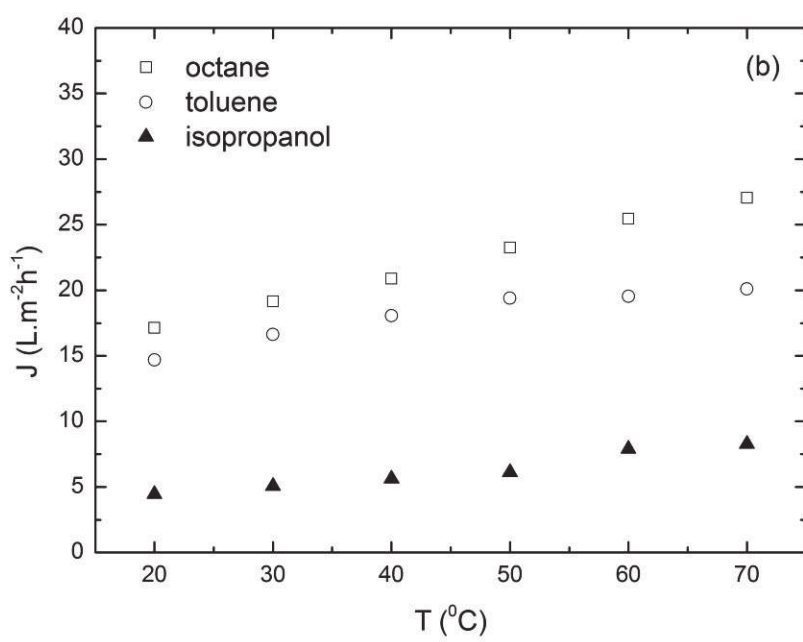
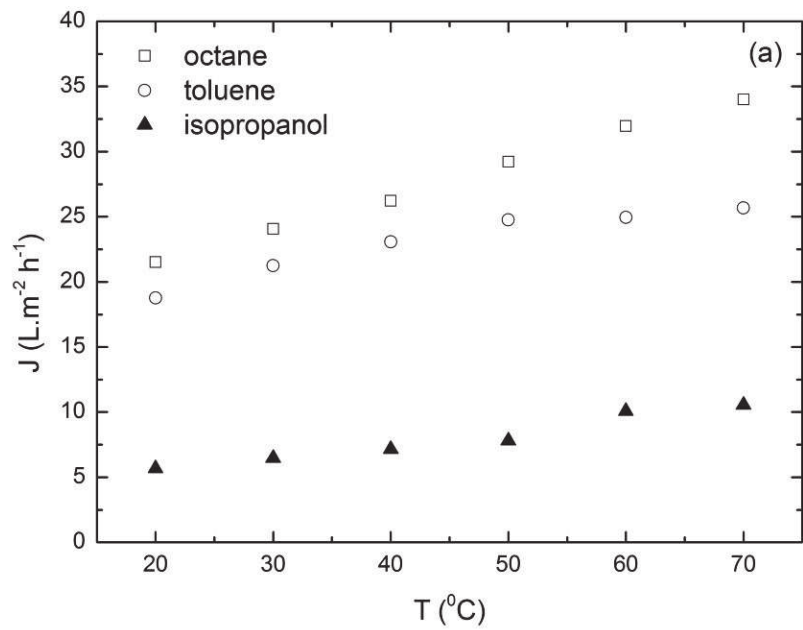


Figure 3.5. Flux versus temperature at a constant TMP of 6 bar for a) M2 and b) M3 membranes

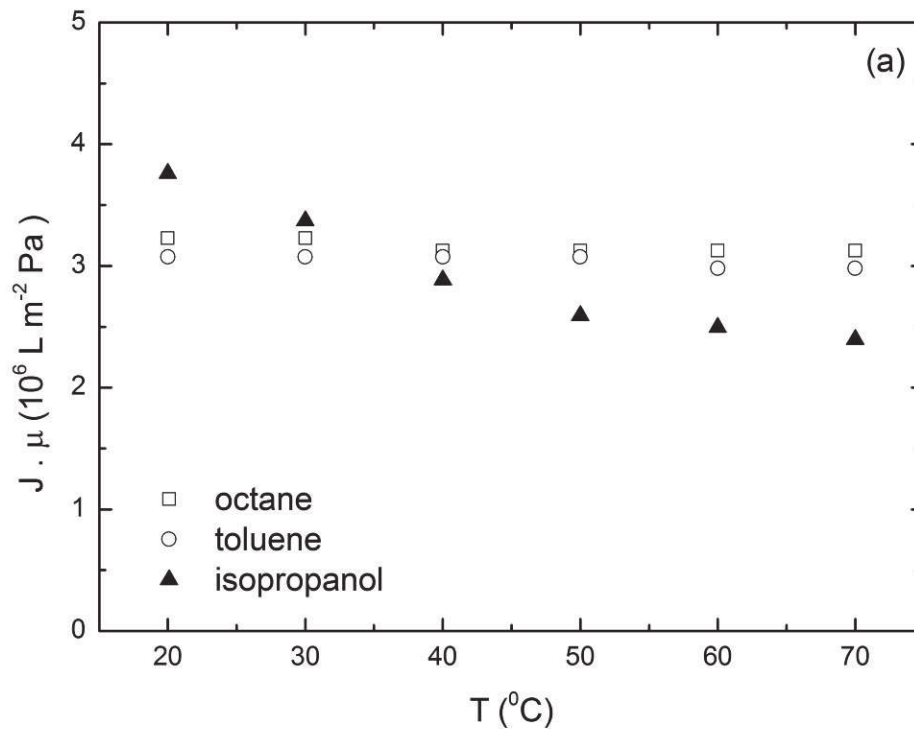
It can be seen from Figure 3.5 that the flux increases with increasing temperature. The increased movements of individual molecules at higher temperature reduce the intermolecular forces resulting in a decrease of solvent viscosity. Besides, there is also an

enhanced polymer chain mobility at elevated temperatures. The solvent viscosities as function of temperature are given in Table 3.6.

Table 3.6. Solvent viscosity at elevated temperatures (26)

T (°C)	Viscosity $\mu$ (mPa.s)		
	octane	toluene	isopropanol
20	0.54	0.59	2.39
30	0.48	0.52	1.88
40	0.43	0.48	1.45
50	0.39	0.45	1.20
60	0.35	0.43	0.89
70	0.33	0.42	0.82

The viscosity corrected flux, according to Darcy's law, are plotted in Figure 3.6 as a function of permeation temperature.



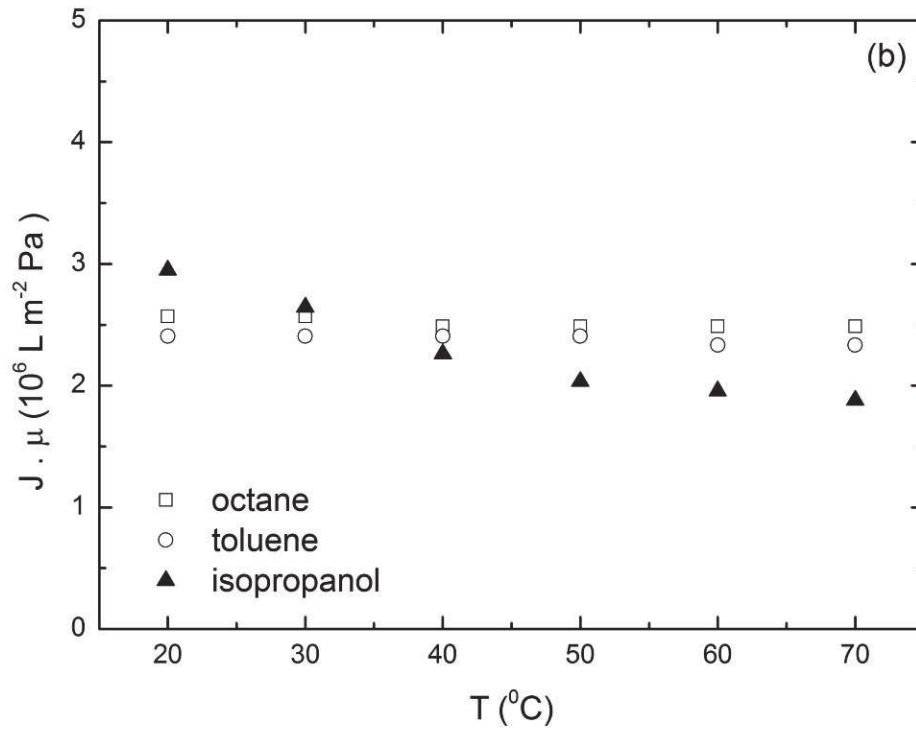


Figure 3.6. Solvent fluxes corrected for the solvent viscosity versus T for a) M2 and b) M3 membranes

It can be seen from Figure 3.6 that the permeability of isopropanol decreases for both membranes with increasing temperature after being corrected for the solvent viscosity at the pertinent temperatures. For octane and toluene on the other hand, the viscosity corrected flux was found to be constant with the increase in temperature.

The differences in permeability behavior as function of temperature between octane and toluene on one side and isopropanol on the other side might indicate a difference in sorption behavior of PDMS in the different solvents for the studied temperature range. Table 3.7 shows the sorption values ( $V_{s,T}$ ) of PDMS at different temperatures for the respective solvents.

Table 3.7. Sorption values of PDMS samples as function of temperature

T (°C)	Sorption values $V_{s,T}(\text{cm}^3/\text{g})$			Normalized sorption values $V_{s,T}' = V_{s,T}/V_{s,20^\circ\text{C},\text{isopropanol}} (-)$		
	octane	toluene	isopropanol	octane	toluene	isopropanol
20	0.54	0.53	0.47	1.15	1.13	1.00
30	0.54	0.53	0.51	1.15	1.13	1.09
40	0.55	0.53	0.56	1.17	1.13	1.19
50	0.55	0.53	0.59	1.17	1.13	1.26
60	0.55	0.54	0.60	1.17	1.15	1.28
70	0.55	0.54	0.61	1.17	1.15	1.30

A significant dependency of the sorption value with temperature is observed for PDMS-isopropanol systems. A dependency of sorption value with temperature is also observed for PDMS-octane or PDMS-toluene systems.

The increasing sorption of isopropanol in the grafted moiety at increasing temperature might be the reason for the decrease in isopropanol permeability, as shown in Figure 3.6a and b. To check whether solvent sorption also affects the solvent transport through grafted membranes as function of temperature, the viscosity corrected flux is further on corrected for the sorption of solvent at the pertinent temperature according to (see also Equation 3.16)

$$\frac{J \cdot \mu}{(A - B \cdot V_{s,T}')} = k_{ref} \cdot \Delta P \quad (3.17)$$

If similar parameters affecting the membrane permeability as function temperatures,

$\frac{J \cdot \mu}{(A - B \cdot V_{s,T}')}$  should be constant against the permeation temperature.

The fluxes corrected with the  $\frac{1}{A - B \cdot V_{s,T}'}$  for each membrane types plotted against the permeation temperature are given in Figure 3.7.



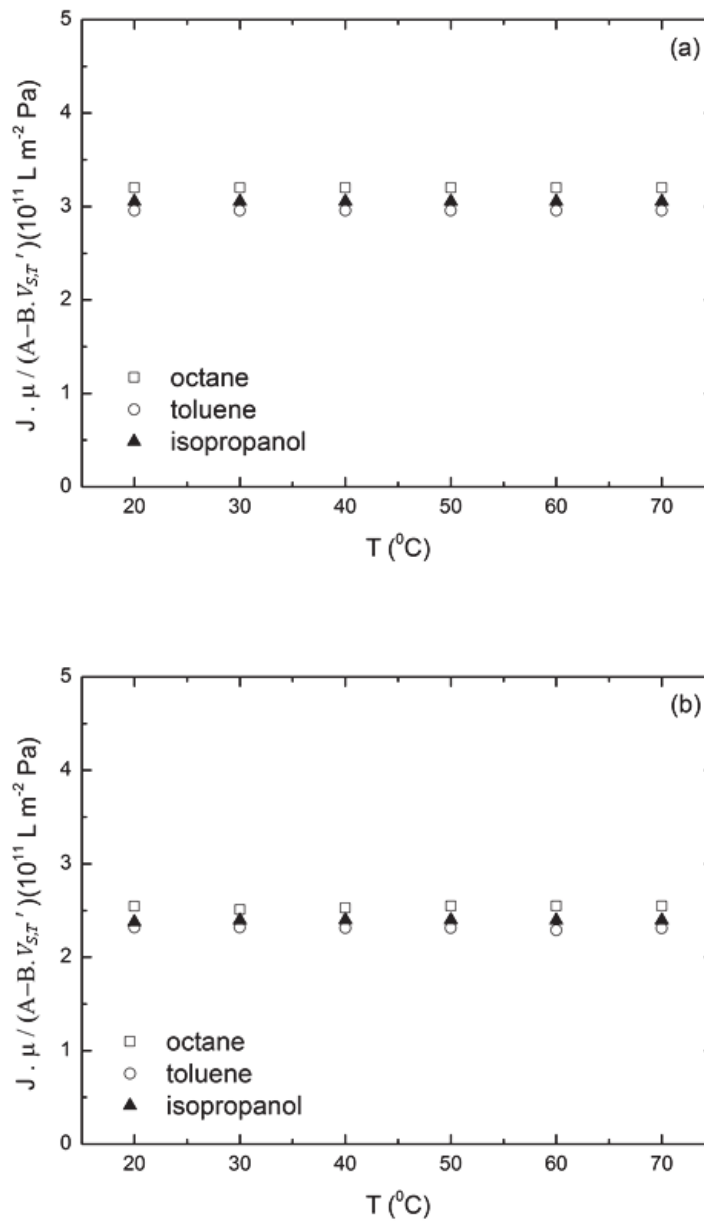


Figure 3.7. The fluxes corrected with  $\frac{1}{A-B.V_{s,T}'}$  plotted against the permeation temperature using A and B values calculated previously for a) M2 and b) M3 membranes

As can be seen from Figure 3.7 Equation 3.17 can be applied for describing the membrane permeability behavior. From all these results it can be concluded that the permeability of PDMS-grafted  $\gamma$ -alumina ceramic membranes, as studied in this work, is dominated by the solvent viscosity and the solvent sorption of the grafted moiety in a solvent when used in a temperature range of 20 - 70  $^{\circ}\text{C}$ .

## 5. Conclusions

Prepared PDMS-grafted alumina membranes are stable for permeation of different types of solvent for at least 10 days. No compaction or shear flow-induced behavior was observed during solvent transport through the grafted membranes at trans-membrane pressures up to 20 bars. The solvent permeation of these ceramic membranes was found to be mainly governed by Darcy's and Hagen-Poiseuille law, but with taking into account swelling of the grafted moiety. An empirical model, derived from the Hagen-Poiseuille model, using the sorption tendency of the grafted material in different solvents, can be used to describe the membrane permeability behavior.

## Acknowledgement

The authors acknowledge the financial support from the European Union – The Education, Audiovisual and Culture Executive Agency (EACEA) under the Program “Erasmus Mundus Doctorate in Membrane Engineering” – EUDIME (FPA 2011-2014) and I.A.P. grant sponsored by the Belgian Federal Government.

## References

1. Vandezande, P., Gevers, L. E. M., and Vankelecom, I. F. J. (2008) Solvent resistant nanofiltration: Separating on a molecular level, *Chemical Society Reviews* 37, 365-405.
2. Leger, C., De Lira, H. L., and Paterson, R. (1996) Preparation and properties of surface modified ceramic membranes. Part II. Gas and liquid permeabilities of 5 nm alumina membranes modified by a monolayer of bound polydimethylsiloxane (PDMS) silicone oil, *Journal of Membrane Science* 120, 135-146.
3. Faibish, R. S., and Cohen, Y. (2001) Fouling-resistant ceramic-supported polymer membranes for ultrafiltration of oil-in-water microemulsions, *Journal of Membrane Science* 185, 129-143.
4. Yoshida, W., and Cohen, Y. (2003) Ceramic-supported polymer membranes for pervaporation of binary organic/organic mixtures, *Journal of Membrane Science* 213, 145-157.
5. Yoshida, W., and Cohen, Y. (2004) Removal of methyl tert-butyl ether from water by pervaporation using ceramic-supported polymer membranes, *Journal of Membrane Science* 229, 27-32.

6. Popat, K. C., Mor, G., Grimes, C. A., and Desai, T. A. (2004) Surface Modification of Nanoporous Alumina Surfaces with Poly(ethylene glycol), *Langmuir* 20, 8035-8041.
7. Sang Won, L., Hao, S., Richard, T. H., Vania, P., and Gil, U. L. (2005) Transport and functional behaviour of poly(ethylene glycol)-modified nanoporous alumina membranes, *Nanotechnology* 16, 1335.
8. Pinheiro, A. F. M., Hoogendoorn, D., Nijmeijer, A., and Winnubst, L. (2014) Development of a PDMS-grafted alumina membrane and its evaluation as solvent resistant nanofiltration membrane, *Journal of Membrane Science* 463, 24-32.
9. Tanardi, C. R., Pinheiro, A. F. M., Nijmeijer, A., and Winnubst, L. (2014) PDMS grafting of mesoporous  $\gamma$ -alumina membranes for nanofiltration of organic solvents, *Journal of Membrane Science* 469, 471-477.
10. Castro, R. P., Cohen, Y., and Monbouquette, H. G. (1993) The permeability behavior of polyvinylpyrrolidone-modified porous silica membranes, *Journal of Membrane Science* 84, 151-160.
11. Castro, R. P., Monbouquette, H. G., and Cohen, Y. (2000) Shear-induced permeability changes in a polymer grafted silica membrane, *Journal of Membrane Science* 179, 207-220.
12. Aerts, S., Vanhulsel, A., Buekenhoudt, A., Weyten, H., Kuypers, S., Chen, H., Bryjak, M., Gevers, L. E. M., Vankelecom, I. F. J., and Jacobs, P. A. (2006) Plasma-treated PDMS-membranes in solvent resistant nanofiltration: Characterization and study of transport mechanism, *Journal of Membrane Science* 275, 212-219.
13. Gevers, L. E. M., Vankelecom, I. F. J., and Jacobs, P. A. (2006) Solvent-resistant nanofiltration with filled polydimethylsiloxane (PDMS) membranes, *Journal of Membrane Science* 278, 199-204.
14. Gevers, L. E. M., Vankelecom, I. F. J., and Jacobs, P. A. (2005) Zeolite filled polydimethylsiloxane (PDMS) as an improved membrane for solvent-resistant nanofiltration (SRNF), *Chemical Communications*, 2500-2502.
15. Mulder, M. (1996) *Basic principles of membrane technology*, 2nd ed., Kluwer Academic Publisher, Netherlands.
16. Vankelecom, I. F. J., De Smet, K., Gevers, L. E. M., Livingston, A., Nair, D., Aerts, S., Kuypers, S., and Jacobs, P. A. (2004) Physico-chemical interpretation of the SRNF transport mechanism for solvents through dense silicone membranes, *Journal of Membrane Science* 231, 99-108.
17. Wijmans, J. G., and Baker, R. W. (1995) The solution-diffusion model: a review, *Journal of Membrane Science* 107, 1-21.
18. Wang, J., Dlamini, D. S., Mishra, A. K., Pendergast, M. T. M., Wong, M. C. Y., Mamba, B. B., Freger, V., Verliefe, A. R. D., and Hoek, E. M. V. (2014) A critical review of transport through osmotic membranes, *J. Membr. Sci.* 454, 516-537.

19. Jonsson, G. (1980) Overview of theories for water and solute transport in UF/RO membranes, *Desalination* 35, 21-38.
20. Robinson, J. P., Tarleton, E. S., Millington, C. R., and Nijmeijer, A. (2004) Solvent flux through dense polymeric nanofiltration membranes, *Journal of Membrane Science* 230, 29-37.
21. Zeidler, S., Kätzel, U., and Kreis, P. (2013) Systematic investigation on the influence of solutes on the separation behavior of a PDMS membrane in organic solvent nanofiltration, *Journal of Membrane Science* 429, 295-303.
22. Postel, S., Spalding, G., Chirnside, M., and Wessling, M. (2013) On negative retentions in organic solvent nanofiltration, *Journal of Membrane Science* 447, 57-65.
23. Nijmeijer, A., Bladergroen, B. J., and Verweij, H. (1998) Low-temperature CVI modification of  $\gamma$ -alumina membranes, *Microporous and Mesoporous Materials* 25, 179-184.
24. Cuperus, F. P., Bargeman, D., and Smolders, C. A. (1992) Permporometry: the determination of the size distribution of active pores in UF membranes, *Journal of Membrane Science* 71, 57-67.
25. Vandezande, P., Gevers, L. E. M., Paul, J. S., Vankelecom, I. F. J., and Jacobs, P. A. (2005) High throughput screening for rapid development of membranes and membrane processes, *Journal of Membrane Science* 250, 305-310.
26. Perry, R. H., Green, D. W., Maloney, J. O., Abbott, M. M., Ambler, C. M., and Amero, R. C. (1997) *Perry's chemical engineers' handbook*, Vol. 7, McGraw-hill New York.
27. Lide, D. (2002) CRC handbook of chemistry and physics: a ready-reference book of chemical and physical data, ed. DR Lide, Boca Raton, FL: CRC Press.
28. Daubert, T. E., and Danner, R. P. (1989) *Physical and Thermodynamic Properties of Pure Chemicals: Design institute for physical property data*, American institute of chemical engineers. *vp*, Hemisphere Publishing Corporation.
29. Dean, J. A. Lange's handbook of chemistry, 1999, McGraw-Hill, New York.
30. Cannella, W. J. (2000) Xylenes and Ethylbenzene, In *Kirk-Othmer Encyclopedia of Chemical Technology*, John Wiley & Sons, Inc.
31. Logsdon, J. E., and Loke, R. A. (2000) Isopropyl Alcohol, In *Kirk-Othmer Encyclopedia of Chemical Technology*, John Wiley & Sons, Inc.
32. Li, X., Monsuur, F., Denoulet, B., Dobrak, A., Vandezande, P., and Vankelecom, I. F. J. (2009) Evaporative light scattering detector: toward a general molecular weight cutoff characterization of nanofiltration membranes, *Anal Chem* 81, 1801-1809.

33. Pinheiro, A. F. M. (2013) Development and Characterization of Polymer-grafted Ceramic Membranes for Solvent Nanofiltration, In *PhD Thesis*, University of Twente, Enschede.
34. Paul, D. R., Paciotti, J. D., and Ebra-Lima, O. M. (1975) Hydraulic permeation of liquids through swollen polymeric networks. II. Liquid mixtures, *Journal of Applied Polymer Science* 19, 1837-1845.
35. Lee, J. N., Park, C., and Whitesides, G. M. (2003) Solvent Compatibility of Poly(dimethylsiloxane)-Based Microfluidic Devices, *Analytical Chemistry* 75, 6544-6554.

### Supporting Information for Chapter 3

In order to determine the A and B values as given in Equation 3.13, the normalized values of  $k_i (k_i')$  was plotted against  $V_{s,i}'$ . The values of  $k_i$  are obtained from the slope of J versus TMP/ $\mu$  curves for each solvent as given in Figure 3.3. These values are normalized towards the  $k_i$  of isopropanol which is chosen as a solvent of reference.

By plotting  $k_i'$  (see Table 3.A.1) versus  $V_{s,i}'$  (see Table 3.5) Figure 3.A.1a and b are obtained for respectively membrane M2 and M3. In this way for membrane M2 A and B values of respectively  $1.68 \pm 0.07$  and  $0.68 \pm 0.09$  were calculated while for membrane M3 A and B values were respectively  $2.27 \pm 0.09$  and  $1.27 \pm 0.07$

Table 3.A.1. Values of  $k_i$ , normalized towards the  $k_i$  of isopropanol ( $= k_i'$ )

Solvent	$k_i'$ for M2	$k_i'$ for M3
Isopropanol	1.00	1.00
Ethyl acetate	0.96	0.92
Octane	0.86	0.85
Toluene	0.85	0.81
p-Xylene	0.79	0.56
Hexane	0.69	0.48
Cyclooctane	0.62	0.36

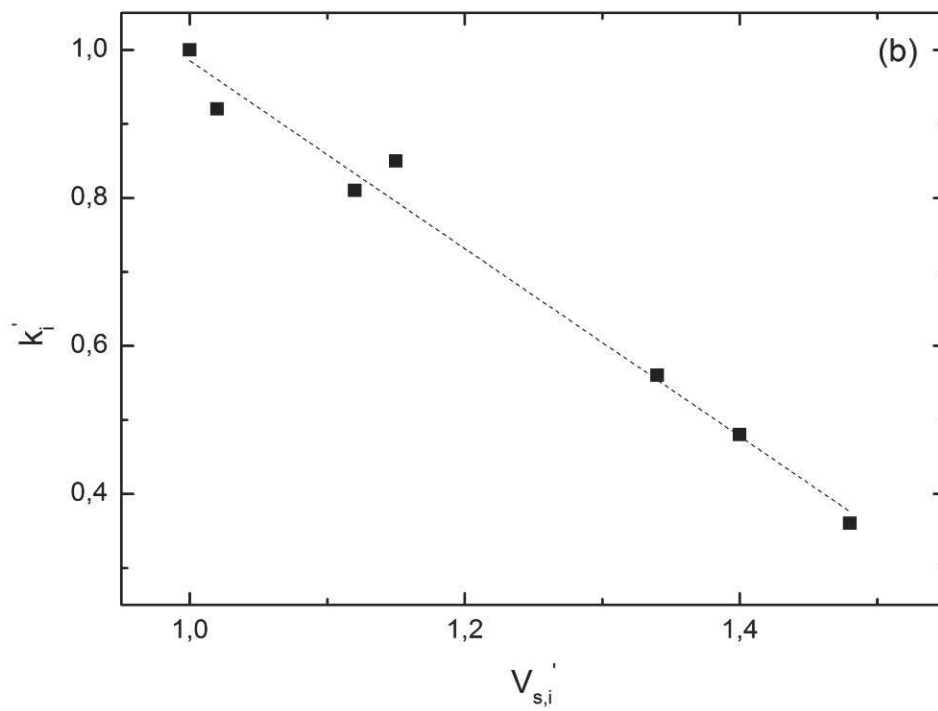
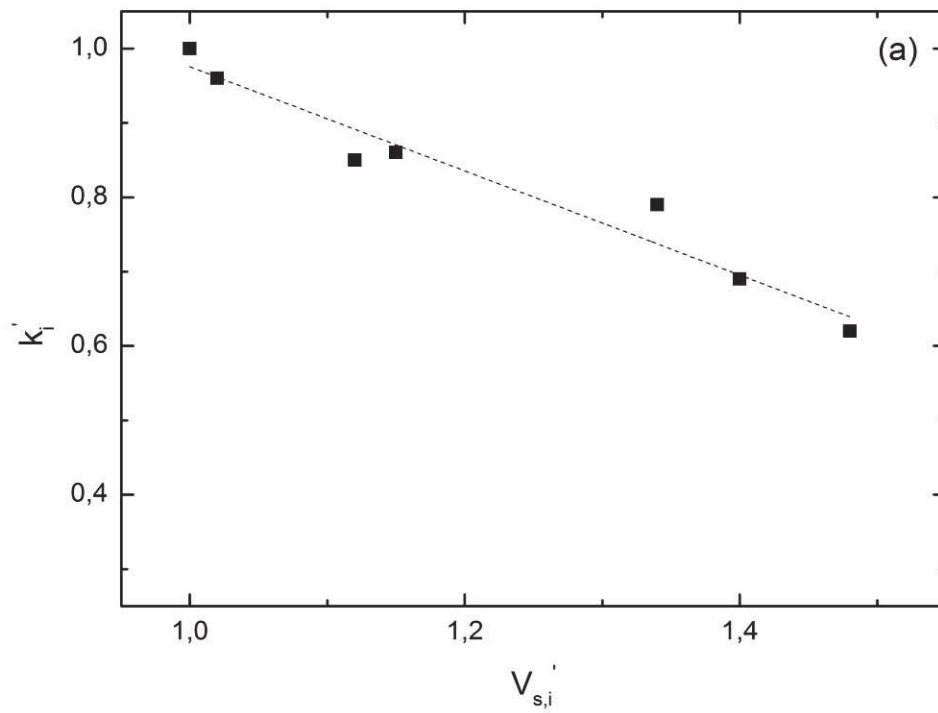


Figure 3.A.1. Plot of  $k_i'$  versus  $V_{s,i}'$  for a) M2 and b) M3 membranes





# Chapter 4

## Solute Rejection in SRNF using PDMS Grafted $\gamma$ -Alumina Membranes

This chapter has been submitted for publication as:

Tanardi, C.R., Vankelecom, I. F. J., Nijmeijer, A., Winnubst, L. Solute Rejection in SRNF using PDMS Grafted  $\gamma$ -Alumina Membranes

## Abstract

The solute rejection of PDMS grafted  $\gamma$ -alumina membranes was investigated for different solvent-solute pairs. In contrast to the behavior of pure PDMS polymeric membranes, higher rejections were found in nonpolar solvents, like toluene, than in polar solvents, such as isopropanol. It is suggested that the transport of solute is following a size based exclusion mechanism as the solute rejection is related to the ratio solute diameter/pore diameter. The Ferry, Verniory and steric hindrance pore (SHP) models were used to predict the membrane rejection using the pore diameter information from  $N_2$  physisorption measurements as the pore size if no solvent was present. For dye solutes in isopropanol, the experimental data fall in the range of the predicted rejection values for Ferry, Verniory, and SHP model, while under-predicted values resulted for solutes in the toluene system. The difference of dyes rejection in isopropanol and toluene can be attributed to the change in the membrane pore size as a result of the membrane-solvent interaction. The effective solute diameter and the ability of one component to create a hydrogen bond with either membrane, solvent, or solute are important factors determining the separation performance of these SRNF membranes.

#### 4.1. Introduction

Solvent resistant nanofiltration (SRNF) is a useful tool for separations in organic media, such as the removal of impurities from used solvents, recycling of solvents or the recovery of products from reaction mixtures in chemical, petrochemical, and pharmaceutical industries (1-2). For these kinds of applications, continuous exposure towards organic solvents is expected, giving a need for a robust membrane.

Membrane preparation by means of grafting of polymers inside the pores of ceramic membranes offers the possibility of integrating pore size tuning and surface wettability/functionality process into one single fabrication step. Several examples of modifying porous inorganic membranes by grafting are known for various applications (3-10) indicating the potential of grafting as a method to prepare selective and chemically stable membranes.

The solvent and solute transport mechanism of membranes, prepared in this way, has not been described in literature yet. To enable process modelling and facilitate process design of SRNF processes, the major parameters as well as transport mechanisms, which influence the transport of solvents and solutes through the membranes, must be quantified.

Variables such as the type of module as well as the process parameters during operation (e.g. feed concentrations, applied pressures and temperatures) can be important parameters influencing the observed selectivity (1-2, 11-12). The properties of the membrane material (e.g. pore size, swelling resistance, and surface properties), as well as the properties of the solvent (e.g. viscosity, polarity, molecular size, and/or surface tension) or the solute (e.g. size, shape, and/or charges of the solute) play a vital role in determining the observed membrane rejection (1-2, 11-12). The separation performance for SRNF is the result of the interactions between membrane, solvents and solutes (1). Due to the overlapping effect of the above mentioned parameters on the observed membrane permeability and selectivity, quantification of each factor that determine the NF separation performance, can be challenging.

The pore-flow and the solution-diffusion models are commonly used for aqueous applications (13-15). A general strategy that can be utilized to identify the transport mechanism of a membrane (despite the many possible contributing factors) is looking whether transport models previously applied for aqueous systems can be used to describe the transport behavior of a SRNF membrane. By identifying the dominant transport mechanism, the important parameters, governing solvent and solute transport, can be singled out first before going for an investigation of the more subtle factors influencing nanofiltration. For a PDMS-based SRNF membrane, both pore-flow and solution-diffusion

models have been used in literature to describe the process. Vankelecom et al. (16) suggested that a viscous flow model can be used to describe the permeation of pure solvents through PDMS membranes by taking into account membrane swelling. This finding was later confirmed by Robinson et al. (17), who successfully used a pore-flow model to describe the transport behavior of PDMS membranes for nonpolar solvents based on the reasoning that the swollen PDMS layer may form a pore-like structure in the presence of nonpolar solvents. Meanwhile, Zeidler et al. (18) observed negative rejections of dye solutes in ethanol through PDMS membranes. It was confirmed that in the presence of swelling solvents like n-heptane and THF, a viscous flow behavior was observed for PDMS membranes. On the other hand, in the presence of non-swelling solvents, like ethanol, it was proposed that the rejection by PDMS might be closer to that of the solution-diffusion mechanism. Postel et al. (19) examined this phenomenon and successfully used the solution-diffusion model to describe the negative rejections of dye solutes by PDMS membranes using ethanol as a solvent. These studies show that the existing transport models for aqueous applications can be used as a starting point to investigate the transport behavior of SRNF membranes. Once the identification of the major parameters is carried out in this way, the identification of the more subtle factors influencing the membrane transport may be progressed further by studying whether there is any difference between the experimental data and the existing model.

By following this strategy, the dominant parameters, which determine the transport of several pure solvents through PDMS-grafted ceramic membranes, were identified (20). It was found that pure solvent permeation through these membranes can be described by a pore flow behavior by taking into account the solvent viscosity and the effect of sorption of the solvent in the grafted moiety. It is suggested that the membrane permeation volume reduces if a solvent is strongly sorbed. Since SRNF involves a variety of solvent and solute combination, it is very important to study the rejection behavior of the membranes for different solvent-solute systems.

In this work the major parameters, governing the SRNF performance and the transport mechanism for the rejection of solutes, are described. First, the effect of Trans Membrane Pressures on solute transport is discussed. Second, the effect of solvent or solute type on membrane selectivity is explored. Finally, the applicability of existing solute rejection models, based on a size-exclusion mechanism, to describe the solute rejection behavior of the PDMS-grafted ceramic membranes is discussed. An estimate of pore sizes of the membranes, based on solute rejection measurements and existing transport models will be provided.

#### 4.2. Existing solute transport models based on a size-exclusion mechanism

A general model to describe solute transport for both porous and nonporous membranes is given by the Kedem-Katchalsky model (21), in which the membrane is considered as a black box comprising feed and permeate as the input and output respectively. The flux of the solute through the membrane is described as:

$$J_c = P_c \Delta x \frac{dc}{dx} + (1 - \sigma)J_v \quad (4.1)$$

with  $J_c$  the solute flux,  $P_c$  the solute permeability,  $\Delta x$  the membrane thickness,  $\frac{dc}{dx}$  the concentration gradient over the membrane,  $\sigma$  the reflection coefficient, which is a measure for the rejection of a solute,  $J_c$  the solute flux, and  $J_v$  the solvent flux.

In Equation 4.1, the first term describes the transport of solutes by a diffusion mechanism, while the second term describes the transport of solutes by a convection mechanism. If the contribution of solute flux by diffusion is negligible, Equation 4.1 can be simplified to Equation 4.2 as follows

$$\sigma = 1 - \frac{J_c}{J_v} \quad (4.2)$$

Ferry et al. (22) proposed a solute transport model, which relates the reflection coefficient with the ratio of solute diameter versus pore diameter. In this model it is assumed that solutes, having similar or larger diameter than the membrane pore diameter, are completely rejected and solutes with smaller diameter than the effective diameter of the membrane pores are passing completely. The membrane pore diameter, as well as the diameter of the solute, are defined as average values rather than nominal values. Besides, no interaction between the membrane, solvent and solute is taken into account. Here, the reflection coefficient will develop from 0 to 1 as the ratio of  $d_c/d_p$  increases, with  $d_c$  the average solute diameter and  $d_p$  the mean pore diameter. This means  $\sigma = 0$  for  $d_c/d_p \geq 1$  and  $\sigma=1$  for  $d_c/d_p \leq 1$ . The model of Ferry describes  $\sigma$  in the following way:

$$\sigma = \left( \frac{d_c}{d_p} \left( \frac{d_c}{d_p} - 2 \right) \right)^2 \quad (4.3)$$

The Verniory model (23) considers that solutes with particle diameter smaller than the pore diameter of the membranes are partially rejected due to wall friction drag forces. The Verniory model can be written as:

$$\sigma = 1 - \left( \frac{1 - \frac{2d_c^2}{3d_p} - 0.2\frac{d_c^5}{d_p}}{1 - 0.76\frac{d_c^5}{d_p}} \right) \left( 1 - \frac{d_c}{d_p} \right)^2 \left( 2 - \left( 1 - \frac{d_c}{d_p} \right)^2 \right) \quad (4.4)$$

The Verniory model accounts for the wall friction occurring between the solute and membrane wall while no attractive forces between the solute and membrane are taken into account. The SHP model (24), instead, accounts for a rejection case in which the wall friction effect was negligible due to attractive forces between membrane and solute. As a consequence, solutes having a particle diameter larger than the pore diameter of the membranes were assumed to be partially disseminated. The SHP model is presented as:

$$\sigma = 1 - \left( 1 + \frac{16}{9} \frac{d_c^2}{d_p} \right) \left( 1 - \frac{d_c}{d_p} \right)^2 \left( 2 - \left( 1 - \frac{d_c}{d_p} \right)^2 \right) \quad (4.5)$$

In this work, the applicability of these models to describe the solute rejection behavior of the PDMS grafted  $\gamma$ -alumina membranes will be investigated.

### 4.3. Materials and Methods

Two types of polymer-grafted ceramic membranes were studied. The first series of membranes (M1) consisted of macroporous  $\alpha$ -Al<sub>2</sub>O<sub>3</sub> supports, topped with a 0.3  $\mu$ m thick mesoporous (pore size 5 nm)  $\gamma$ -Al<sub>2</sub>O<sub>3</sub> layer which was modified with 3-aminopropyltriethoxysilane followed by mono(2,3-epoxy)polyetherterminated polydimethylsiloxane ( $n \sim 10$ ). Details of the membrane modification procedure are described elsewhere (9).

The second series of membranes (M2) consisted of macroporous  $\alpha$ -Al<sub>2</sub>O<sub>3</sub> supports, topped with an identical 0.3  $\mu$ m thick mesoporous  $\gamma$ -Al<sub>2</sub>O<sub>3</sub> layer which was modified with mercaptopropyl triethoxysilane followed by monovinyl terminated polydimethylsiloxane ( $n \sim 39$ ). Details of this membrane modification procedure was described in (25). All membranes were flat discs with a diameter of 20 mm and a thickness of 2.5 mm.

The solvents, octane (98% purity), cyclooctane (>99%), p-xylene (>99%), and n-hexane (>99%) were purchased from Sigma-Aldrich. Toluene (100%), ethyl acetate (99.9 %), and isopropanol (100 %) were purchased from VWR. All solvents were dried using zeolite A (molecular mesh 4-8 nm) purchased from Sigma-Aldrich which had been pretreated for 1 hour at 200°C. As solutes, polyethylene glycol (PEG; Fluka) with molecular weights of 200, 400, 600, 1000, 1500, and 2000

g/mol, polystyrene (PS; Sigma-Aldrich) with molecular weights of 500, 1000, and 2000 as well as a series of dyes (Sigma-Aldrich) were used. The chemical structures of the dyes are given in Figure 4.1.

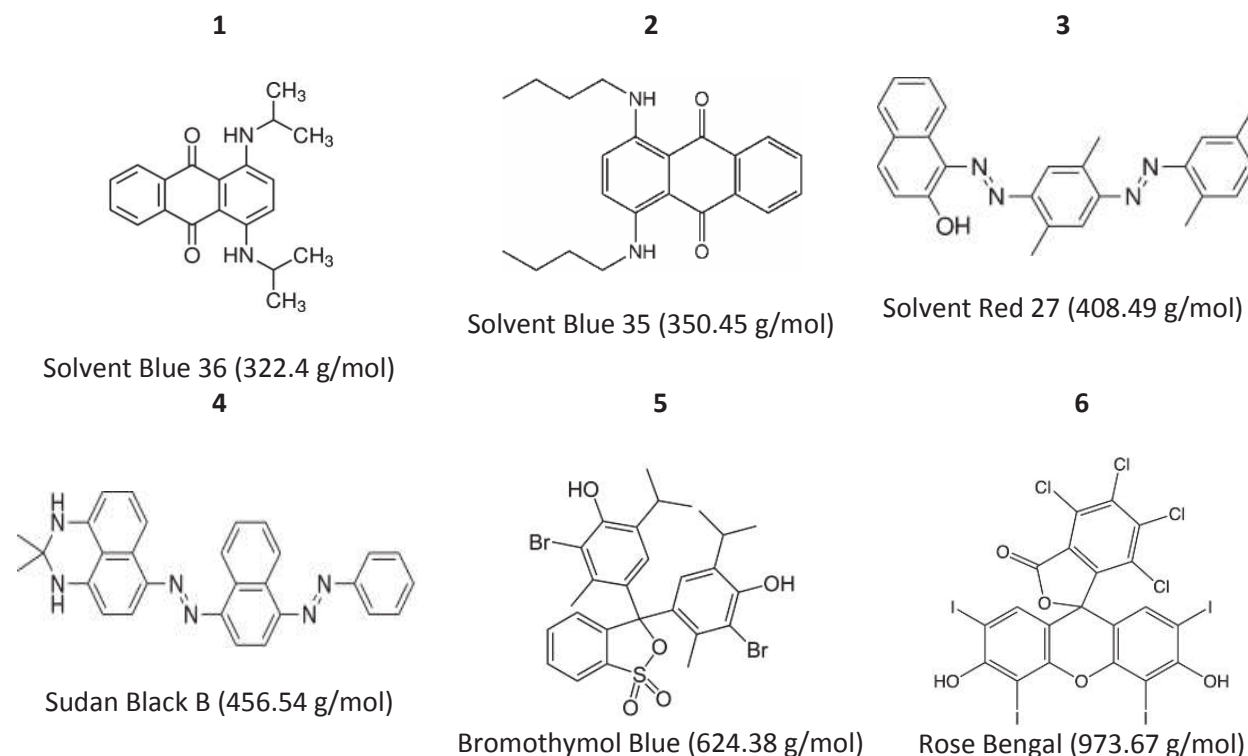


Figure 4.1. The chemical structures of the dyes used

The nanofiltration behavior of Sudan Black B was investigated for all solvents. All other dyes (except Rose Bengal) as well as PEG were studied in toluene and isopropanol, while SRNF selectivity for PS was only studied in toluene due to the insolubility of PS in isopropanol. Rose Bengal was only studied in isopropanol, due to its insolubility in toluene.

Molecular Weight Cut Off (MWCO) measurements were performed using a stainless steel dead-end pressure cell at a 50% recovery. The feed solution was constantly stirred at a speed of 500 rpm to prevent concentration polarization on the membrane surface. 8000 ppm of dye was used in the feed solution. The same solute concentration and procedure was used for PS and PEG samples for each MW. All measurements were performed on three different samples for each type of membrane with three measurements per sample. Between each rejection test, the membranes were rinsed with the previous solvent and subsequently three times ultrasonically cleaned in fresh ethanol 10 minutes at room temperature. After this ultrasonic treatment the membranes were dried in a vacuum oven under nitrogen for 24 hours at 80°C. After being cooled down to room temperature, the membranes were soaked for 24 hours in the solvent to be tested.

Dye solute concentrations in the feed and permeate solution were analyzed using a Perkin-Elmer  $\lambda$ 12 UV-Vis Spectrophotometer. The rejection ( $R$  in %) was calculated by the following equation:  $R = (1 - C_p/C_f) \times 100\%$ , where  $C_p$  and  $C_f$  are the solute concentrations in permeate and feed solution, respectively. PS and PEG solute concentrations in the feed and permeate solution were analyzed by a Thermo Electron Corporation HPLC coupled to an Evaporative Light Scattering Detector (ELSD 2000 ES). A nebulizer temperature of  $80^\circ\text{C}$ , a gas flow of  $2.5\text{ L/min}$ , a column temperature of  $30^\circ\text{C}$  and a sample volume of  $20\ \mu\text{L}$  were used for the ELSD. As eluent for the HPLC  $1\text{ mL/min}$  of THF was used. The feed and permeate solute concentration ( $C_f$  and  $C_p$ ) were determined as a function of total area from a plot of electric potential versus time. The rejection ( $R$ ) was calculated by the following equation:  $R = (1 - C_p/C_f) \times 100\%$ , where  $C_p$  and  $C_f$  are the solute concentrations in permeate and feed solution, respectively.

In order to check whether any concentration polarization occurs, the solvent permeation of blank feeds (pure solvents without solutes) and those with solutes were compared using a similar set-up. Permeate fluxes were obtained by measuring the weight of the collected permeate as a function of time.

#### 4.4. Results and Discussion

Figure 4.2 shows the results of rejection tests using Sudan Black B in different solvents using trans membrane pressures (TMP) ranging from 6 to 20 bars at 50% recovery.

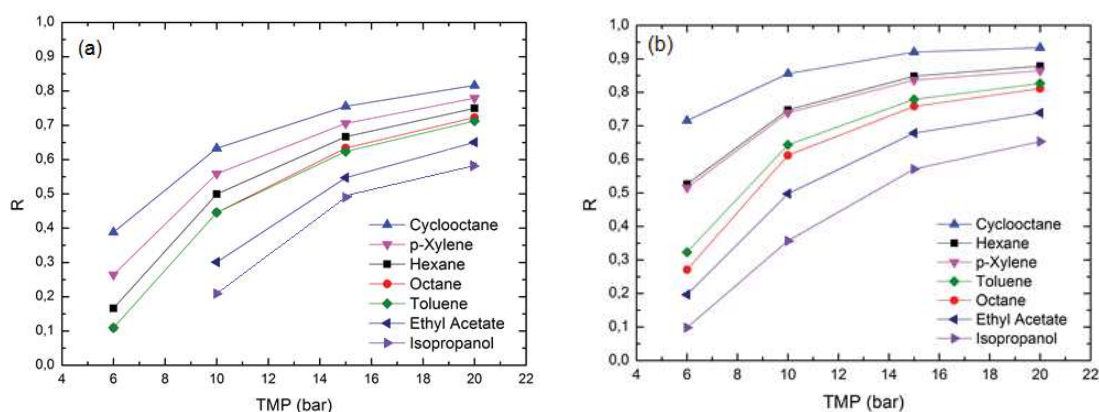


Figure 4.2. Rejection of Sudan Black B in different solvents versus TMPs at room temperature for a) M1 and b) M2 membranes at 50% recovery

From the results in Figure 4.2, it can be seen that dye rejection increases with increasing applied pressure regardless the type of solvents used. If a deformation of the polymer occurs, due to a shear induced behavior, then this results in a larger membrane pore diameter at increasing applied pressure and consequently a decrease in rejection. However, the opposite is found, namely an



increase in rejection at higher TMP. This is in agreement with the previous observation on the same type of membranes that a shear rate flow induced behavior is not present which might be due to the nanostructure of the rigid ceramic substrate causing a negligible shear at the pressure range studied (20).

Further it can be observed in Figure 4.2 that different rejections were found for the same Sudan Black B in different solvents. The highest rejection was found for Sudan Black B in cyclooctane, while the lowest rejection was found in isopropanol.

No significant differences were observed between the permeation of blank feeds (pure solvents without solutes) (20) and those with solutes, suggesting that no concentration polarization of solutes occurred during the measurements. In Table 4.1, rejection values ( $R$ ) of Sudan Black B at a TMP of 20 bars for M1 and M2 membranes at 50% recovery are given. In order to see whether there is a relation between the rejection and the solvent viscosity, the viscosity values are also given in Table 4.1. Another factor, which can influence the rejection, is the degree of polymer swelling as function of the type of solvent. A measure of polymer swelling is the solvent sorption ( $S$ ) by the polymer (PDMS) as defined in (20). Several solvent sorption values are given in Table 4.1.

Table 4.1. The rejection ( $R$ ) of Sudan Black B in different solvents for M1 and M2 membranes at TMP of 20 bar at 50% recovery

Solvent Types	$\mu^{(1)}$ (mPa.s)	$S^{(2)}$ $V_{s,i}$ (cm <sup>3</sup> /g)	$R_{M1}$ (%)	$R_{M2}$ (%)
Isopropanol	2.39	0.47	55 ± 1	66 ± 1
Ethyl acetate	0.45	0.48	64 ± 1	75 ± 1
Octane	0.54	0.54	71 ± 1	80 ± 1
Toluene	0.59	0.53	72 ± 1	83 ± 1
p-xylene	0.64	0.63	75 ± 1	87 ± 1
Hexane	0.31	0.66	78 ± 1	88 ± 1
Cyclooctane	2.13	0.70	82 ± 1	93 ± 1

(1) Solvent viscosity (at 20°C); (2) Sorption value as described in (20)

The results in Table 4.1 show that for solvents with comparable viscosity, e.g. isopropanol and cyclooctane, higher rejection is achieved for cyclooctane than isopropanol. In a previous study where pure solvent permeation was studied on the same membranes (20), it was indicated that both solvent viscosity and sorption of the solvent in the grafted moiety determine solvent transport through the membrane. It is possible that the sorbed solvent does not only influence the solvent transport, but also the solute rejection of the membrane. In this case, the relatively stronger sorption of cyclooctane in the grafted moiety compared to that of isopropanol may result in a

smaller membrane pore size in the presence of cyclohexane, thus a higher rejection observed in cyclohexane than isopropanol.

For free (or unconfined) PDMS polymeric membranes, a lower rejection is observed in the presence of toluene whereas a higher rejection is observed in the presence of isopropanol (16, 26-27). The results of the work described in this chapter, as summarized in Table 4.1, show the opposite behavior, meaning a higher solute rejection in toluene than in isopropanol for both types of PDMS grafted ceramic membranes (M1 and M2). This again emphasizes the different behavior of a “free” PDMS membrane compared to that of membranes where PDMS is confined in a ceramic matrix. For a “free” PDMS membrane, the sorption of solvent leads to swelling, thus a more open membrane structure, while for grafted membranes, it is suggested that a strongly sorbed solvent leads to a more closed structure of the grafted membranes (20). This may explain the higher solute rejection in the presence of toluene than that in the presence of isopropanol (see Table 4.1).

Besides the solvent-membrane interaction as discussed above, the solvent-solute and solute-membrane interactions may also play a role in the nanofiltration performance. Figure 4.3 shows the rejection for PEG in toluene and isopropanol and PS in toluene. No differences were observed between the solvent flux containing the probe solutes and that of the pure solvent showing that in this case also no concentration polarization occurred during the measurements.

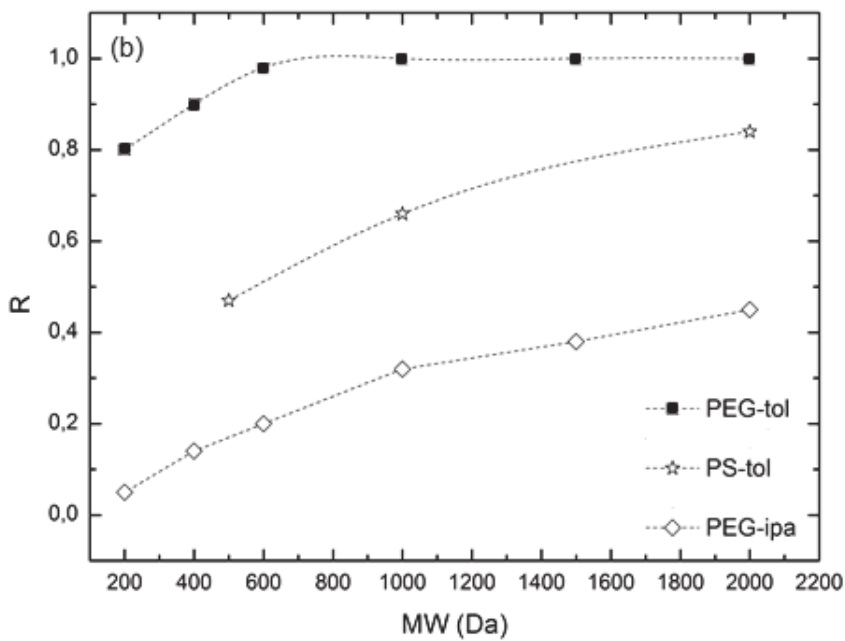
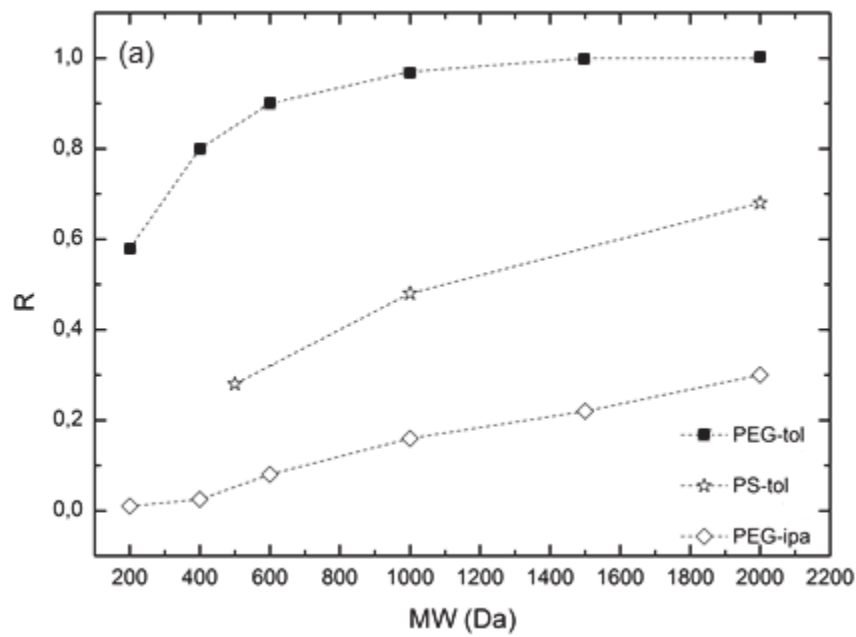


Figure 4.3. Rejection results of PEG and PS in toluene (*tol*) and isopropanol (*ipa*) at TMP = 10 bars for a) M1 and b) M2 membranes

It can be seen in Figure 4.3 that the solute rejection is a function of the solute molecular weight with a higher rejection for a higher solute molecular weight. The M1 membranes show in general a lower rejection than the M2 membranes for all solvent-solute systems. The results in Figure 4.3 also show

that the rejection differs for each solvent-solute pair for both membranes. A lower rejection is found for PEG in isopropanol, followed by PS in toluene with the highest rejection values for PEG in toluene.

The dependence of the rejection on the solute molecular weight suggests that the rejection is a function of solute size. This leads to the hypothesis that solute transport is according to a size based exclusion mechanism. To provide a quantitative comparison whether rejection can be described as a function of solute size and membrane pore diameter, the experimental rejection data were compared with the calculated values predicted by the three size-based exclusion solute transport models as described in section 2. The way these models quantitatively describe the membrane rejection behavior for different solvent-solute systems may provide insight in the identification of important parameters governing the transport of solutes through these types of membranes. In order to use these models, an appropriate approximation of the solute diameter and the membrane pore diameter is required.

The dynamic properties of oligomers moving in a solvent can be represented by the hydrodynamic diameter, as calculated from the Einstein viscosity relation (28):

$$r_h = \left( \frac{3[\eta]M_w}{4\pi 2.5N_A} \right)^{0.33} \quad (4.9)$$

with  $d_h$  is the hydrodynamic radius,  $\eta$  the intrinsic viscosity,  $M_w$  the molecular weight, and  $N_A$  Avogadro number. The intrinsic viscosity  $[\eta]$  can be calculated from the Mark-Houwink parameters using the following equation:

$$[\eta] = KM_w^\alpha \quad (4.10)$$

where  $K$  and  $\alpha$  are the Mark Houwink parameters, depending on the particular polymer-solvent system (28), and  $M_w$  the molecular weight in g/mol. The  $K$  and  $\alpha$  values for PS in toluene are 0.012 and 0.71 respectively (28). The  $K$  and  $\alpha$  values for PEG in toluene are 0.014 and 0.7, while for PEG in isopropanol these values are 0.07 and 0.57 (28) respectively. The calculated hydrodynamic diameters for PS in toluene, PEG in toluene, and PEG in isopropanol and the experimental rejection values are given in Table 4.2.

Table 4.2. Hydrodynamic diameters ( $d_H$ ) of various solutes as calculated by Equation 4.9 and 4.10 and the experimental rejection values at TMP = 10 bars in toluene or isopropanol for membranes M1 (=  $R_{M1}$ ) and M2 (=  $R_{M2}$ )

Solute	$M_w$ (g/mol)	Toluene			Isopropanol		
		$d_H$ (nm)	$R_{M1}$ (%)	$R_{M2}$ (%)	$d_H$ (nm)	$R_{M1}$ (%)	$R_{M2}$ (%)
PS	500	0.86	28 ± 1	47 ± 1	-	-	-
	1000	1.28	48 ± 1	66 ± 1	-	-	-
	2000	1.88	68 ± 1	84 ± 1	-	-	-
PEG	200	0.54	58 ± 1	80 ± 1	0.72	1 ± 1	5 ± 1
	400	0.78	80 ± 1	90 ± 1	1.02	3 ± 1	14 ± 1
	600	1.00	90 ± 1	98 ± 1	1.26	8 ± 1	20 ± 1
	1000	1.32	97 ± 1	100 ± 0	1.66	16 ± 1	32 ± 1
	1500	1.66	100 ± 0	100 ± 0	2.04	22 ± 1	38 ± 1
	2000	1.96	100 ± 0	100 ± 0	2.38	30 ± 1	45 ± 1

It can be seen from Table 4.2 that the rejection increases when the solute diameter increases, meaning that a size-exclusion rejection mechanism is appropriate.

The rejection of the several dyes in toluene or isopropanol is summarized in Table 4.3. The average molecular diameter of the dye solutes is calculated by using the *CS 3D Model* software by taking into account the bond length, the corresponding Van der Waals radius, and the bond angle as given in (29-30). Since the dye solute can be positioned in different conformations when approaching the membrane pores and assuming that the different conformations may have a similar probability to occur (31), an average value for each type of dye is used, representing the average size of the solute molecular diameter in the axial, horizontal and lateral direction. These calculated average molecular diameters are also given in Table 4.3.

Table 4.3. Average molecular diameter ( $d_{avg}$ ) of the dye solutes and its experimental rejection values at TMP = 10 bar in toluene or isopropanol for membranes M1 (=  $R_{M1}$ ) and M2 (=  $R_{M2}$ )

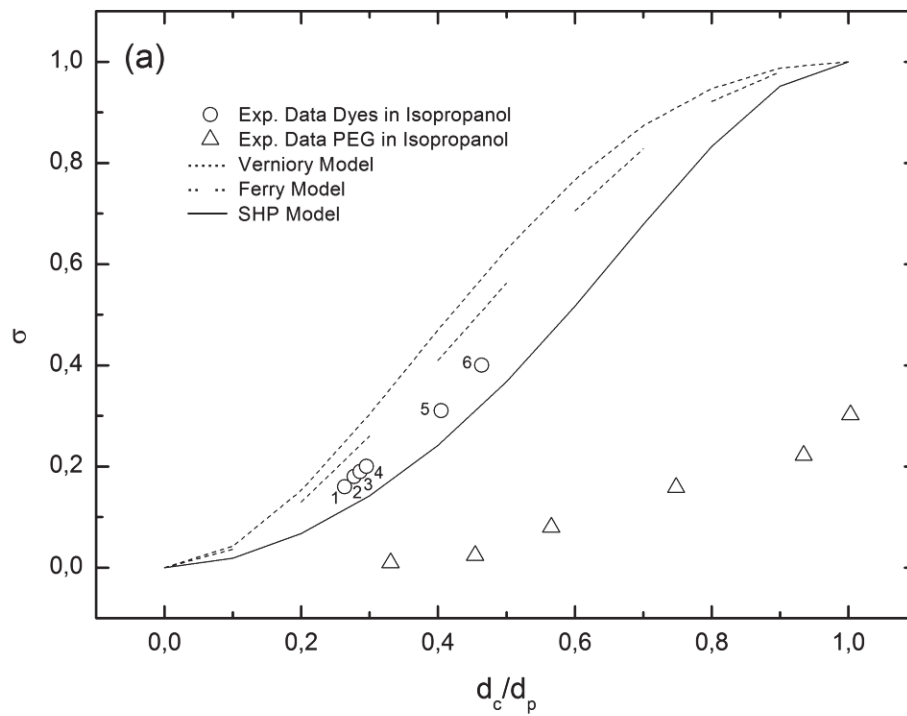
Solute	$d_{avg}$ (nm)	Toluene		Isopropanol	
		$R_{M1}$ (%)	$R_{M2}$ (%)	$R_{M1}$ (%)	$R_{M2}$ (%)
Solvent blue 35	0.58	40 ± 1	55 ± 1	16 ± 1	28 ± 1
Solvent blue 36	0.61	44 ± 1	60 ± 1	18 ± 1	31 ± 1
Solvent Red 27	0.63	46 ± 1	62 ± 1	19 ± 1	33 ± 1
Sudan Black B	0.65	45 ± 1	64 ± 1	20 ± 1	35 ± 1
Bromothymol blue	0.89	65 ± 1	81 ± 1	31 ± 1	53 ± 1
Rose bengal	1.02	-	-	40 ± 1	65 ± 1

Also from Table 4.3 it can be logically seen that the rejection increases when the solute diameter increases. Since the size-exclusion separation mechanism is dependent on the pore size besides the size of solute (as can be seen in Equation 4.3, 4.4, and 4.5), an actual pore size of the membranes is required under the experimental conditions with regard to the solvent used. As a first approximation, the analysis of nitrogen adsorption/desorption isotherms on grafted  $\gamma$ -alumina was used to obtain a pore diameter value, which is an indication of the actual pore diameter of the grafted M1 and M2 membranes in the presence of no solvent (32). Based on the  $N_2$  physisorption isotherms of the M1 and M2 grafted  $\gamma$ -alumina flakes, uniform pores were observed with the estimated pore diameter of 2.2 nm for the grafted M1  $\gamma$ -alumina flakes (32) and 1.8 nm for the grafted M2  $\gamma$ -alumina flakes. These pore size values can be regarded as the diameter of the pores of PDMS-grafted membranes under dry, non-swollen, conditions.

At a first approximation, the reflection coefficient ( $\sigma$ ) values, as described in the the Ferry (Equation 4.3), the Verniory (Equation 4.4) and the SHP model (Equation 4.5), can be calculated by using the solute diameters as given in Tables 4.2 and 4.3 and the membrane pore diameter in the dry, non-swollen state, as provided by the nitrogen physisorption measurements on the grafted  $\gamma$ - $Al_2O_3$  flakes. The reflection coefficient (or rejection values), calculated from the solute transport models ( $\sigma = R_{predicted}$ ) can then be compared with the rejection data obtained experimentally ( $\sigma = R_{exp}$ ). In this regard, the predicted  $\sigma$  by the solute transport model is assumed to be representative for the rejection observed when there is no solvent present. Thus, this comparison can give information of the actual membrane pore diameter ( $d_p$ ) in the presence of a specific solvent. If for example the

experimental rejection results are higher than those calculated by the models, it means that the actual  $d_p$  in the presence of that specific solvent is smaller than the  $d_p$  when no solvent is present.

A comparison of the experimental results with the calculated rejection values for the solutes in isopropanol system is presented in Figure 4.4.



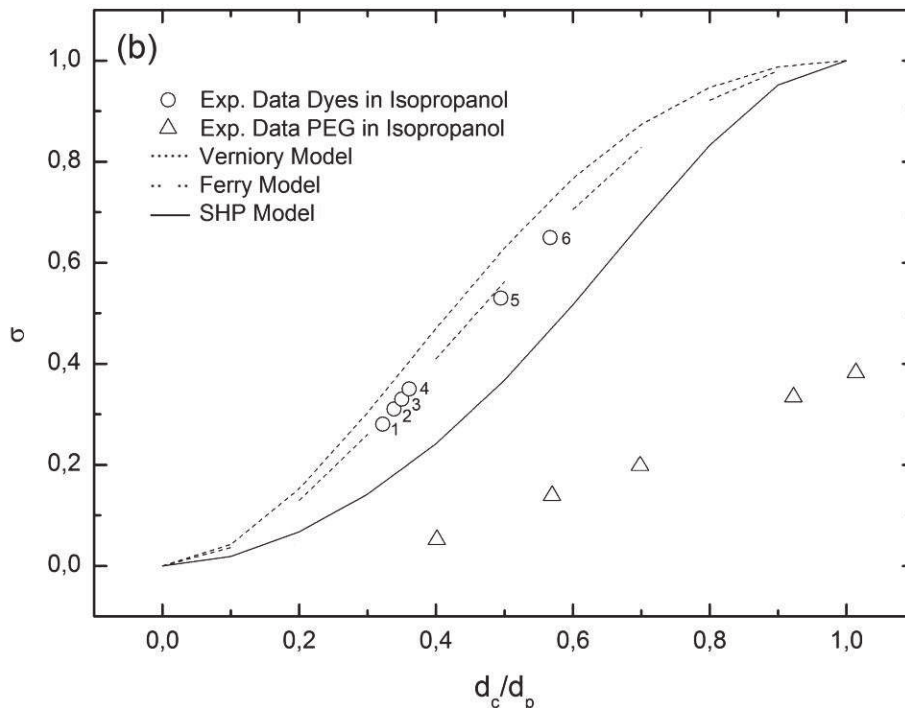


Figure 4.4. Comparison of experimental rejection results with the calculated rejection values from the Verniory, Ferry and SHP model for different solutes in isopropanol for a) M1 ( $d_p = 2.2$  nm) b) M2 ( $d_p = 1.8$  nm) membranes. The number of the dyes (1-6) refer to the numbers as given in Figure 4.1. PEG with  $M_w$  of 200-2000 is shown in (a) while PEG with  $M_w$  of 200-1500 is shown in (b).

For both membranes, it can be seen in Figure 4.4 that for the dye solutes in isopropanol, the experimental data fall in the range of the predicted  $\sigma$  by the solute transport models. For the M2 membranes the results almost coincide with the Ferry model. The pore diameter ( $d_p$ ) of the M1 and M2 membrane in the presence of isopropanol, as calculated by the Ferry model (Equation 4.3), are respectively 2.5 and 1.8 nm, using the experimental rejection data of the several dyes in isopropanol and the  $d_c$  of the dyes given in Table 4.3. These calculated pore diameters are is close to the pore diameters as determined by  $N_2$  physisorption measurements. This may imply that, assuming there is no important solvent-solute or solute-membrane interaction present in the observed rejection behavior, the membrane actual pore diameter in the presence of isopropanol can be described with the pore diameter when no solvent is present. This means that for a rather polar solvent, like isopropanol, no strong solvent sorption by the grafted PDMS moiety occurs, resulting in almost no decrease in pore size by swelling. This seems in contradiction to a previous study, in which isopropanol sorption does occur though in lesser degree than that of toluene, meaning that the



membrane pore diameter in the presence of isopropanol should not be comparable, but should be slightly smaller, than that predicted when no solvent is present (20). This contradiction along with the slightly different observation between Figure 4.4a and b with regard to the comparison of the experimental data and the solute transport models for dyes and PEG in isopropanol, may highlight the complexity of the system in the presence of isopropanol. The interaction between the dyes and the grafted moiety, as well as between the dyes and isopropanol, must be investigated further as they may mask the contribution of the membrane-solvent interaction alone on the membrane selectivity.

In Figure 4.4, it can be seen that for both M1 and M2 system, the rejection of PEG in isopropanol as a function of  $d_c/d_p$  is lower than that of dyes in isopropanol. The lower rejection of PEG in isopropanol can be attributed to a strong solute-solvent interaction. A strong solute-solvent interaction may occur between the PEG and isopropanol due to the hydrogen bonding. Hydrogen bonding between the PEG solutes and the isopropanol may increase the flexibility of PEG, resulting in a decrease in solute rejection. Based on the experimental rejection data the diameter of the PEG is calculated to be 0.3-0.4 its hydrodynamic diameter, assuming that the rejection of PEG can be modeled by Ferry.

A comparison of the experimental results ( $\sigma=R_{experimental}$ ) of all solutes in toluene for M1 and M2 membranes with the calculated rejection values ( $\sigma=R_{predicted}$ ) using the Ferry, SHP, and Verniory model is given in Figure 4.5.

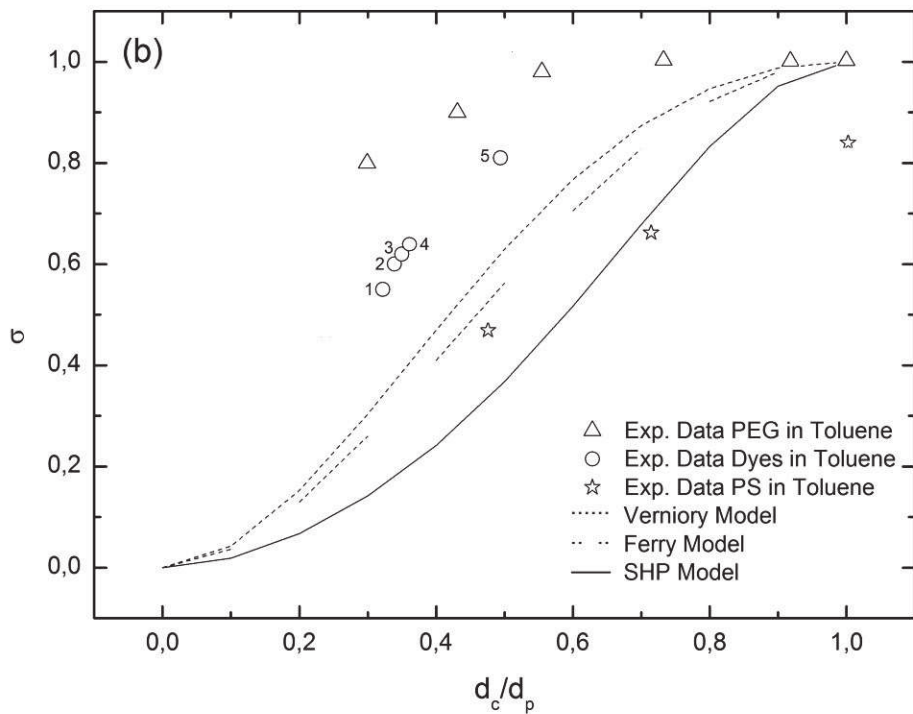
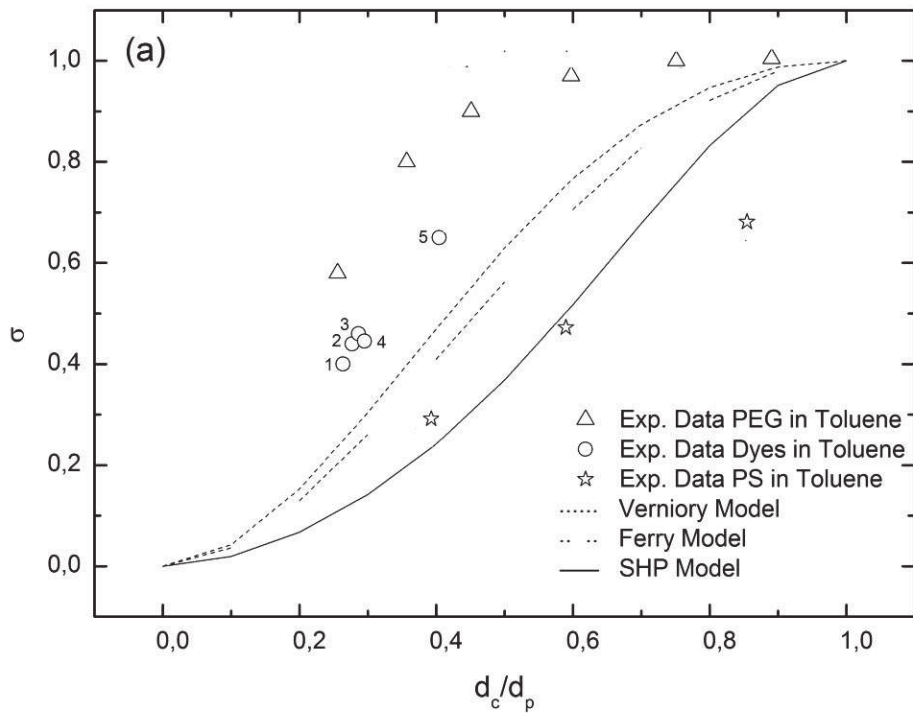


Figure 4.5. Comparison of the experimental rejection results ( $\sigma=R_{\text{experimental}}$ ) with the calculated rejection values ( $\sigma=R_{\text{predicted}}$ ) from the Ferry, SHP, and Verniory model for solutes in toluene for a) M1

b) M2 membranes. The number of the dyes refer to the numbers as given in Figure 4.1. PEG with  $M_w$  of 200-2000 is shown in (a) and (b).

Figure 4.5 shows that for the toluene-solute systems the experimental data are far above the predicted  $\sigma$  values for all transport models used. Further on, as can be seen from the figures 4.2, 4.4 and 4.5 rejection of the dyes in toluene is much higher than in isopropanol. This may suggest that the actual membrane pore diameter ( $d_p$ ) is much smaller in the presence of toluene than isopropanol. Assuming that the Ferry model is applicable to describe rejection of the dyes in toluene for M1 and M2 membranes,  $d_p$  of these membranes in toluene can be calculated by Equation 4.3, using the experimental rejection results and  $d_c$  values of the dyes as given in Table 4.3. In this way a pore diameter of 1.6 nm for M1 membranes and 1.3 nm for M2 membranes in the presence of toluene was determined.

From Figure 4.5 it can be seen that rejection of PS is lower than that of the dyes in toluene. A strong solvent-solute interaction may increase the flexibility of PS, resulting in a decrease in solute rejection. Based on the experimental rejection data, the diameter of the PS is calculated to be 0.7-0.9 its hydrodynamic diameter, assuming that the rejection of PS can be modeled by Ferry.

Finally, at a given  $d_c/d_p$  value, the rejection of PEG in toluene is higher than that of the dyes in toluene (Figure 4.5). This is just the other way around when compared to the rejection behavior of PEG in isopropanol (see Figure 4.4), where the rejection of PEG is lower than that of the dyes. The different order of PEG rejection as compared to those of dyes in the two different solvents might be attributed to the hydrophilicity of PEG. Hydrophilic PEG solutes may form clusters in the presence of nonpolar solvents like toluene by means of hydrogen bonds between the PEG solutes. In turn, this will cause a higher rejection of PEG in toluene (than that of the non-hydrogen-bonded dyes in toluene) since the diameter of a PEG cluster is larger than that of a calculated single PEG solute. Based on the experimental rejection data the diameter of the PEG clusters in toluene can be calculated to be 1.6-2 times that of a single PEG solute, assuming that the rejection of PEG follows the same mechanism as that of the dyes.

#### 4.5. Conclusions

For PDMS-grafted  $\gamma$ -alumina ceramic membranes higher rejection values of an identical solute were found in the presence of nonpolar solvents, like toluene, than in polar solvents, like isopropanol. A relation was observed between solute rejection and the ratio of solute diameter versus membrane pore diameter, indicating that a size-exclusion mechanism may be applicable to describe the membrane solute rejection.

The Ferry, Verniory, and SHP size-exclusion models were used to identify the rejection characteristics of these membranes. For the dye solutes in isopropanol, the experimental rejection data are in the range of the predicted rejection ( $\sigma$ ) as based on all three models, using the pore diameter information, obtained from N<sub>2</sub> physisorption measurements when no solvent is present. This is an indication that polar solvents, like isopropanol, do not significantly swell the PDMS in its confined, ceramic environment. No further conclusion can be drawn as the interactions between the dyes and the grafted moiety, as well as between the dyes and isopropanol, must be investigated further to see, as these effects may mask the contribution of the membrane-solvent interaction on membrane selectivity.

If using the pore diameter, obtained from N<sub>2</sub> physisorption measurements, the calculated rejections of the dyes or PEG by using the three solute transport models in toluene were much lower than experimentally observed. This is an indication of a more closed pore structure of the membranes in toluene than in isopropanol, caused by a strong swelling of PDMS in the apolar solvent. The higher rejection of PEG in toluene than that of the dyes may be attributed to the ability of the hydrophilic PEG solutes to form clusters in the presence of nonpolar solvents, such as toluene, by means of internal hydrogen bonds.

### **Acknowledgement**

The authors acknowledge the financial support from the European Union – The Education, Audiovisual and Culture Executive Agency (EACEA) under the Program “Erasmus Mundus Doctorate in Membrane Engineering” – EUDIME (FPA 2011-2014) and an I.A.P. grant supported by the Belgian Government under Supramolecular Analysis.

### **References**

1. Vandezande, P., Gevers, L. E. M., and Vankelecom, I. F. J. (2008) Solvent resistant nanofiltration: Separating on a molecular level, *Chemical Society Reviews* 37, 365-405.
2. Marchetti, P., Jimenez Solomon, M. F., Szekely, G., and Livingston, A. G. (2014) Molecular Separation with Organic Solvent Nanofiltration: A Critical Review, *Chemical Reviews* 114, 10735-10806.
3. Leger, C., De Lira, H. L., and Paterson, R. (1996) Preparation and properties of surface modified ceramic membranes. Part II. Gas and liquid permeabilities of 5 nm alumina membranes modified by a monolayer of bound polydimethylsiloxane (PDMS) silicone oil, *Journal of Membrane Science* 120, 135-146.
4. Faibish, R. S., and Cohen, Y. (2001) Fouling-resistant ceramic-supported polymer membranes for ultrafiltration of oil-in-water microemulsions, *Journal of Membrane Science* 185, 129-143.

5. Yoshida, W., and Cohen, Y. (2003) Ceramic-supported polymer membranes for pervaporation of binary organic/organic mixtures, *Journal of Membrane Science* 213, 145-157.
6. Yoshida, W., and Cohen, Y. (2004) Removal of methyl tert-butyl ether from water by pervaporation using ceramic-supported polymer membranes, *Journal of Membrane Science* 229, 27-32.
7. Popat, K. C., Mor, G., Grimes, C. A., and Desai, T. A. (2004) Surface Modification of Nanoporous Alumina Surfaces with Poly(ethylene glycol), *Langmuir* 20, 8035-8041.
8. Sang Won, L., Hao, S., Richard, T. H., Vania, P., and Gil, U. L. (2005) Transport and functional behaviour of poly(ethylene glycol)-modified nanoporous alumina membranes, *Nanotechnology* 16, 1335.
9. Pinheiro, A. F. M., Hoogendoorn, D., Nijmeijer, A., and Winnubst, L. (2014) Development of a PDMS-grafted alumina membrane and its evaluation as solvent resistant nanofiltration membrane, *Journal of Membrane Science* 463, 24-32.
10. Tanardi, C. R., Pinheiro, A. F. M., Nijmeijer, A., and Winnubst, L. (2014) PDMS grafting of mesoporous  $\gamma$ -alumina membranes for nanofiltration of organic solvents, *Journal of Membrane Science* 469, 471-477.
11. Darvishmanesh, S., Degreève, J., and Van Der Bruggen, B. (2010) Mechanisms of solute rejection in solvent resistant nanofiltration: The effect of solvent on solute rejection, *Physical Chemistry Chemical Physics* 12, 13333-13342.
12. Yang, X. J., Livingston, A. G., and Freitas dos Santos, L. (2001) Experimental observations of nanofiltration with organic solvents, *J. Membr. Sci.* 190, 45-55.
13. Mulder, M. (1996) *Basic principles of membrane technology*, 2nd ed., Kluwer Academic Publisher, Netherlands.
14. Wang, J., Dlamini, D. S., Mishra, A. K., Pendergast, M. T. M., Wong, M. C. Y., Mamba, B. B., Freger, V., Verliefe, A. R. D., and Hoek, E. M. V. (2014) A critical review of transport through osmotic membranes, *J. Membr. Sci.* 454, 516-537.
15. Jonsson, G. (1980) Overview of theories for water and solute transport in UF/RO membranes, *Desalination* 35, 21-38.
16. Vankelecom, I. F. J., De Smet, K., Gevers, L. E. M., Livingston, A., Nair, D., Aerts, S., Kuypers, S., and Jacobs, P. A. (2004) Physico-chemical interpretation of the SRNF transport mechanism for solvents through dense silicone membranes, *Journal of Membrane Science* 231, 99-108.
17. Robinson, J. P., Tarleton, E. S., Millington, C. R., and Nijmeijer, A. (2004) Solvent flux through dense polymeric nanofiltration membranes, *Journal of Membrane Science* 230, 29-37.
18. Zeidler, S., Kätzel, U., and Kreis, P. (2013) Systematic investigation on the influence of solutes on the separation behavior of a PDMS membrane in organic solvent nanofiltration, *Journal of Membrane Science* 429, 295-303.
19. Postel, S., Spalding, G., Chirnside, M., and Wessling, M. (2013) On negative retentions in organic solvent nanofiltration, *Journal of Membrane Science* 447, 57-65.

20. Tanardi, C. R., Vankelecom, I. F. J., Pinheiro, A. F. M., Tetala, K. K. R., Nijmeijer, A., and Winnubst, L. (2015) Solvent Permeation Behavior of PDMS Grafted  $\gamma$ -Alumina Membranes.
21. Kedem, O., and Katchalsky, A. (1958) Thermodynamic analysis of the permeability of biological membranes to non-electrolytes, *Biochimica et Biophysica Acta* 27, 229-246.
22. Ferry, J. D. (1936) Ultrafilter membranes and ultrafiltration, *Chemical Reviews* 18, 373-455.
23. Verniory, A., du Bois, R., Decoodt, P., Gasee, J. P., and Lambert, P. P. (1973) Measurement of the permeability of biological membranes. Application to the glomerular wall, *Journal of General Physiology* 62, 489-507.
24. Nakao, S.-I., and Kimura, S. (1982) Models of membrane transport phenomena and their applications for ultrafiltration data, *Journal of Chemical Engineering of Japan* 15, 200-205.
25. Tanardi, C. R., Pinheiro, A. F. M., Nijmeijer, A., and Winnubst, L. PDMS Grafting of Mesoporous  $\gamma$ -Alumina Membranes for Nanofiltration of Organic Solvents.
26. Paul, D. R., and Ebra-Lima, O. M. (1970) Pressure-induced diffusion of organic liquids through highly swollen polymer membranes, *Journal of Applied Polymer Science* 14, 2201-2224.
27. Paul, D. R., Paciotti, J. D., and Ebra-Lima, O. M. (1975) Hydraulic permeation of liquids through swollen polymeric networks. II. Liquid mixtures, *Journal of Applied Polymer Science* 19, 1837-1845.
28. Mark, J. E. (1999) *Polymer Data Handbook*, Oxford University Press, Oxford.
29. Allen, F. H., Kennard, O., Watson, D. G., Brammer, L., Orpen, A. G., and Taylor, R. (1987) Tables of bond lengths determined by X-ray and neutron diffraction. Part 1. Bond lengths in organic compounds, *Journal of the Chemical Society, Perkin Transactions 2*, S1-S19.
30. Bondi, A. (1964) van der Waals Volumes and Radii, *The Journal of Physical Chemistry* 68, 441-451.
31. Santos, J. L. C., de Beukelaar, P., Vankelecom, I. F. J., Velizarov, S., and Crespo, J. G. (2006) Effect of solute geometry and orientation on the rejection of uncharged compounds by nanofiltration, *Separation and Purification Technology* 50, 122-131.
32. Pinheiro, A. F. M. (2013) Development and Characterization of Polymer-grafted Ceramic Membranes for Solvent Nanofiltration, In *PhD Thesis*, University of Twente, Enschede.

# Chapter 5

## **Coupled-PDMS Grafted Mesoporous $\gamma$ -Alumina Membranes for Solvent Nanofiltration**

This chapter has been submitted for publication as:

Tanardi, C. R., Nijmeijer, A., and Winnubst, L. Coupled-PDMS Grafted Mesoporous  $\gamma$ -Alumina Membranes for Solvent Nanofiltration.

## Abstract

In this paper grafting of mesoporous  $\gamma$ -alumina membranes with hydride terminated polydimethylsiloxane is described. Vinyltriethoxysilane is used as linking agent and tetrakis(vinyl dimethylsiloxy)silane as a coupling agent, to create a dense network structure that is grafted in the ceramic pores. Grafting performance of the organic moieties on  $\gamma$ -alumina powders was analyzed by FTIR and TGA. The results indicate that grafting reactions were successfully carried out. SEM-EDX and contact angle analysis on the grafted membranes showed that grafting occurs throughout the  $\gamma$ -alumina layer and that the resulting membrane surface had a water contact angle of  $108^\circ$ . From permeability and rejection tests using Sudan Black in toluene, ethyl acetate or isopropanol, the use of a coupling agent was found to result in a more dense network structure grafted in the gamma alumina pores. This resulted in a higher selectivity for nanofiltration of solvents but at the cost of a lower solvent permeability, when compared with PDMS-grafted alumina membranes where no coupling of PDMS was applied.



## 5.1. Introduction

Organic Solvent Nanofiltration (OSN) is a potential technology to recover solvents (1-2). For this application, a chemically stable membrane is required that can endure continuous exposure towards organic solvents. Grafting of porous ceramic substrates by an organic moiety is an interesting way to prepare chemically and mechanically stable membranes for nanofiltration of solvents (3-4). During organic grafting of oxide ceramic membranes the OH-groups that are present at the oxide surface, react with hydrolysable groups from an organic moiety to produce a stable covalent bond. Most work done in this area describes a two-step reaction, in which the surface hydroxyl groups are first reacted with organosilanes to provide reactive sites for the organic moiety to be grafted (3-9).

Several examples of membrane preparation by organic grafting of ceramic membranes are given in literature (3-10). Pinheiro et al. (3) and Tanardi et al. (4) graft low molecular weight (MW) PDMS to silylated  $\gamma$ -alumina porous supports (pore size 5 nm) for the fabrication of nanofiltration membranes. Here a "grafting to" method was used, in which a low MW polymer was grafted to the ceramic mesoporous substrate without additional growing of the organic chain from the surface of the pore wall. Another way of grafting is the "grafting from" method where the polymer chains are synthesized from the monomer molecules by initiating chain growth from an active centre on the ceramic surface, e.g. via free radical polymerization between the organic molecules in order to result in a as small as possible membrane pore diameter (5-7). Faibish et al. (5) used free-radical graft polymerization of vinylpyrrolidone monomers to grow the organic layer during grafting of silylated zirconia membranes for the fabrication of ultrafiltration membranes. This way of grafting resulted in a reduction in pore size of around 25 %. Yoshida et al. made a layer of a terminally bonded polymer via free radical graft polymerization of vinyl acetate or vinyl pyrrolidone monomers on the silylated surface of gamma alumina tubular support (pore size 5 nm) (6) and silica membranes (pore size of 20 nm) (7) for pervaporation application. Besides free-radical polymerization, another way to increase the thickness of the grafted organic layer is by means of reactions between organic molecules and a coupling agent. Popat et al. (8) and Lee et al. (9) employed a catalyzed covalent reaction between low MW poly(ethylene glycol) and a coupling agent (in this case silicon tetrachloride) so that the organic chain was grown from

the surface of the pore wall during the grafting of straight pore alumina (“anodisc”) membranes to be used for ultrafiltration.

Different from (3) and (4), in which a low MW PDMS was grafted to the ceramic mesoporous substrate without additional covalent coupling for growing of the organic chain from the pore wall, in this work a covalent reaction between PDMS molecules and a coupling agent was used in order to result in a more dense organic network grafted inside the pores. It is expected that this method may lead to a smaller membrane pore diameter compared to the results given in (3) and (4) to accommodate the need for removing very small impurities during solvent recycling.

In this paper the grafting of mesoporous  $\gamma$ -alumina membranes with hydride terminated polydimethylsiloxanes is described. Vinyltriethoxysilane is used as linking agent and tetrakis(vinyldimethylsiloxy)silane as coupling agent, in order to generate a membrane for solvent nanofiltration. The grafting behaviour of the organic moiety was studied by Fourier Transform Infrared spectroscopy (FTIR) and TGA. Contact angle measurements and SEM-EDX analyses were used to characterize the grafted membrane properties. Permeation tests with toluene, isopropanol, and ethyl acetate, as well as rejection tests with Sudan Black B were performed to characterize the membrane performance.

## 5.2. Experimental procedure

Anhydrous toluene, ethyl acetate, and isopropanol were obtained from Sigma-Aldrich. Vinyltriethoxysilane and Tetrakis(vinyldimethylsiloxy)silane were purchased from ABCR. Hydride terminated polydimethylsiloxane (PDMS), with an average number of repeating monomers ( $n$ ) of 10, was purchased from Gelest. All chemicals were used as received. Flat  $\alpha$ - $\text{Al}_2\text{O}_3$  supported  $\gamma$ - $\text{Al}_2\text{O}_3$  membranes with a diameter of 39 mm were purchased from Pervatech. The mean pore diameter of the 3  $\mu\text{m}$  thick  $\gamma$ - $\text{Al}_2\text{O}_3$  layer and the 1.7 mm thick  $\alpha$ - $\text{Al}_2\text{O}_3$  support were 5 nm and 80 nm, respectively (11-12). The  $\gamma$ - $\text{Al}_2\text{O}_3$  powder was bought from Alfa-Aesar, having a BET surface area of 84.38  $\text{m}^2/\text{g}$ .

The unmodified  $\gamma$ - $\text{Al}_2\text{O}_3$  membranes were soaked in an ethanol/water (2:1) solution for 24 hours at ambient temperature to remove dust and provide suitable hydroxylation. The

membranes were then dried at 100°C for 24 hours under vacuum and stored at room temperature under nitrogen atmosphere until further use.

Inside a glove box, under nitrogen atmosphere, a 100 ml toluene solution of 25 mM of the linking agent, vinyltriethoxysilane, was prepared in a 250 ml five-necked round flask. After removing the linking agent/toluene solution from the glove box a  $\gamma$ -Al<sub>2</sub>O<sub>3</sub> membrane was placed in a sample holder located a few centimeters above the vinyltriethoxysilane solution. The solution was stirred and heated to perform the grafting reaction between vinyltriethoxysilane vapour and  $\gamma$ -Al<sub>2</sub>O<sub>3</sub> at 90°C for 4 hours under nitrogen flow. Details on this Vapour Phase Deposition (VPD) method are provided elsewhere (3, 13). After the reaction mixture was allowed to cool down to room temperature, the membrane was retrieved from the sample holder and rinsed with toluene before being dried in a vacuum oven at 100°C for 2 hours.

Grafting of PDMS combined with the coupling agent tetrakis(vinyldimethylsiloxy)silane was performed through hydrosilylation (14) on the vinyl grafted membranes by a solution phase deposition (SPD) method. A 100 ml solution of 37.5 mM of hydride terminated PDMS in toluene was added under stirring at room temperature to a 500 ml flask containing a vinyl-grafted membrane, submerged in toluene. A 100 ml solution of 12.5 mM tetrakis(vinyldimethylsiloxy)silane was added under stirring to this solution, and subsequently 10 mg of a Pt catalyst (50% of Pt-divinyltetramethyldisiloxane complex and 50% of Pt-cyclovinylmethylsiloxane complex, Fluka) was added to this solution under stirring. The mixture was heated under reflux at 60 °C for 0.5 h to initiate the addition reaction between the vinyl groups of the linker and coupling agent with the hydride terminated PDMS. Afterwards, the membrane was retrieved from the solution and rinsed three times with toluene, dried overnight in a fumehood and further dried at 100°C in a vacuum oven for 2 hours.

In order to study the grafting performance of  $\gamma$ -Al<sub>2</sub>O<sub>3</sub> by means of FTIR, a  $\gamma$ -Al<sub>2</sub>O<sub>3</sub> powder was used as starting inorganic material. To remove dust and provide suitable hydroxylation, the  $\gamma$ -Al<sub>2</sub>O<sub>3</sub> powder was soaked in an ethanol/water (2:1) solution for 24 hours at ambient temperature. The powder was then dried at 100°C for 24 h under vacuum and stored under

nitrogen atmosphere prior to grafting. Grafting of the  $\gamma$ -Al<sub>2</sub>O<sub>3</sub> powder was performed as follows. Inside a glove box, under nitrogen atmosphere, a 100 ml solution of 25 mM vinyltriethoxysilane in anhydrous toluene was prepared in a 250 ml two-necked round flask. The round flask was removed from the glove box and connected with an U-shaped glass tube to another 250 ml round flask where 600 mg of  $\gamma$ -Al<sub>2</sub>O<sub>3</sub> powder was placed. Both flasks were heated at 90°C for 4 hours under nitrogen flow to allow the grafting reaction between vinyltriethoxysilane vapor and  $\gamma$ -Al<sub>2</sub>O<sub>3</sub>. Details on this vapor phase deposition (VPD) method are given elsewhere (13, 15). After 4 hours, both flasks were cooled to ambient temperature. Immediately after, the modified powder was retrieved and rinsed with toluene to remove any physically absorbed vinyltriethoxysilane. The powder was further dried for 2 hours at 100°C in a nitrogen vacuum oven.

Grafting of PDMS coupled with tetrakis(vinyl dimethylsiloxy)silane was performed on the vinyl grafted powder by a solution phase deposition (SPD) method. A 100 ml solution of 37.5 mM of hydride terminated PDMS in toluene was added to a 500 ml flask containing a submerged vinyl grafted powder at room temperature. A 100 ml solution of 12.5 mM tetrakis(vinyl dimethylsiloxy)silane was added to the solution and stirred. 10 mg of Pt catalyst (1 : 1 of Pt-divinyltetramethyldisiloxane complex and Pt-cyclovinylmethylsiloxane complex) was added to this solution under stirring. The mixture was heated under reflux at 60 °C for 0.5 h to initiate the addition reaction between the vinyl groups of the linker and coupling agent with the hydride terminated PDMS. Afterwards, the powder was retrieved from the solution and rinsed with toluene before being dried overnight in the fume hood before being dried at 100°C in a vacuum oven for 2 hours.

### *Characterization*

FTIR analysis was performed using a Bruker Optik GmbH Tensor 27 TGA-IR spectrometer equipped with a universal ATR polarization accessory. The FTIR spectra were recorded at room temperature over a scanning range of 700-3000 cm<sup>-1</sup> with a resolution of 4.0 cm<sup>-1</sup>. The grafted  $\gamma$ -Al<sub>2</sub>O<sub>3</sub> powder sample is considered to have the same chemical characteristics as the actual  $\gamma$ -Al<sub>2</sub>O<sub>3</sub> membrane and therefore can be used to describe the chemical reactions that occur between ceramic membrane and grafting agent.

Thermogravimetric analysis on the PDMS-grafted powder was conducted from room temperature until 700°C in nitrogen. The measurement was performed at a heating rate of 10°C per minute.

Water contact angles of the membrane surfaces were measured by the sessile drop method to evaluate the surface wettability for grafted and ungrafted membranes. 5  $\mu\text{L}$  *Millipore Q2* water was dropped at a speed of 2  $\mu\text{L s}^{-1}$  on a membrane surface using a *Hamilton Microliter* syringe. The water contact angle data were collected by the Data Physics Optical Contact Angle instrument (OCA 20).

Morphologies of the membranes were observed by scanning electron microscopy (SEM-EDX, Thermo NORAN Instruments).

Solvent permeation tests were carried out at room temperature using a dead-end pressure cell made from stainless steel. Membranes to be tested were soaked in the organic solvent for 12 hours prior to each experiment for preconditioning. The cell was filled with the feed solution and helium was used to pressurize the cell. Solvent permeation values were obtained by measuring the weight of the collected permeate as a function of time. Three different membrane samples were analysed for each data point to ensure reproducibility and measurements were performed three times for each sample.

Rejection tests using Sudan Black B were performed using the same dead-end pressure cell at 50% recovery. The cell was filled with feed solution and helium was used to pressurize the cell. The feed solution was constantly stirred at a speed of 500 rpm to prevent concentration polarization on the membrane surface. Sudan Black B (Fluka, MW 456.54 g/mol) was used at a concentration of 8000 ppm as probe solute in pure solvents. The rejection test was performed until an equilibrium retention value was reached. All measurements were performed on three different membrane samples to ensure reproducibility and three measurements were done for each sample. UV-Vis Spectrophotometer was used to analyze the Sudan Black concentrations in the feed and permeate. In order to check for the occurrence of any concentration polarization, fluxes of solvents with solutes were compared with those of pure solvents. Between each cycle, the samples were rinsed with the previous solvent and subsequently three times ultrasonically cleaned in ethanol for 10 minutes at

room temperature. After this ultrasonic treatment the membranes were dried in a vacuum oven under nitrogen for 24 hours at 30°C. After being cooled down, membranes were soaked for 24 hours in the solvent to be tested.

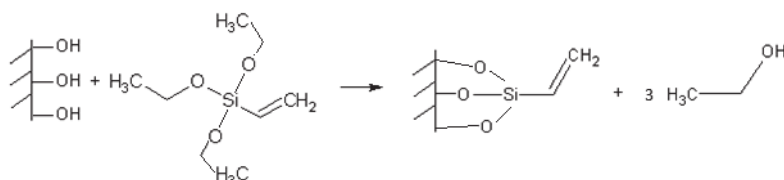
The solvent fluxes and the rejection results of the membranes developed in this work were compared with those of two other types of PDMS-grafted ceramic membranes as developed in previous works. These are  $\gamma$ -alumina membranes grafted with a mono-vinyl-terminated PDMS (n=39), using mercaptopropylsilane as the linker, hereinafter referred to as M2 (4), and  $\gamma$ -alumina membranes grafted with mono-epoxy-terminated PDMS (n=10) and aminosilane as the linker, hereinafter referred to as M3 (3). All membranes were tested in the same equipment for flux and rejection measurements.

### 5.3. Results and Discussion

#### 5.3.1. Grafting performance

In this work chemical grafting was carried out using two consecutive steps as shown in Figure 5.1.

Step 1:



Step 2:

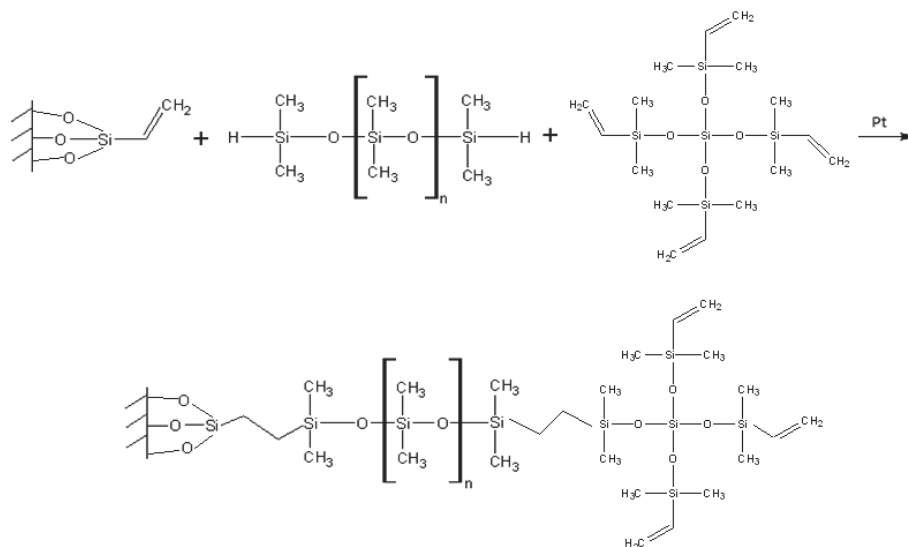
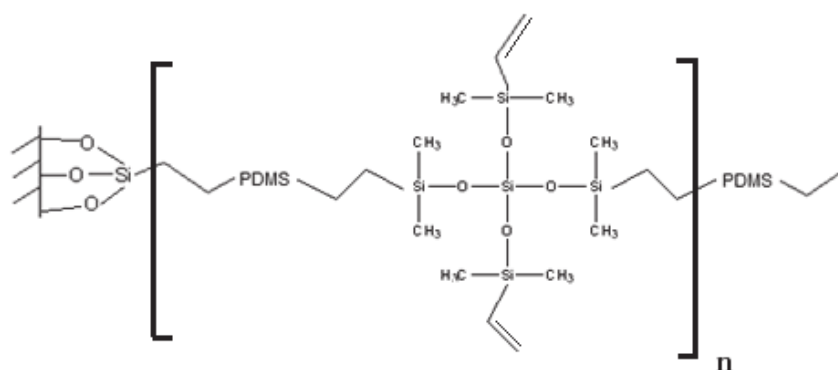
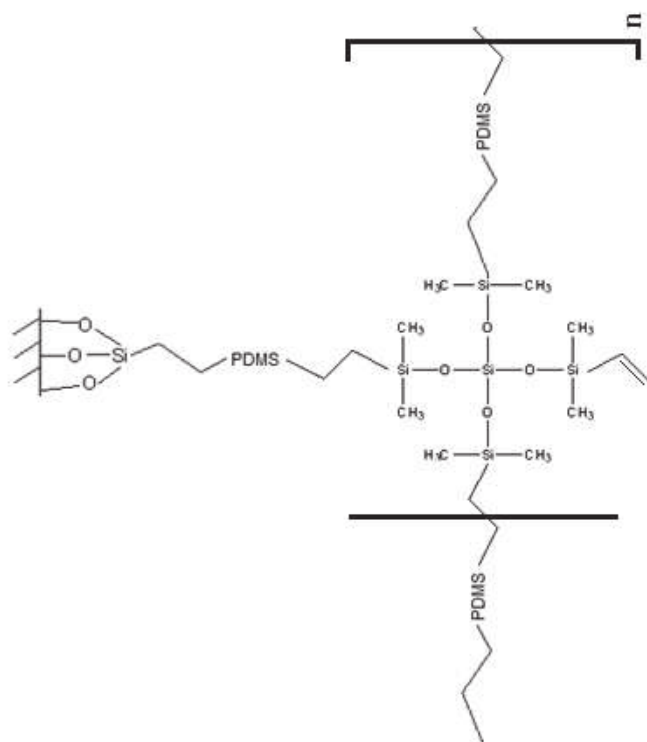


Figure 5.1. The reaction steps of grafting  $\gamma$ -alumina with the linker (step 1) and PDMS plus coupling agent (step 2)

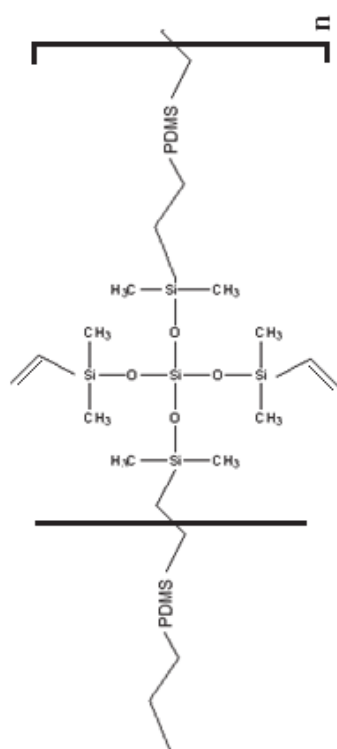
The first step is the grafting of vinyltriethoxysilane to the ceramic pore wall as depicted in step 1 of Figure 5.1. Grafting proceeds according to the reaction between a surface hydroxyl group with an ethoxysilane group resulting in a vinyl-terminated surface with a covalent Si-O-Al bond to the ceramic. In the second reaction step, the hydride terminated PDMS is reacted with the available vinyl group of the linker and of the tetrakis(vinyl)dimethylsiloxane through a hydrosilylation reaction using a Pt catalyst, which is the addition of the H-Si bond across the C double bond (Figure 5.1, step 2). The two step reaction as shown in Figure 5.1 is aimed to create a random network structure grafted inside the membrane pores.



(a)



(b)



(c)

Figure 5.2. Several possible structures resulted during random grafting: (a) and (b) possible morphologies of grafting on the inorganic surface; (c) "free" polymer, formed without reaction with the inorganic surface



Figure 5.2 shows the possible structures formed during the grafting reaction. The morphologies (a) and (b) are the result of respectively grafting the organic moiety parallel or perpendicular to the membrane pore wall. Morphology (c) is a result when “free” polymers are formed without reaction with the inorganic surface. It is expected that the latter morphology will be removed from the grafted system by washing (see experimental).

Figure 5.3 shows the results of FTIR analysis on the unmodified, vinyl-grafted and coupled-PDMS-grafted  $\gamma$ -Al<sub>2</sub>O<sub>3</sub> powders.

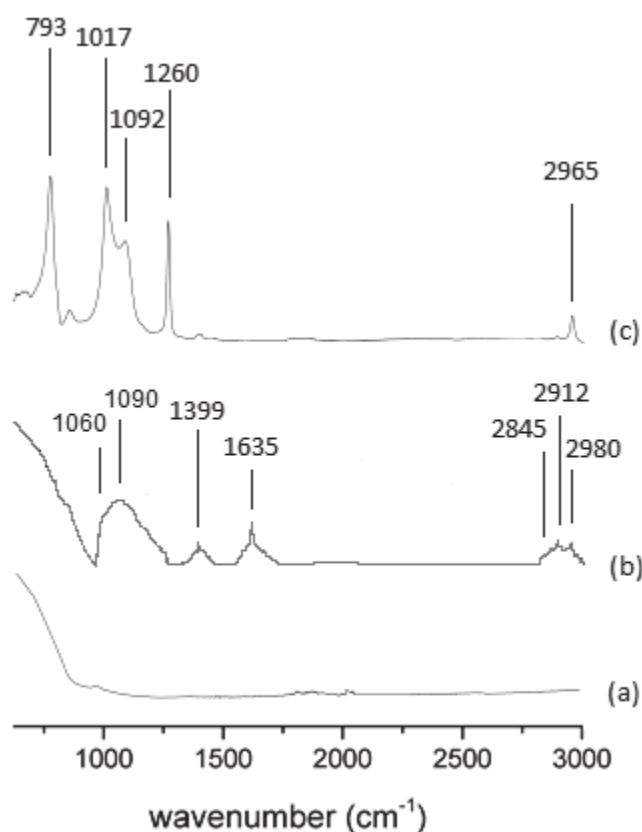


Figure 5.3. FTIR absorbance spectra of a) unmodified  $\gamma$ -Al<sub>2</sub>O<sub>3</sub> b) vinyl grafted  $\gamma$ -Al<sub>2</sub>O<sub>3</sub> c) coupled-PDMS grafted  $\gamma$ -Al<sub>2</sub>O<sub>3</sub>

In the FTIR spectrum of the vinyl grafted powder (Figure 5.3b), the broad peak at around 1000 - 1100 cm<sup>-1</sup> consists of a peak at 1060 cm<sup>-1</sup> and a peak at 1090 cm<sup>-1</sup> which can be attributed to the formation of covalent Si-O-Al and Si-O-Si bonds respectively (16-18). One or more hydrolysable groups out of total three functional alkoxy groups that are present at the vinyltriethoxysilane linking agent can react with the surface hydroxyl groups of  $\gamma$ -Al<sub>2</sub>O<sub>3</sub> forming a covalent Si-O-Al bond or with the adjacent silanols through the reaction of -Si-OH

+ Si-OH  $\rightarrow$  -Si-O-Si- + H<sub>2</sub>O, forming a covalent Si-O-Si bond. In Figure 5.3b, the peak at 1399 cm<sup>-1</sup> is ascribed to the bending of CH<sub>2</sub> of the vinyl (-CH=CH<sub>2</sub>) groups, while the peak at 1635 cm<sup>-1</sup> is a characteristic absorption peak for the bending of the C=C groups (19). The peaks at 2845 and 2912 cm<sup>-1</sup> can respectively be attributed to the asymmetric and symmetric stretching of CH<sub>2</sub> and furthermore the peak at 2980 cm<sup>-1</sup> is attributed to the symmetric stretching of C=C of the vinylsilanes (20).

During the reaction between the PDMS with the grafted silanes as well as with the coupling agent, the hydrides of the PDMS will react with the vinyl groups from the grafted linker and/or coupling agent through a hydrosilylation reaction forming a stable covalent bond. The peaks at 1399 cm<sup>-1</sup> and 1635 cm<sup>-1</sup>, ascribed to C=C bending of the vinyl groups as present in the silane grafted  $\gamma$ -Al<sub>2</sub>O<sub>3</sub> system (Figure 5.3b), are no longer observed after the reaction with PDMS (Figure 5.3c). This confirms the hydrosilylation reaction between the hydride and vinyl groups, which indicate the reaction between the hydride PDMS and the vinyl of the coupling agent and/or the linking agent on the gamma alumina surface. In the FTIR spectrum of the PDMS grafted powder (Figure 5.2c), the peak at 793 cm<sup>-1</sup> is attributed to the stretching of Si-C from the SiCH<sub>3</sub> group of PDMS (18). The two peaks at 1017 and 1092 cm<sup>-1</sup> can be ascribed to the Si-O-Si group of dimethylsiloxanes (18, 20). A characteristic peak at 1260 cm<sup>-1</sup> is attributed to symmetric C-H bending from the SiCH<sub>3</sub> group. The peak at 2965 cm<sup>-1</sup> can be assigned to the asymmetric stretching of C-H of the methyl groups of the PDMS (20). The presence of all these IR peaks indicates the presence of PDMS on the grafted powder and that the reactions, as given in Figure 5.1, have occurred (15, 18, 20).

Figure 5.4 shows the TGA results of 11.635 mg of PDMS grafted  $\gamma$ -Al<sub>2</sub>O<sub>3</sub> powder. A first stage of weight loss (around 0.3%, 0.035 mg) was observed up to 200°C. This initial weight loss can be attributed to the evaporation of adsorbed solvents from the samples. A second stage in weight loss of 8.7% (1.009 mg) was found at higher temperatures with a maximum loss observed in the temperature range between 300°C and 400°C. This significant weight loss can be attributed to the decomposition of the organic groups from the grafted samples. The decomposition temperature of the organic groups is higher than the boiling point of the individual grafting agents which are 205°C, 160°C, and 130°C, respectively for the hydride PDMS, vinyltriethoxysilane, and tetrakis(vinyldimethylsiloxy)silane. Thus, the TGA analysis

suggests that due to grafting an increase in the thermal stability of the organic moieties is achieved.

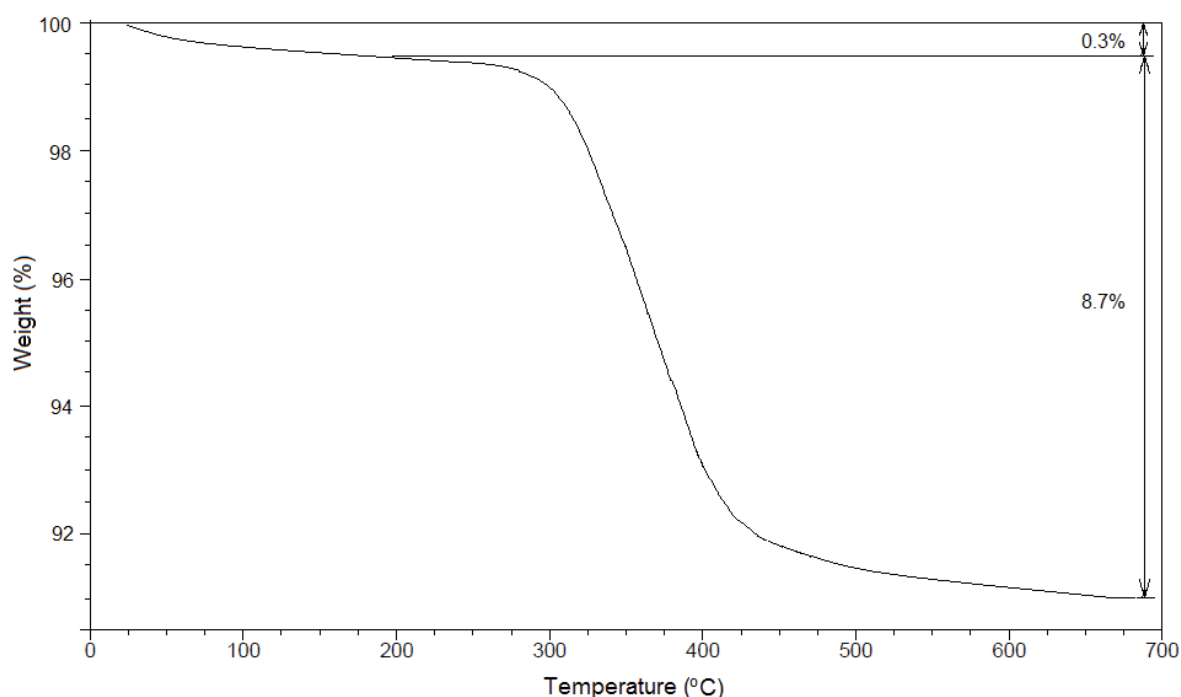


Figure 5.4. TGA results of the PDMS grafted  $\gamma$ - $\text{Al}_2\text{O}_3$  powder

### 5.3.2. Membrane Characteristics

In order to characterize the grafting performance of the  $\gamma$ - $\text{Al}_2\text{O}_3$  membranes, SEM-EDX and contact angle analyses were conducted. A SEM picture and EDX mappings of the coupled PDMS grafted  $\gamma$ - $\text{Al}_2\text{O}_3$  membrane are shown in Figure 5.5.

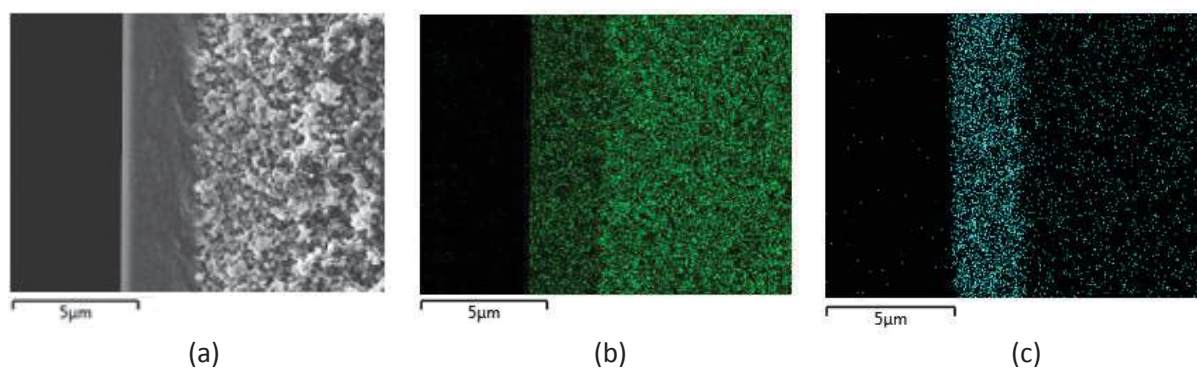


Figure 5.5. SEM-EDX maps for the coupled PDMS grafted  $\gamma$ - $\text{Al}_2\text{O}_3$  membrane (a) SEM picture, (b) Al-mapping (green), (c) Si-mapping (blue)

In Figure 5.5a, the modified  $\gamma$ - $\text{Al}_2\text{O}_3$  layer is shown at the left side of the SEM picture, while the  $\alpha$ - $\text{Al}_2\text{O}_3$  support layer appears on the right side of the same picture. The presence of Al

and Si in the modified membranes were shown on the EDX maps in Figure 5.3b and c, respectively. As can be seen from the EDX mapping of Si, grafting occurs throughout the  $\gamma$ -alumina layer with an observed thickness of about 3  $\mu\text{m}$ .

The results of the contact angle measurements of the unmodified, silane-grafted, and polymer-grafted  $\gamma\text{-Al}_2\text{O}_3$  membranes are given in Table 5.1. The contact angle values are the average of contact angles taken from 5 different points on the membrane surface. The almost negligible standard deviation indicates that the grafting reaction has occurred homogeneously over the membrane surface.

For the unmodified gamma-alumina membrane, the water droplet immediately wetted the membrane surface. A corresponding water contact angle of  $0^\circ$  is therefore assumed, indicating the hydrophilic character of the  $\gamma\text{-Al}_2\text{O}_3$  membrane due to natural occurrence of hydroxyl (OH-) groups on the ceramic surface. A relatively higher contact angle was observed after modification of  $\gamma\text{-Al}_2\text{O}_3$  with vinyl triethoxysilane. The higher contact angle might be attributed to the presence of the vinyl groups. Vinyl (C=C) groups are less polar than hydroxyl (OH-) groups, causing a weaker attraction between the water droplet and the vinyl-grafted  $\gamma\text{-Al}_2\text{O}_3$  membrane, and thus a relatively higher contact angle. Other factors such as the nanotextures of the grafted moieties as a result of the molecule orientation, the grafting density of the grafted moieties, as well as the presence of the pores can contribute to the actual contact angle value (21).

Table 5.1. Water contact angle of unmodified  $\gamma\text{-Al}_2\text{O}_3$ , vinyl grafted  $\gamma\text{-Al}_2\text{O}_3$ , and PDMS grafted  $\gamma\text{-Al}_2\text{O}_3$

	Unmodified ( $\gamma\text{-Al}_2\text{O}_3$ membrane)	After silanization with vinyltriethoxysilane	After reaction with PDMS and tetrakis(vinyldimethylsiloxy)silane
Contact Angle ( $^\circ$ )	0	$63 \pm 2$	$108 \pm 1$

After grafting with PDMS and coupling agent an increase in contact angle was observed. A higher contact angle for the PDMS-grafted membranes relative towards the vinyl grafted  $\gamma\text{-Al}_2\text{O}_3$  membranes might be attributed to the nonpolarity of dimethylsiloxane groups. The contact angle measurement suggests that a change in the membrane surface wettability has

occurred after grafting. For a comparison, a contact angle in the range of 91 to 97 degree were observed for  $\gamma$ -alumina membranes grafted with a mono-epoxy-terminated PDMS (n=10), using an aminosilane as the linker (3), and a contact angle of 95 degrees was observed for  $\gamma$ -alumina membranes grafted with a mono-vinyl-terminated PDMS (n=39), using mercaptopropylsilane as the linker (4). The slightly larger contact angle observed in this work, when compared to the previously reported results, might be attributed to the more dense structure realized due to the use of a coupling agent.

### 5.3.3. Membrane Performance

Figure 5.6 shows the flux of toluene, ethyl acetate and isopropanol through the modified membranes at different trans membrane pressures (TMPs) at 20°C.

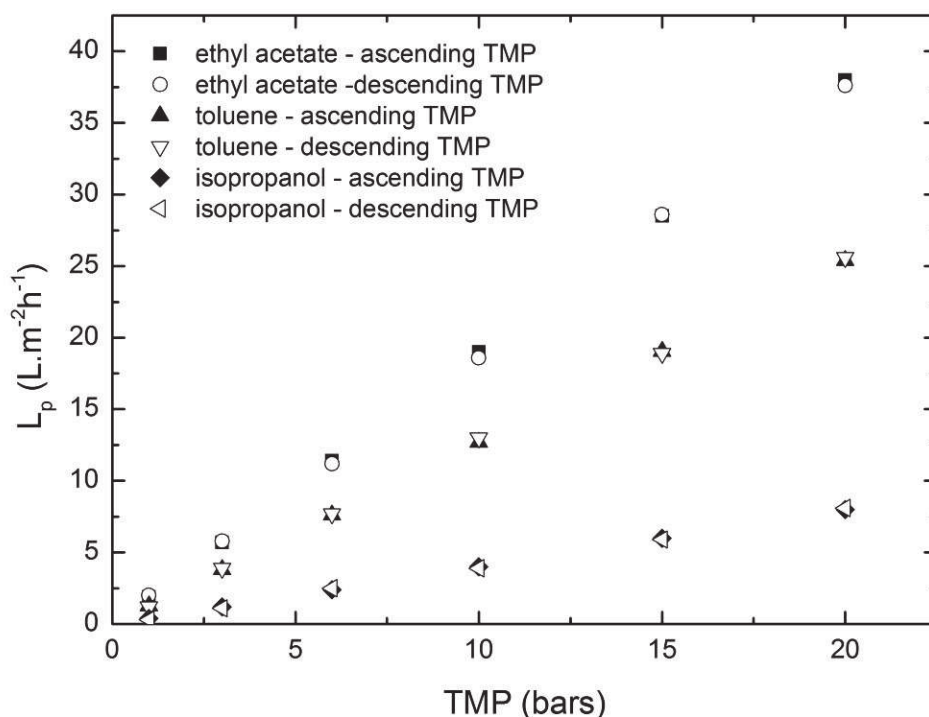


Figure 5.6. Flux of toluene, ethyl acetate, and isopropanol through the modified membranes as a function of trans membrane pressure (TMP) at 20°C

A linear relationship of flux versus pressure was observed for increasing as well as decreasing trans membrane pressure (TMP). The linearity of flux versus TMP suggests that the membrane structure does not deform under the applied TMP.

In Table 5.2, the fluxes of toluene, ethyl acetate, and isopropanol and the rejection results of Sudan Black in different types of solvents at 20°C and TMP of 10 bar for the three types of membranes are given. No significant differences were observed between the flux of the solvent with solutes and that of the pure solvents suggesting that no concentration polarization occurred during the rejection measurements at 50% recovery.

A membrane permeability constant ( $k$ ) is determined from the Hagen-Poiseuille relation ( $J_i = \frac{k_i}{\mu_i} \Delta P$ ) (Table 5.2). This viscosity-corrected membrane permeability constant is a function of the parameters representing the membrane pore geometry as given by:

$k_i = \frac{\varepsilon_i r_{p,i}^2}{8\tau l}$ , where  $\varepsilon_i$  is the membrane porosity,  $r_{p,i}$  the pore diameter,  $\tau$  the membrane tortuosity, and  $L$  the membrane thickness.

Table 5.2. Solvent fluxes ( $J$ ), Hagen-Poiseuille membrane permeability constants ( $k$ ) and Sudan Black rejections ( $R$ ) in different solvents at 20°C and TMP of 10 bar for different PDMS-grafted alumina membranes

Solvent Type	J (L.m <sup>-2</sup> .h <sup>-1</sup> )					
	M1		M2*		M3*	
	A**	B**	A**	B**	A**	B**
Toluene	12.7 ± 0.4	12.7 ± 0.3	23.8 ± 1.0	23.7 ± 1.0	30.6 ± 1.2	30.6 ± 1.2
Ethyl Acetate	19.0 ± 0.7	19.0 ± 0.7	35.7 ± 1.4	35.8 ± 1.0	44.8 ± 1.8	44.7 ± 1.7
Isopropanol	4.0 ± 0.1	4.0 ± 0.1	7.5 ± 0.3	7.6 ± 0.2	9.0 ± 0.4	9.0 ± 0.3
	k <sup>(1)</sup> (L.m <sup>-2</sup> )					
	M1		M2		M3	
Toluene	0.21 ± 0.02		0.40±0.02		0.51±0.02	
Ethyl Acetate	0.24 ± 0.02		0.46±0.02		0.57±0.02	
Isopropanol	0.27 ± 0.02		0.50±0.02		0.60±0.02	

	R at 50% recovery (%)		
	M1	M2	M3
Toluene	95 ± 1	65 ± 1	45 ± 1
Ethyl Acetate	88 ± 1	47 ± 1	30 ± 1
Isopropanol	80 ± 1	35 ± 1	20 ± 1

(1)  $k$  for pure solvent: The viscosity corrected membrane permeability constants according to the Hagen-Poiseuille equation,  $k = J \frac{\mu}{\Delta P}$ , with  $J$  solvent flux,  $\mu$  the solvent viscosity, and  $\Delta P$  the applied pressure

A\*\*: Pure solvent flux

B\*\*: Flux of solvent containing 8000 ppm Sudan Black B

\* Details on fabrication of M2 and M3 membranes can respectively be found in ref (4) and (3)

The results in Table 5.2 indicate that there is an increase in flux and permeability constant and a decrease in retention from M1 to M2 to M3. A trade-off is seen between the flux and rejection in which a higher flux accompanied by a lower rejection.

If for all solvents the membrane-solvent interaction is identical,  $k$  should be independent of the type of the permeating solvent. However, the results in Table 5.2 indicate that for all three membranes (M1, M2, and M3) different  $k$  values were observed for each solvent and each membrane types. The ratio of  $k$  in one solvent towards that in a reference solvent can be used to indicate the effect of the membrane-solvent interaction between the membrane and the permeating solvent on the membrane pore geometry as described in (22). In mathematical form, it is given by

$$k_i' = \frac{k_i}{k_{ref}} = \frac{\frac{\varepsilon_i r_{p,i}^2}{8\tau l}}{\left(\frac{\varepsilon_i r_{p,i}^2}{8\tau l}\right)_{ref}} = f(V_{s,i}') = A - B V_{s,i}' \quad (5.1)$$

with  $k_i$  the membrane permeability constant for solvent  $i$ ,  $k_i'$  the membrane permeability constant for solvent  $i$  normalized for the  $k$  value of a reference solvent  $k_{ref}$ ,  $V_{s,i}'$  the sorption volume of sorbed solvent  $i$  per mass of the grafted material, normalized towards solvent of reference, and  $A$  the intercept and  $B$  the slope of a plot of  $k_i'$  versus  $V_{s,i}'$ . By making this correction for the sorbed volume, identical values (thus independent of solvent) of the permeability constant were observed (22).

Toluene has the strongest interaction with PDMS, followed by ethyl acetate and finally by isopropanol. According to Equation 5.1, the membrane permeable volume reduces if the solvent is strongly swelling the membrane material. The Hagen-Poiseuille pore flow model, corrected for solvent sorption, can be applied for all three membranes. For the M1 (the coupled PDMS grafted membrane), the strongest interaction of toluene with the grafted PDMS, results in the smallest membrane permeable volume compared to those of ethyl acetate and isopropanol.

The more closed membrane structure in the presence of toluene, as a result of a stronger membrane-solvent interaction, is therefore the cause of the higher Sudan Black rejection observed in toluene as compared to those in other solvents. As a similar ceramic porous ceramic substrate is used for all types of grafted membranes, the higher Sudan Black rejection (selectivity) of M2 compared to that of M3 might be explained by the difference in the chain length of the PDMS used for grafting. When the flux data of grafted membranes with identical PDMS chain length ( $n=10$ ) with (M1) and without the use of a coupling agent (M3), then it can be seen that M1 showed 2.3 - 2.4 times lower flux than M3. A higher selectivity is achieved for as well for M1 if compared with M3. This is an indication that the pore size of M1 is smaller than of M3. This may be a result of the thicker grafted material in the pores due to the use of coupling agent.

It is worth to mention that the increase of the membrane selectivity obtained from the use of coupling agent during grafting came at the cost of the permeability, as indicated by the low permeability of M1 compared to M3. Comparing M1 with M2, and assuming a similar transport model, it can be seen that a stronger pore size reduction is realized for M1 by using a coupling agent, than that of M2 in which a longer chain length of PDMS was used. This indicates that from M1 to M3, there is a trend in decreasing pore size or decreasing thickness of grafted organic moiety layer in the gamma alumina pores.

#### **5.4. Conclusion**

A method was presented of grafting a mesoporous  $\gamma$ -alumina layer, supported on macro porous  $\alpha$ -alumina membrane, with hydride terminated polydimethylsiloxane coupled with tetrakis(vinyl dimethylsiloxy)silane, by using vinyltriethoxysilane as linking agent in order to



create a coupled grafted PDMS network in the ceramic pores for solvent nanofiltration. Grafting performance of the organic moieties on  $\gamma$ -alumina powders was analyzed by FTIR and TGA indicating that grafting of vinyltriethoxysilane and hydrosilylation between the hydride group of PDMS and the vinyl group of the linking and/or coupling agent were successfully carried out. SEM-EDX and contact angle analysis on the grafted membranes showed that the grafting occurs throughout the  $\gamma$ -alumina layer and that the resulting membrane surface had a water contact angle of 108°. From pure solvent permeability and rejection tests in toluene, ethyl acetate, and isopropanol using Sudan Black as probe solute, an increased selectivity was found for membranes grafted with the use of coupling agent than those without the use of coupling agent. The use of a coupling agent increases the grafted organic layer thickness in the gamma alumina pores and thus a higher selectivity for nanofiltration of solvents but with the cost of lower permeability, if compared with PDMS-grafted alumina membranes where no PDMS-coupling agent was applied.

### Acknowledgement

The authors acknowledge the financial support from the European Union – The Education, Audiovisual and Culture Executive Agency (EACEA) under the Program “ Erasmus Mundus Doctorate in Membrane Engineering” – EUDIME (FPA 2011-2014).

### References

1. Vandezande, P., Gevers, L. E. M., and Vankelecom, I. F. J. (2008) Solvent resistant nanofiltration: Separating on a molecular level, *Chemical Society Reviews* 37, 365-405.
2. Marchetti, P., Jimenez Solomon, M. F., Szekely, G., and Livingston, A. G. (2014) Molecular Separation with Organic Solvent Nanofiltration: A Critical Review, *Chemical Reviews* 114, 10735-10806.
3. Pinheiro, A. F. M., Hoogendoorn, D., Nijmeijer, A., and Winnubst, L. (2014) Development of a PDMS-grafted alumina membrane and its evaluation as solvent resistant nanofiltration membrane, *Journal of Membrane Science* 463, 24-32.
4. Tanardi, C. R., Pinheiro, A. F. M., Nijmeijer, A., and Winnubst, L. (2014) PDMS grafting of mesoporous  $\gamma$ -alumina membranes for nanofiltration of organic solvents, *Journal of Membrane Science* 469, 471-477.

5. Faibish, R. S., and Cohen, Y. (2001) Fouling-resistant ceramic-supported polymer membranes for ultrafiltration of oil-in-water microemulsions, *Journal of Membrane Science* 185, 129-143.
6. Yoshida, W., and Cohen, Y. (2003) Ceramic-supported polymer membranes for pervaporation of binary organic/organic mixtures, *Journal of Membrane Science* 213, 145-157.
7. Yoshida, W., and Cohen, Y. (2004) Removal of methyl tert-butyl ether from water by pervaporation using ceramic-supported polymer membranes, *Journal of Membrane Science* 229, 27-32.
8. Popat, K. C., Mor, G., Grimes, C. A., and Desai, T. A. (2004) Surface Modification of Nanoporous Alumina Surfaces with Poly(ethylene glycol), *Langmuir* 20, 8035-8041.
9. Sang Won, L., Hao, S., Richard, T. H., Vania, P., and Gil, U. L. (2005) Transport and functional behaviour of poly(ethylene glycol)-modified nanoporous alumina membranes, *Nanotechnology* 16, 1335.
10. Leger, C., De Lira, H. L., and Paterson, R. (1996) Preparation and properties of surface modified ceramic membranes. Part II. Gas and liquid permeabilities of 5 nm alumina membranes modified by a monolayer of bound polydimethylsiloxane (PDMS) silicone oil, *Journal of Membrane Science* 120, 135-146.
11. Nijmeijer, A., Bladergroen, B. J., and Verweij, H. (1998) Low-temperature CVI modification of  $\gamma$ -alumina membranes, *Microporous and Mesoporous Materials* 25, 179-184.
12. Cuperus, F. P., Bargeman, D., and Smolders, C. A. (1992) Permporometry: the determination of the size distribution of active pores in UF membranes, *Journal of Membrane Science* 71, 57-67.
13. Sripathi, V. G. P., Mojet, B. L., Nijmeijer, A., and Benes, N. E. (2013) Vapor phase versus liquid phase grafting of meso-porous alumina, *Microporous and Mesoporous Materials* 172, 1-6.
14. Marciniak, B., (Ed.) (2009) *Hydrosilylation of Alkenes and Their Derivatives*, Vol. 1, Springer Science+Business Media B. V.
15. Pinheiro, A. F. M. (2013) Development and Characterization of Polymer-grafted Ceramic Membranes for Solvent Nanofiltration, In *PhD Thesis*, University of Twente, Enschede.
16. Jakobsson, S. (2002) Determination of Si/Al Ratios in Semicrystalline Aluminosilicates by FT-IR Spectroscopy, *Spectroscopy Techniques* 56, 797-799.
17. Sinko K., M. R., Rohonczy, J., Frazl P. (1999) Gel Structures Containing Al(III), *Langmuir* 15, 6631-6636.
18. Anderson, D. R. (1974) *Analysis of Silicones*, Wiley-Interscience, New York.

19. Esteves, A. C. C., Brokken-Zijp, J., Laven, J., Huinink, H. P., Reuvers, N. J. W., Van, M. P., and de With, G. (2009) Influence of cross-linker concentration on the cross-linking of PDMS and the network structures formed, *Polymer* 50, 3955-3966.
20. Bellamy, L. J. (1975) *The Infra-red Spectra of Complex Molecules*, 3rd ed., Chapman and Hall, London.
21. Faibish, R. S., Yoshida, W., and Cohen, Y. (2002) Contact Angle Study on Polymer-Grafted Silicon Wafers, *Journal of Colloid and Interface Science* 256, 341-350.
22. Tanardi, C. R., Vankelecom, I. F. J., Pinheiro, A. F. M., Tetala, K. K. R., Nijmeijer, A., and Winnubst, L. (2015) Solvent Permeation Behavior of PDMS Grafted  $\gamma$ -Alumina Membranes.



# **Chapter 6**

## **Polyethyleneglycol Grafting of $\gamma$ -Alumina Membranes for Solvent Resistant Nanofiltration**

This chapter has been submitted for publication as:

Tanardi, C. R., Catana, R., Barboiu, M., Ayrat, A., Vankelecom, I. F., Nijmeijer, A., and Winnubst, L.  
Polyethyleneglycol Grafting of  $\gamma$ -Alumina Membranes for Solvent Resistant Nanofiltration.

## Abstract

A method is presented for the grafting of a mesoporous  $\gamma$ -alumina layer, supported on a macro porous  $\alpha$ -alumina membrane, by polyethylene glycols (PEG). The grafting performance of  $\gamma$ - $\text{Al}_2\text{O}_3$  powder with various PEG grafting agents having different molecular weights, alkoxy groups, and ureido functionality were analysed by TGA,  $^{29}\text{Si}$ -NMR, FTIR, and BET to see the effects of different properties of the grafting agent on the grafting results. The molecular weights, the presence of the ureido functionality, and the number of hydrolyzable groups of the grafting agents were found to influence the grafting density. FTIR analysis indicated that grafting of the  $\gamma$ - $\text{Al}_2\text{O}_3$  powders has occurred. The degree of self-condensation is almost identical for most of the grafting agents. The grafting density increases with decreasing chain length of the grafting agents. The highest grafting density in this work is obtained by using a silylated ureido PEG with the shortest chain length ( $n=10$ ). The number of alkoxy groups of the grafting agents influences the structural configuration of the grafted moiety. Moreover, for grafting agents having an ureido functionality, the chain length of the grafting agents was found the structural configuration of the grafted moiety. Contact angle measurements, solvent permeability tests, and rejection tests were used to assess the grafted membrane performance. A higher contact angle was observed after grafting. A lower solvent permeation of both ethanol and hexane was observed due to the presence of the grafted moiety inside the membranes reducing the membrane pore diameter. The permeability behavior with respect to different types of permeating solvent (polar and nonpolar) was investigated. Lower permeability of ethanol than hexane was observed accompanied by a higher retention of Sudan Black in ethanol than in hexane. This effect is explained by the difference in solvent sorption in the grafted moiety for different types of permeating solvents.

## 6.1. Introduction

Solvent resistant nanofiltration (SRNF), a type of pressure-driven membrane separation, is a potential economic and energy-efficient solution for solvent recovery in various industries due to the lower amount of energy it consumes than evaporation or distillation (1). With regard to separation performance, nanofiltration generally has nominal molecular weight cutoffs ranging from 200 to 1000 Da (neutral solutes), using membranes with pore sizes of around 0.5–2 nm (2). In order for SRNF to be applicable for industrial applications, the membranes need to be chemically stable and robust to endure a continuous exposure towards organic solvents.

Grafting of ceramic substrates by organic moieties is a convenient method to prepare chemically stable membranes for various purposes (3-10). During grafting a specific organic moiety is chemically bonded to an inorganic substrate. The hydrolysable groups of the to-be-grafted organic moiety will react with the OH- groups of an oxide ceramic surface to produce a stable covalent bond. Faibish et al.(3) grafted zirconia membranes with polyvinylpyrrolidone using free-radical graft polymerization, resulting in a reduction in pore size of around 25 % after grafting (no pore size values are given in this paper), suitable for ultrafiltration. Here a vinyl silane was used as linker to the zirconia membranes. Popat et al. (6) and Lee et al. (7) grafted polyethylene glycol to straight pore alumina membranes (“anodisc”), with a pore size of 25 and 80 nm, using a silane coupling agent to obtain anti-fouling ultrafiltration membranes. Yoshida et al. made a layer of terminally bonded polymer via free radical graft polymerization of vinyl acetate or vinyl pyrrolidone monomers on the surface of  $\gamma$ -alumina tubular supports (pore size 5 nm) using silane as a linker (10), while in other work of the same group (5) silica membranes (pore size of 20 nm) were used as inorganic substrate to be grafted using the same monomers as in (10) for pervaporation. Pinheiro et al. (8) and Tanardi et al. (9) grafted low molecular weight PDMS in  $\gamma$ -alumina membranes(pore size 5 nm) using alkoxy-silanes as the linker suitable for nanofiltration.

Recent work has been dedicated to prepare hydrophobic PDMS grafted  $\gamma$ -alumina membranes for the filtration of nonpolar solvents (8-9). The PDMS grafted  $\gamma$ -alumina

membranes are less attractive for the filtration of polar solvents since these membranes show a lower membrane selectivity in polar solvents than in non-polar solvents. This can be explained by the difference in the sorption behavior of the grafted moiety in different types of solvents affecting the effective membrane pore diameter (11-12). As such, hydrophilic grafted ceramic membranes may be more interesting for the filtration of polar solvents, as opposed to the hydrophobic grafted membranes which are more directed for the filtration of nonpolar solvents.

In this work, grafting of mesoporous  $\gamma$ -alumina by different types of silylated poly (ethylene glycols) (PEGs) was performed in order to result in Solvent Resistant NanoFiltration (SRNF) grafted ceramic membranes for the filtration of polar solvents. The different PEG compounds are chosen in such a way that they vary in terms of molecular weight, number of alkoxy groups, and self-assembling ability as indicated by the number of ureido functionalities present. The chemical structures of all grafting agents used in this study (compound **A** to **H**) are given in Figure 6.1.



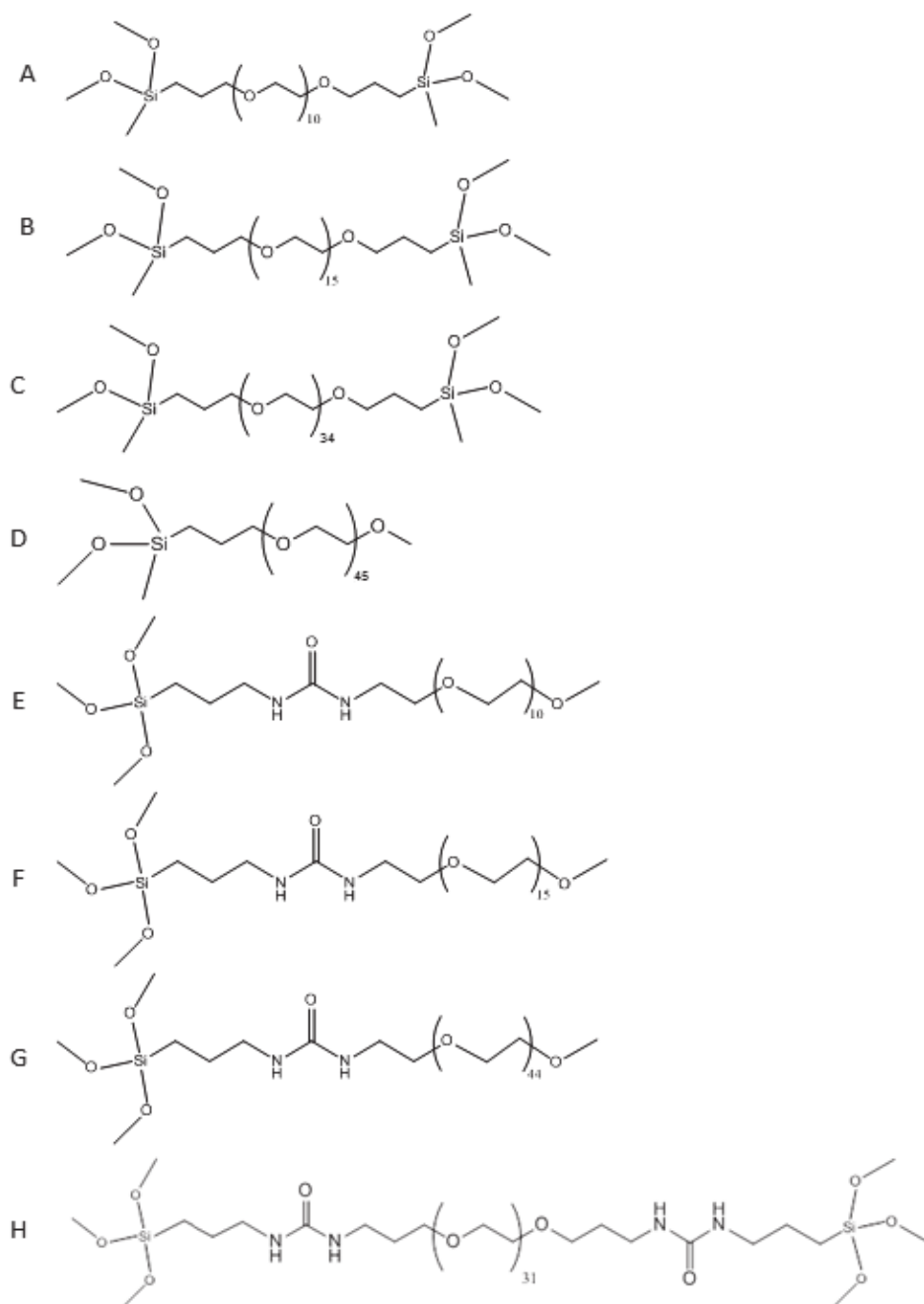


Figure 6.1. The chemical structures of the grafting agents studied

The grafting performance of each grafting agent on inorganic,  $\gamma$ -alumina, particles (acting as surrogate membrane surfaces) was analyzed by means of FTIR,  $^{29}\text{Si}$ -NMR, TGA, and BET. In this work, the  $\gamma$ -alumina membranes were grafted with the grafting agent that gave the highest grafting density according to the TGA analysis. The performance of the grafted membranes was assessed by means of water contact angle measurements, as well as permeability and rejection tests.

## 6.2. Experimental Methods

Compounds **A** till **D** (silylated PEG with an average molecular weight,  $M_n$ , of 740, 950, 1820, and 2170 g/mol respectively) were purchased from Specific Polymers. Compounds **E** till **H** (silylated ureido PEGs) were prepared by a reaction between amine terminated PEGs with an average molecular weight ( $M_n$ ) of respectively 500, 750, 1500, and 2000 g/mol (Sigma Aldrich) and isocyanate triethoxysilane (95%, Sigma Aldrich). The solvents, acetonitrile (99.9%) and toluene (99.9%), were dried using zeolite A with a particle size of 4-8 nm and pore diameter of 4 Å (Sigma Aldrich).  $\gamma$ -alumina powder with a BET surface area of 84.36 m<sup>2</sup>/g was purchased from Alfa Caesar. Flat  $\gamma$ -Al<sub>2</sub>O<sub>3</sub> membranes supported on  $\alpha$ -Al<sub>2</sub>O<sub>3</sub> supports with a diameter of 39 mm were purchased from Pervatech. The mean pore diameter of the 3  $\mu$ m thick  $\gamma$ -Al<sub>2</sub>O<sub>3</sub> layer and the 1.7 mm thick  $\alpha$ -Al<sub>2</sub>O<sub>3</sub> support were 5 nm and 80 nm, respectively (13-14).

### 6.2.1. Synthesis of grafting agents with ureido functionality

The silylated ureido PEG grafting agents (compounds **E** - **H**) were prepared by a reaction between isocyanates and amines to result in ureido groups (15-16). The reaction rate of an aliphatic isocyanate increases with the addition of a primary aliphatic amine (15-16). Figure 6.2 gives the chemical structure of the reactants and products. Details on the experimental procedures and purification steps are given in the **Supporting Information**.

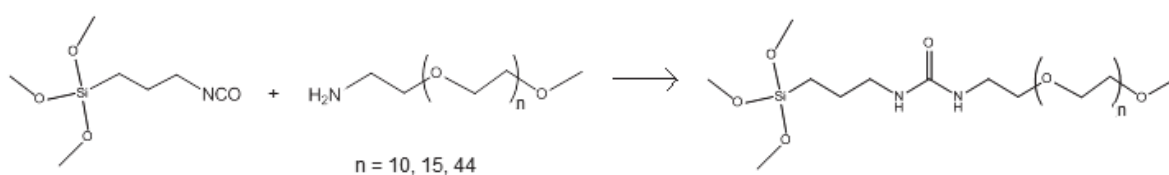


Figure 6.2. The reaction between isocyanate triethoxysilanes and the corresponding amine terminated PEG to result in the ureido PEG

### 6.2.2. Grafting method for $\gamma$ -Al<sub>2</sub>O<sub>3</sub> powders and membranes

Grafting of the  $\gamma$ -Al<sub>2</sub>O<sub>3</sub> powder was performed as follows.

The  $\gamma$ -Al<sub>2</sub>O<sub>3</sub> powder was soaked in an ethanol/water (2:1) solution for 8 hours at room temperature to remove dust and provide suitable hydroxylation and subsequently dried

at 100°C for 2 hours under vacuum and stored under nitrogen atmosphere until further use.

In a fumehood, a 50 mL solution of 3 mM of a silane terminated PEG in toluene was prepared. The solution was added into a flask containing 1.8 g  $\gamma$ -Al<sub>2</sub>O<sub>3</sub> powder. The mixture was stirred and heated under reflux with a Dean Stark apparatus (a laboratory glassware used in combination with a reflux condenser to remove side products such as water and alcohols from a batch reactor containing a reaction performed at a reflux temperature) for 24 hours at 110°C for the silylation reaction between the silane terminated PEG and the  $\gamma$ -Al<sub>2</sub>O<sub>3</sub> powder. Afterwards, the mixture was cooled to room temperature. The powders were retrieved by centrifuging the mixture and were 3 times washed with fresh toluene. Afterwards, the powders were placed in a vacuum oven for 2 hours at 115°C.

The  $\gamma$ -Al<sub>2</sub>O<sub>3</sub> membranes were soaked in an ethanol/water (2:1) solution for 8 hours at room temperature to remove dust and provide suitable hydroxylation. The membranes were then dried at 100°C for 2 hours under vacuum and stored under nitrogen atmosphere until further processing.

In a fumehood, a 50 mL solution of 3 mM of a silane terminated PEG in toluene was prepared in a flask. The unmodified  $\gamma$ -Al<sub>2</sub>O<sub>3</sub> membrane was placed in a sample holder and kept in the solution throughout the reaction. The grafting reaction between the silane terminated PEG and the hydroxylated  $\gamma$ -Al<sub>2</sub>O<sub>3</sub> was carried out under continuous stirring and reflux at 110°C for 24 hours. After 24 hours, the reaction mixture was allowed to cool down. The membrane was retrieved from the mixture and rinsed 3 times with toluene before placing in a vacuum oven at 115°C for 2 hours.

### **6.2.3.Characterization**

<sup>1</sup>H NMR spectra of the in-house prepared grafting agents (compounds E - H) were acquired using a Bruker Avance 300 NMR spectrometer.

FTIR analysis on ungrafted and grafted  $\gamma$ -alumina powders was conducted using a Thermo-Fischer Nicolet 710 spectrometer. The FTIR spectra were recorded at room temperature over a scanning range of 400-4000  $\text{cm}^{-1}$  with a resolution of 4.0  $\text{cm}^{-1}$  using 32 scans. The samples were in the form of  $\gamma\text{-Al}_2\text{O}_3$  powders which were modified using the same grafting procedure as the actual membrane. The sample in powder form is considered to have the same chemical characteristics as the actual membrane and can therefore be used to describe the chemical reactions that occur between the membrane and the grafting agent.

Solid-state  $^{29}\text{Si}$  NMR experiments on the grafted  $\gamma$ -alumina powders were performed on a Bruker Avance III spectrometer with a 9.4-T wide bore superconducting magnet. The spectrometer operated at 79.51 MHz for  $^{29}\text{Si}$ . Samples were placed in a 3.2 mm rotor in diameter for spinning at magic angle.

TGA analysis on the grafted  $\gamma$ -alumina powders was conducted by a coupled DSC/TGA 2960 from TA Instruments at a heating rate of 10°C/minute under nitrogen atmosphere. In all cases a run from room temperature up to 700°C was performed and around 11 mg of sample was used.

Nitrogen sorption studies were conducted on ungrafted and grafted  $\gamma$ -alumina powders by a Micromeritics Instruments ASAP-2020. The BET method was used to calculate the constant (c) and specific surface areas in the pressure range of  $P/P_0 = 0.05 - 0.35$  at 77 K. Prior to each measurement, the sample was degassed at 200°C for 12 hours.

Water contact angle data using the sessile drop method were collected on grafted  $\gamma$ -alumina membranes by a QCM Optical Contact Angle instrument.

Permeation tests on the grafted  $\gamma$ -alumina membranes were carried out at room temperature using a dead-end high pressure cell made from stainless steel. Membranes to be tested were soaked in the organic solvent for 12 hours prior to each experiment for preconditioning. The cell was filled with feed solution and helium was used to pressurize the cell. Permeate fluxes were obtained by measuring the weight of the collected

permeate as a function of time. All measurements were performed on three different membrane samples and two measurements per sample.

Rejection tests were performed on the grafted  $\gamma$ -alumina membranes using the same stainless steel dead-end pressure cell. 8000 ppm Sudan Black in hexane or ethanol was used as feed. The feed solution was constantly stirred at a speed of 500 rpm to prevent concentration polarization on the membrane surface. The rejection tests were performed until an equilibrium retention value was reached. Here also the measurements were performed on three different membrane samples of each composition with two measurements per sample. Sudan Black concentrations in the feed and permeate solution were analyzed using a Perkin-Elmer  $\lambda$ 12 UV-Vis Spectrophotometer. The rejection (R in %) was calculated by the following equation:  $R = (1 - C_p/C_f) \times 100\%$ , where  $C_p$  and  $C_f$  are the solute concentrations in permeate and feed, respectively. Between each rejection test the membranes were rinsed with the previous solvent and subsequently three times ultrasonically cleaned in fresh ethanol 10 minutes at room temperature. After this ultrasonic treatment the membranes were dried in a vacuum oven under nitrogen for 24 hours at 80°C. After cooling to room temperature, the membranes were soaked for 24 hours in the solvent to be tested. In order to check whether any concentration polarization occurs, the solvent permeation of blank feeds (pure solvents without solutes) and those with Sudan Black solute were compared using a similar set-up.

### **6.3. Results and Discussion**

#### **6.3.1. Chemical Reaction Background**

In previous work (8-9), chemical grafting was carried out using two consecutive steps, in which a silane linking agent was first grafted onto the pore wall, using a vapour phase deposition method and then reacted with oligomers. In this work, a different strategy was utilized, in which the organics were silylated first and then grafted onto the ceramic pore wall.

The grafting reaction between the silylated PEG and the surface hydroxyls proceeds by hydrolysis of the alkoxy groups upon reaching the hydroxyl groups of the membrane surface, followed by a condensation reaction, resulting in a stable covalent Al-O-Si bond between the oxide surfaces and the PEG (17-18). In this reaction, moisture from the substrate acts as a catalyst for the hydrolysis (17-18). For the silanes to access the hydroxyl groups on the membrane surface, no more than 2 or 3 monolayers of water should exist on the substrate surface (17). In order to limit the amount of moisture present, the substrate was stored under nitrogen atmosphere prior to grafting and dried toluene was used as solvent for the grafting reaction. The grafting reaction between the surface hydroxyls and the silylated PEG is depicted in Figure 6.3. The hydroxyl groups on the  $\gamma$ -alumina surface act as the active sites for the grafting reaction. The grafting was done under reflux to remove side products such as water and alcohols from the reaction medium and to shift the reaction equilibrium to the product side.

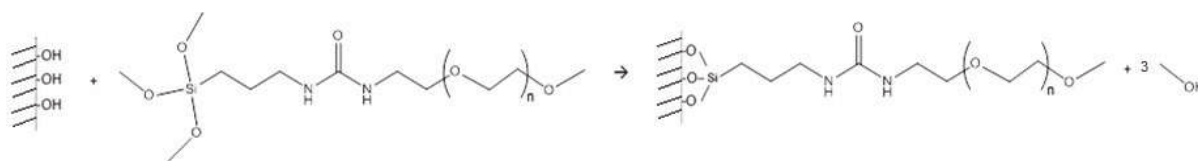


Figure 6.3. Schematic representation of ideal grafting reaction between the surface hydroxyls of the  $\gamma$ -alumina substrate and silylated PEG grafting agents

For compounds E to H, the silylated PEG with ureido groups, the oxygen from the ureido group can form a hydrogen bond with the amide from the adjacent ureido group. This results in the formation of ribbon type aggregates by self assembling, which could potentially promote a higher grafting density. For compound A to D, the non-ureido functionalized PEGs, a random statistical displacement of grafting agents on the pore wall is expected. Figure 6.4 illustrates the grafting mechanism by the non-self-assembling (Figure 6.4a) versus the self-assembling silylated ureido PEG grafting agents (Figure 6.4b).

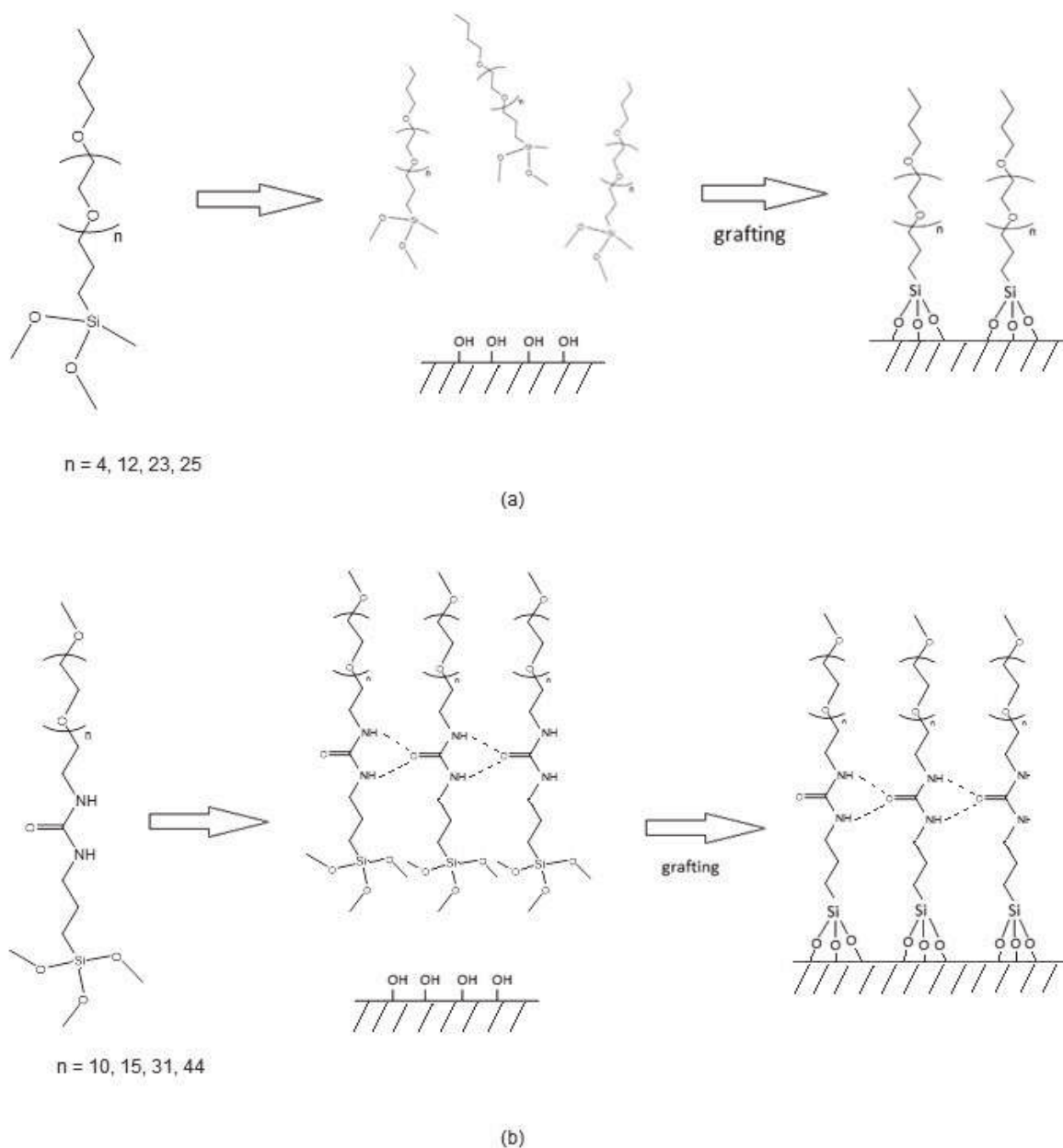


Figure 6.4. Schematic representation of the grafting mechanism by (a) the non-self-assembling silylated PEG grafting agents (from compounds A-D) versus (b) the self-assembling silylated ureido PEG grafting agents (from compounds E-H).

The type of grafting agent may affect the grafting density and the chemical structure of the grafted organosilanes (19-25). The characterization strategy for the chemical structure is summarized in Figure 6.5. In addition to the grafting reaction between the silylated PEG and the  $\gamma$ -Al<sub>2</sub>O<sub>3</sub> powder, the silanol groups can also react with adjacent silanols, resulting in a siloxane network through the formation of the covalent Si-O-Si

bond (19, 21, 25) through the following condensation reaction:  $-\text{Si}-\text{OH} + \text{Si}-\text{OH} \rightarrow -\text{Si}-\text{O}-\text{Si}- + \text{H}_2\text{O}$ . The importance of the formation of the Si-O-Si bond than that of Si-O-Al bonds was semi-quantitatively investigated by FTIR.

Depending on the amount of alkoxy groups per PEG molecule, who can form a covalent Si-O-Al bond with the  $\gamma\text{-Al}_2\text{O}_3$  surface, several different possible configurations exist, namely  $\text{D}^1$  and  $\text{D}^2$  for compounds A to D (Figure 6.5a), and  $\text{T}^1$ ,  $\text{T}^2$ , and  $\text{T}^3$  for compounds E to H (Figure 6.5b). The ratio of each D and T structure after grafting by each type of grafting agent was investigated by  $^{29}\text{Si}$ -NMR.

The grafting efficiency, i.e. the mole ratio of grafted PEG versus the available surface hydroxyls on the surface of  $\gamma$ -alumina per  $\text{nm}^2$  were analyzed by TGA. Here the decomposed mass was related to the presence of organics in the sample (after subtracting the mass loss due to the absorbed water), while the weight, remaining after the TGA measurement, was related to the presence of inorganics in the sample.

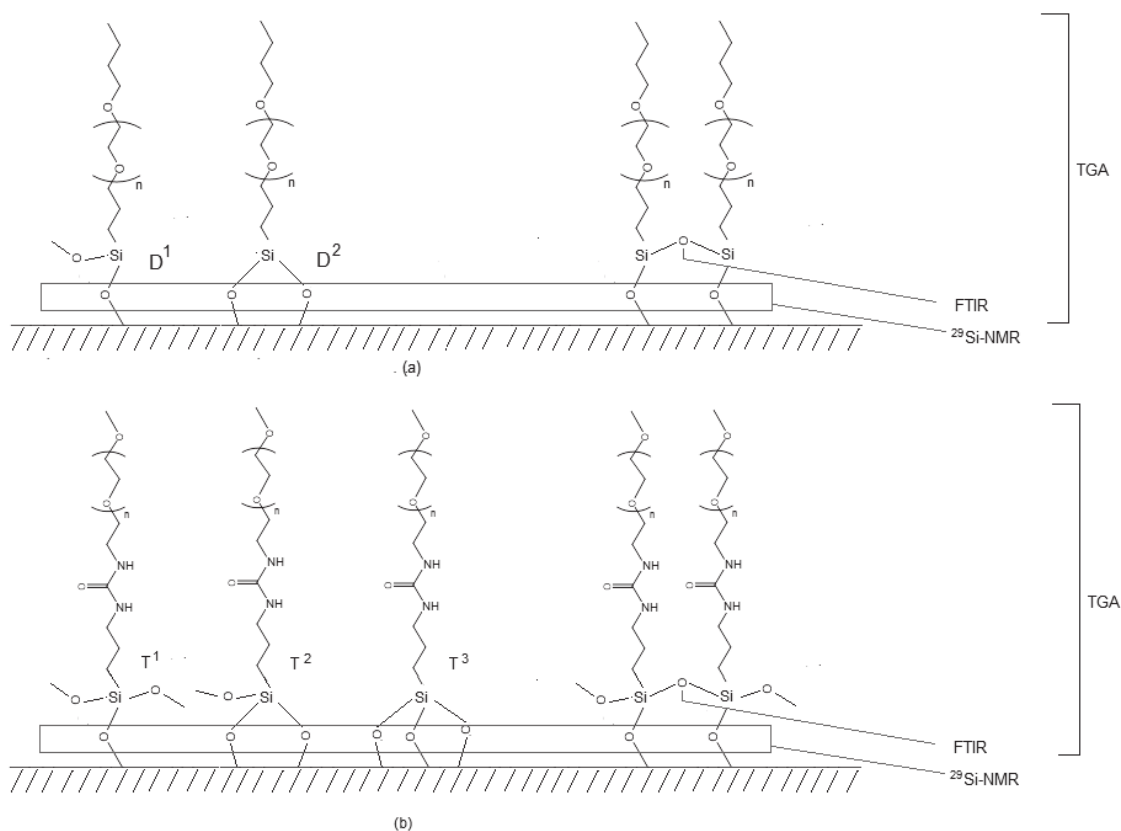


Figure 6.5. The characterization strategy employed in this work to study the grafting nature of different types of PEG grafting agents



### 6.3.2. FTIR Analysis of grafting performance and the presence of self-condensation

The presence or disappearance of transmittance peaks in the FTIR spectra for the grafted, compared with the ungrafted powder, is an indication whether the grafting reaction has occurred. Figure 6.6 shows the IR spectra of the unmodified (Figure 6.6a) and of one type of the grafted  $\gamma$ -Al<sub>2</sub>O<sub>3</sub> powders, namely compound E (silylated ureido PEG with n = 10, Figure 6.6b). For all types of grafted powders the IR spectra are more or less identical with the one given in Figure 6.6b. In Figure 6.6a and b, the absorption band at 800 cm<sup>-1</sup> is attributed to the Al-O stretching (26). In the grafted  $\gamma$ -Al<sub>2</sub>O<sub>3</sub> spectra the bands at 1060 cm<sup>-1</sup> and 1092 cm<sup>-1</sup> can be attributed to the formation of covalent Si-O-Al and Si-O-Si bonds respectively (27-29). In Figure 6.6b, the bands at 1241, 1355, 1452, 1557, 1636, and 2876 cm<sup>-1</sup> indicate the presence of PEG (26). The band at 1241 cm<sup>-1</sup> is ascribed to the wagging of Si(CH<sub>2</sub>), while the bands at 1355 cm<sup>-1</sup> and 1452 cm<sup>-1</sup> are attributed to the wagging of C-CH<sub>2</sub> and the bending of CH<sub>2</sub> of the grafted PEG (26). The two maxima at 1557 and 1636 cm<sup>-1</sup> are ascribed to the bending of N-H of the ureido groups (26). The band at 2876 cm<sup>-1</sup> is caused by the asymmetric stretching of -CH<sub>2</sub>- of the grafted PEG (26). The FTIR analysis indicated that the grafting reaction has occurred for the grafted  $\gamma$ -Al<sub>2</sub>O<sub>3</sub> powder.

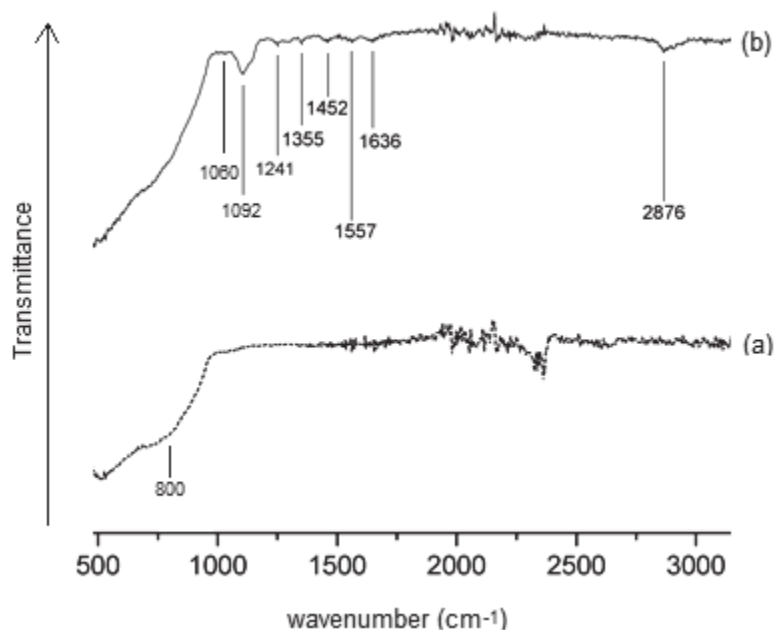


Figure 6.6. FTIR Transmittance Spectra of a) unmodified and b) grafted  $\gamma$ -Al<sub>2</sub>O<sub>3</sub> powder grafted with compound E (silylated ureido PEG with n = 10)

During the grafting reaction between the silanated PEG and the  $\gamma$ -Al<sub>2</sub>O<sub>3</sub> powder, the hydrolyzable alkoxy groups that do not form Si-O-Al bonds with the inorganic surface hydroxyl groups may self-condense with the adjacent silanols through the reaction: -Si-OH + Si-OH  $\rightarrow$  -Si-O-Si- + H<sub>2</sub>O forming a covalent Si-O-Si bond. The degree of self-condensation for each type of grafting agent can be semi-quantitatively analyzed by comparing the ratio of the Si – O absorbance peak at 1092 cm<sup>-1</sup> versus the Al –O absorbance band at 800 cm<sup>-1</sup>. The band at 800 cm<sup>-1</sup> is associated with the maximum IR absorbance due to the Al-O vibrations of the  $\gamma$ -alumina, while the band at 1092 cm<sup>-1</sup> is associated with the maximum IR absorbance due to the Si-O-Si vibrations of amorphous silica (27-29). It is assumed that the band at 1092 cm<sup>-1</sup> is only due to the Si-O-Si vibrations. Table 6.1 shows the ratio  $I_{\text{Si-O}}/I_{\text{Al-O}}$  of the Si-O and Al-O IR band intensities representing the importance of self-condensation among the hydrolyzable groups during grafting. The band intensities are the average of three FTIR spectra taken for each grafted sample type.

Table 6.1. Ratio of the Si-O versus Al-O IR bands ( $I_{\text{Si-O}}/I_{\text{Al-O}}$ ) as an indication of the degree of self-condensation among the hydrolyzable groups of the grafting agents.

Type	Si – O band intensity at 1092 cm <sup>-1</sup> $I_{\text{Si-O}}$	Al –O band intensity at 800 cm <sup>-1</sup> $I_{\text{Al-O}}$	$I_{\text{Si-O}}/I_{\text{Al-O}}$
A	0.020 ± 0.003	0.305 ± 0.012	0.066 ± 0.005
B	0.033 ± 0.003	0.328 ± 0.013	0.100 ± 0.008
C	0.027 ± 0.003	0.300 ± 0.012	0.089 ± 0.007
D	0.032 ± 0.003	0.319 ± 0.013	0.101 ± 0.008
E	0.026 ± 0.003	0.298 ± 0.012	0.088 ± 0.007
F	0.016 ± 0.003	0.298 ± 0.012	0.053 ± 0.004
G	0.034 ± 0.002	0.318 ± 0.013	0.107 ± 0.008
H	0.105 ± 0.004	0.386 ± 0.015	0.271 ± 0.021

Table 6.1 showed that self-condensation has occurred for all types of grafting agents. These results indicated that for most of the grafting agents studied (**A** to **G**) self-condensation (the formation of Si-O-Si bonds) is of the same order. Only a higher degree of self-condensation was observed for grafting agent **H**. From these results it can be

deduced that in most cases there is a comparable degree of resistance for the formation of Si-O-Si bonds regardless of the chain length of the grafting agents.

### 6.3.3. Structural configurations of the grafted moiety

The influence of the type of grafting agent on the number of alkoxy groups per PEG molecule that reacted with the surface hydroxyls was further investigated by  $^{29}\text{Si}$ -NMR analysis. If there are two hydrolysable alkoxy groups in addition to the Si atom ( $=\text{Si}(\text{OR})_2$ ), the grafting agent is called to have a D structure. If there are three hydrolysable alkoxy groups next to the Si atom ( $-\text{Si}(\text{OR})_3$ ) the grafting agent is considered as a T structure. In this work, the grafting agents **A - D** are having the D structure, while the grafting agents **E - H** are having the T structure.

In Figure 6.7  $^{29}\text{Si}$ -NMR spectra of  $\gamma\text{-Al}_2\text{O}_3$  powders grafted with the compounds A-H are given. The peak(s) appearing in the  $^{29}\text{Si}$ -NMR spectra are used to indicate the number of oxygen atoms directly bonded to a Si atom which in itself is bonded to the  $\gamma\text{-Al}_2\text{O}_3$  surface. If one silanol out of two is attached to the  $\gamma\text{-Al}_2\text{O}_3$  surface, a  $\text{D}^1$  annotation is used. If both silanols are attached to the  $\gamma\text{-Al}_2\text{O}_3$  surface, a  $\text{D}^2$  annotation is used. A chemical shift in the range of -10 to -13 ppm is generally assigned to a  $\text{D}^1$  structure and respectively in the range of -20 to -23 ppm to a  $\text{D}^2$  structure (30-31). A similar annotation also applies for the T structure, except that there are three possibilities for the T structure ( $\text{T}^1$ ,  $\text{T}^2$ , and  $\text{T}^3$ ). The chemical shifts in the range of -50 to -45 ppm is commonly ascribed to indicate a  $\text{T}^1$  structure, -55 ppm to -60 ppm to a  $\text{T}^2$  structure and -70 to -61 ppm for a  $\text{T}^3$  structure (32). The  $^{29}\text{Si}$ -NMR results for all types of grafting agents are given in Figure 6.7.

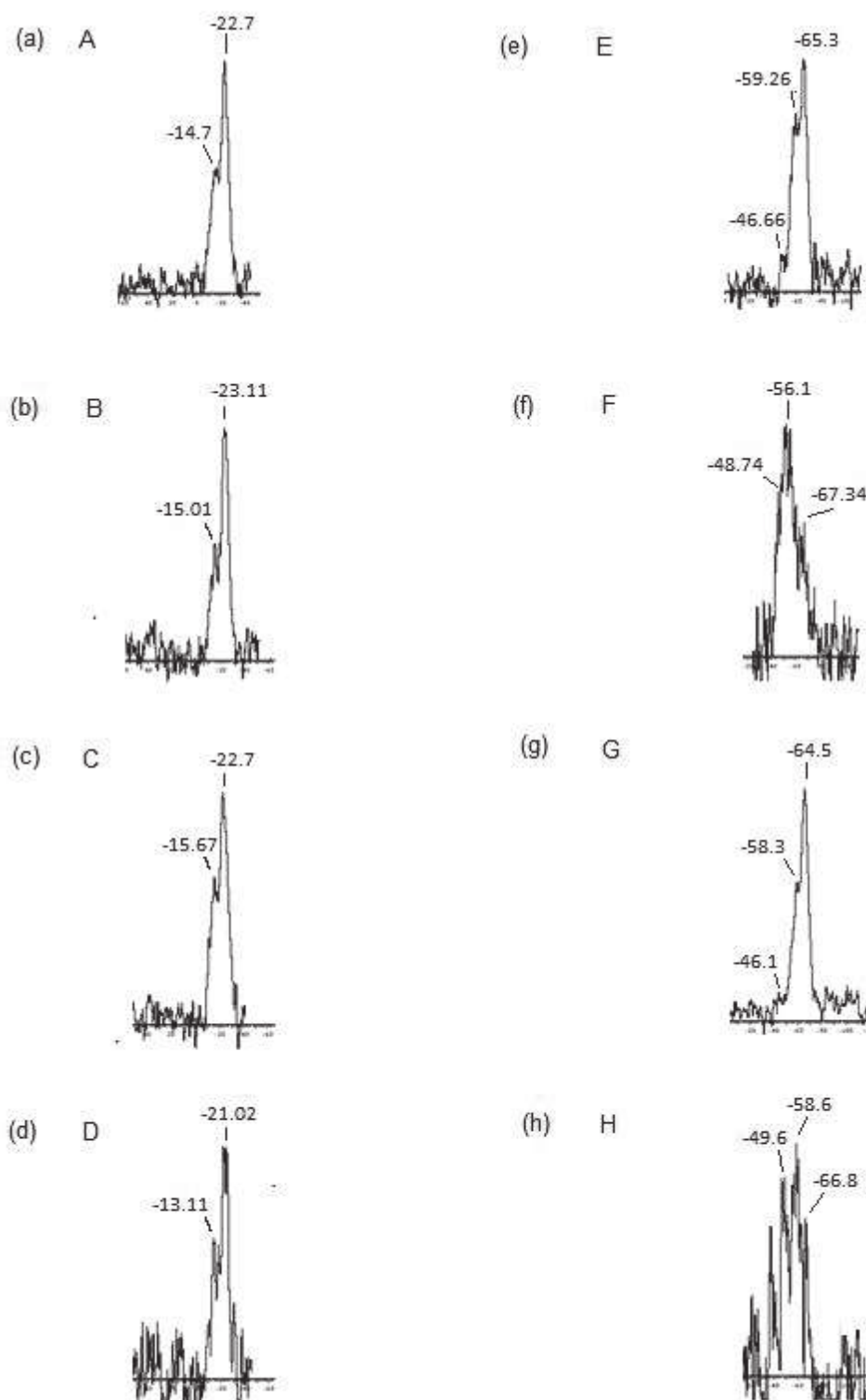


Figure 6.7.  $^{29}\text{Si}$  CP NMR spectra of the grafted  $\gamma\text{-Al}_2\text{O}_3$  powder with grafting agents (a) A to (h) H

In Figure 6.7 (a to d), there are two peaks identified in the  $\text{D}^1$  and  $\text{D}^2$  region indicating that both types of the D structure are present for the grafted  $\gamma\text{-Al}_2\text{O}_3$  by compounds A -

**D.** The peak area ratios for D<sup>1</sup> and D<sup>2</sup> configurations for powders grafted by grafting agents **A - D** are shown in Table 6.2.

Table 6.2. Relative peak area values for D<sup>1</sup> and D<sup>2</sup> configurations of the <sup>29</sup>Si NMR spectra for the powders grafted by grafting agent **A - D**

Type of Grafting Agent	D <sup>1</sup> (%)	D <sup>2</sup> (%)
A	50 ± 2	50 ± 2
B	50 ± 2	50 ± 2
C	50 ± 2	50 ± 2
D	70 ± 2	30 ± 2

From Table 6.2, it was found that the peak area ratios for the D<sup>1</sup> and D<sup>2</sup> for powders grafted with **A** to **C** are similar, while a higher percentage of D<sup>1</sup> structure is found for the powder grafted with **D**. This indicates that for the grafted powders **A**, **B** and **C** with a similar number of alkoxy functional groups but different chain length, the chain length of the grafting agent does not influence the ratio of the D<sup>1</sup> and D<sup>2</sup> configurations. For compound **D** a higher percentage of the grafting agent is bonded with only one siloxane group to the  $\gamma$ -alumina surface. This lower degree of bonding of the siloxane groups for grafting agent **D** can be attributed to the difference in the number of silica alkoxide groups present in the grafting agent **D** (3 groups) in comparison with **A – C** (6 groups; see Figure 6.1).

The relative peak area values for samples grafted with grafting agents **E - H** are given in Table 6.3.

Table 6.3. Relative peak areas for the three configurations for samples grafted with grafting agent **E - H**

Type of Grafting Agent	T <sup>1</sup> (%)	T <sup>2</sup> (%)	T <sup>3</sup> (%)
E	7 ± 1	66 ± 3	27 ± 1
F	25 ± 1	37 ± 1	38 ± 2
G	28 ± 1	7 ± 1	65 ± 3
H	25 ± 1	50 ± 2	25 ± 1

In Figure 6.7 (e to h), all 3 different types of T structures are present for all grafted  $\gamma$ -Al<sub>2</sub>O<sub>3</sub> powders. For powders grafted with **E** till **G** (Table 6.3) a trend can be seen that by

increasing the molecular weight of the grafting agent the percentage of the T<sup>3</sup> structure becomes higher, accompanied by a lower percentage of the T<sup>2</sup> structure. This indicates that the higher the molecular weight of the grafting agents, the more the T<sup>2</sup> structure converts to a T<sup>3</sup> structure. At a higher molecular weight or larger chain length of the grafting agent the distance between one PEG to the adjacent PEG becomes larger due to the higher molecular size. As a result, it may preserve the availability of the surface hydroxyls for reaction with the said grafting molecules rather than reacting with the adjacent PEG.

A different trend was observed for the grafting performance of compound **H** compared with **E-G** (see Table 6.3). This is attributed to the difference in the number of silica alkoxide and ureido groups for grafting agent **H** if compared with the other compounds (see Figure 6.1).

The <sup>29</sup>Si-NMR analysis showed that for  $\gamma$ -alumina powder grafted by ureido PEG, the chain length of the grafting agents influence the structural configuration. For  $\gamma$ -alumina powder grafted by non-ureido PEG, the chain length of the grafting agents does not seem to affect the structural configuration. Moreover, the number of the alkoxy groups also affect the structural configuration of the grafted moiety.

#### 6.3.4. Grafting density

TGA analysis was used to obtain information about the grafting density. The TGA results of the  $\gamma$ -Al<sub>2</sub>O<sub>3</sub> powders grafted with compounds **A** to **H** are shown in Figure 6.8. Two weight loss regions along the temperature axis can be observed. In the first region (20 to 100°C) initial weight losses (up to 1%) were observed. These initial weight losses can be attributed to the evaporation of adsorbed molecular water from the samples. In the second region, starting from 200°C, significant weight losses were observed. These weight losses can be attributed to the thermal decomposition of the organic groups from the samples. Above 500°C or in some cases above 600 to 700°C, no more significant weight losses were observed. The remaining weight (85-95%) observed at 700°C represents the inorganic groups (silica and  $\gamma$ -Al<sub>2</sub>O<sub>3</sub>) present in the samples.

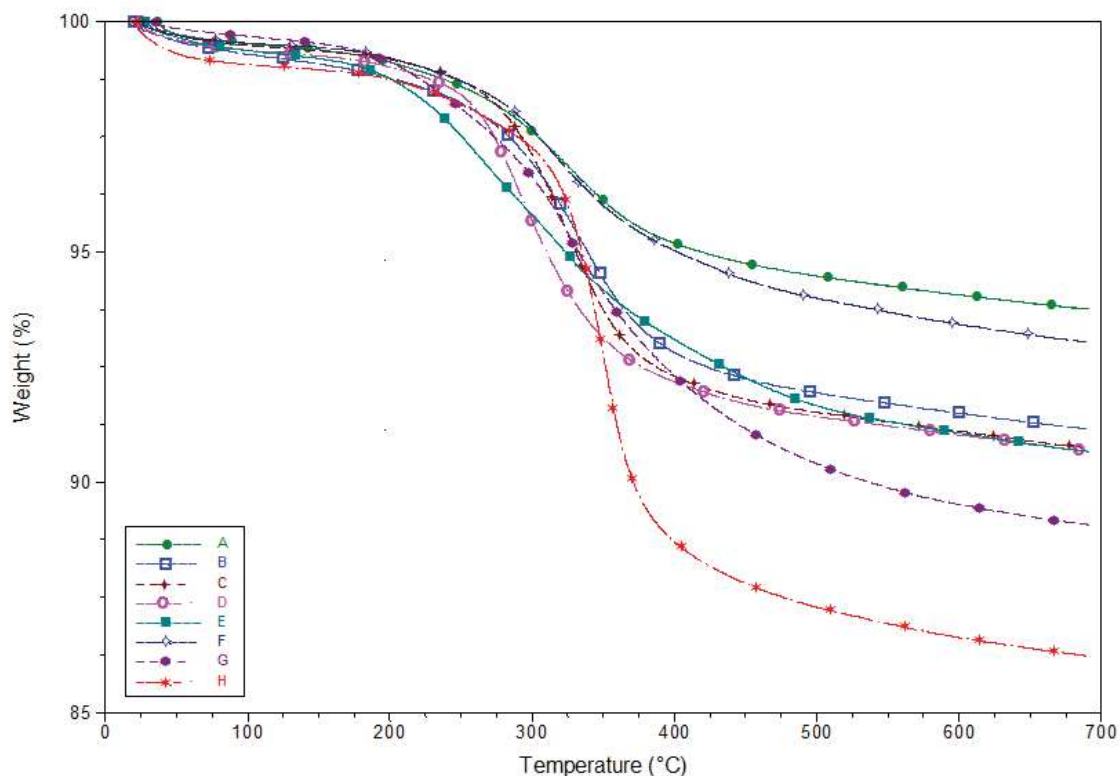


Figure 6.8. TGA results of  $\gamma$ - $\text{Al}_2\text{O}_3$  powders grafted by grafting agents A to H

By evaluating the degree of mass loss and the remaining mass in Figure 6.8, the grafting efficiency ( $G_{\text{eff}}$ ) can be calculated. Detailed information and calculations is provided in Table 6.4.

Table 6.4. Grafting efficiencies  $G_{\text{eff}}$  ( $10^{-6}$  mol/g) of  $\gamma$ - $\text{Al}_2\text{O}_3$  powder grafted by compounds A to H

ID	M1	M2	weight loss organics (%) <sup>*</sup>	weight loss organics (mg) <sup>*</sup>	# moles grafted PEG ( $10^{-6}$ mol) <sup>**</sup>	$W_{\text{Inorganics}}$ (mg) <sup>***</sup>	M3	mass of $\gamma$ - $\text{Al}_2\text{O}_3$ (mg) <sup>****</sup>	$G_{\text{eff}}$
A	733	629	$5.6 \pm 0.2$	$0.63 \pm 0.03$	$1.00 \pm 0.04$	$10.41 \pm 0.42$	104	$10.30 \pm 0.41$	$97 \pm 4$
B	933	829	$5.4 \pm 0.2$	$0.57 \pm 0.02$	$0.69 \pm 0.03$	$9.63 \pm 0.39$	104	$9.56 \pm 0.38$	$72 \pm 3$
C	1803	1699	$8.5 \pm 0.3$	$1.38 \pm 0.06$	$0.81 \pm 0.03$	$14.77 \pm 0.59$	104	$14.69 \pm 0.59$	$55 \pm 2$
D	2170	2121	$8.3 \pm 0.3$	$0.86 \pm 0.03$	$0.41 \pm 0.02$	$9.36 \pm 0.37$	49	$9.34 \pm 0.37$	$44 \pm 2$
E	786	723	$8.5 \pm 0.3$	$0.95 \pm 0.04$	$1.32 \pm 0.05$	$10.15 \pm 0.41$	63	$10.06 \pm 0.40$	$131 \pm 5$
F	1009	947	$6.4 \pm 0.3$	$0.83 \pm 0.03$	$0.88 \pm 0.04$	$11.99 \pm 0.48$	62	$11.93 \pm 0.48$	$73 \pm 3$
G	2240	2174	$10.3 \pm 0.4$	$1.06 \pm 0.04$	$0.49 \pm 0.02$	$9.12 \pm 0.36$	66	$9.09 \pm 0.36$	$54 \pm 2$
H	2037	1917	$12.5 \pm 0.5$	$1.46 \pm 0.06$	$0.76 \pm 0.03$	$10.02 \pm 0.40$	120	$9.93 \pm 0.40$	$77 \pm 3$

M1: Molecular weight of the grafted PEG molecules (A-H)

M2: Molecular weight of the organic parts of the grafted PEG molecules (*organic parts: e.g. C, H, O, N*)

M3: Molecular weight of the inorganic parts of the grafted PEG molecules

$G_{\text{eff}}$ : Grafting efficiency = (# moles grafted PEG)/(mass of  $\gamma$ - $\text{Al}_2\text{O}_3$ ) ( $10^{-6}$  mol/g)

\*The weight loss in the second weight loss region, starting from 200°C (see Figure 6.8), can be ascribed to the decomposition of the organic groups of the grafted PEG.

$$** \# \text{moles grafted PEG} = \frac{W_{\text{loss organics}}}{M2}$$

\*\*\*The remaining weight observed at 700°C (see Figure 6.8) represents the inorganic groups (silica and  $\gamma$ - $\text{Al}_2\text{O}_3$ ) present in the samples (=  $W_{\text{Inorganics}}$ )

$$**** \text{mass of } \gamma\text{-Al}_2\text{O}_3 = W_{\text{Inorganics}} - \# \text{moles grafted PEG} \times M3$$

The  $\gamma\text{-Al}_2\text{O}_3$  powders grafted by compounds **A** to **C** (the silylated PEG without ureido groups and similar number of alkoxy groups) showed that the grafting density decreases with increasing chain length of the grafting agents. For a fair comparison, the grafting agent **D** was not included since this compound has a different number of alkoxy groups compared to grafting agents **A** to **C**. For the  $\gamma\text{-Al}_2\text{O}_3$  powder grafted by compounds **E** to **G** (the silylated PEG with a similar number of ureido and alkoxy groups), the grafting density also decreases with increasing chain length of the grafting agents. The grafting agent **H** was not included here either as it has a different number of alkoxy and ureido groups compared to grafting agents **E** to **G**. The TGA analysis showed that the chain length of the grafting agents affects the grafting density. This can be explained by the difference in steric hindrance, as present during grafting, for grafting agents with different chain lengths. The highest grafting density in this work is obtained by grafting agent **E**, which is the silylated ureido PEG having the shortest chain length ( $n=10$ ). The chain length of the grafting agents is not the only factor affecting the grafting density. Compared to the grafting agent **A**, also with  $n = 10$  and an identical number and position of the alkoxy groups, the only difference is existence of the ureido groups in compound **E**. The self assembling, which takes place for compound **E** (see Figure 6.4b) has a positive influence on the grafting density.

### 6.3.5. Surface characteristics of the grafted powders

BET analysis were used to obtain information as whether the surface wettability of the  $\gamma$ -alumina powder has changed after being grafted. The BET constant ( $c$ ) is useful to indicate the hydrophilicity of the material. The BET constant ( $c$ ) is related to the energy of adsorption in the first adsorbed layer and its value shows the magnitude of the adsorbent/adsorbate interactions. The more hydrophilic the material, the higher the BET constant ( $c$ ) due to the stronger interaction of the powder with the adsorbed



nitrogen (33). Table 6.5 shows the BET specific surface area and the BET constant (c) values of ungrafted and grafted  $\gamma$ -Al<sub>2</sub>O<sub>3</sub> powders.

Table 6.5. BET specific surface area and the BET C constant of ungrafted and grafted  $\gamma$ -Al<sub>2</sub>O<sub>3</sub> powders by grafting agents A - H

Sample	BET constant	Specific Surface Area (m <sup>2</sup> /g)
Unmodified	125.5 ± 1.4	84.4 ± 0.9
A	33.8 ± 0.4	44.5 ± 0.5
B	37.9 ± 0.4	35.0 ± 0.4
C	37.7 ± 0.4	31.6 ± 0.3
D	37.0 ± 0.4	31.6 ± 0.3
E	40.9 ± 0.5	38.7 ± 0.4
F	41.7 ± 0.5	42.8 ± 0.5
G	45.8 ± 0.5	42.6 ± 0.5
H	35.6 ± 0.4	30.7 ± 0.3

It can be seen from Table 6.5 that the specific surface area of the  $\gamma$ -Al<sub>2</sub>O<sub>3</sub> powder decreases significantly after grafting. The lower BET constant (c) of the grafted powders versus that of the ungrafted suggested a weaker interaction between the nitrogen molecules and the sample surface due to the lower polarity of the polyethylene glycol as compared to that of the surface hydroxyl (OH<sup>-</sup>) groups. The BET analysis showed that the surface wettability of the  $\gamma$ -alumina powder has changed after grafting, while there is only a slight difference in wettability between the different grafting agents used.

### 6.3.6. Filtration performance of the grafted membranes

Based on the TGA analysis given in Table 6.1, the grafting agent E was chosen to be used as the grafting agent for the  $\gamma$ -alumina membranes, since it provides the highest grafting density.

Water contact angles were taken from the ungrafted and grafted membranes to investigate the membrane surface property after grafting (Table 6.6). The contact angle measurements were taken at 5 different points on the flat membrane surface and the average values were used. The negligible standard deviation shows that the grafting reaction occurred homogeneously throughout the membrane surface.

Table 6.6. Water Contact Angles (°)

	Ungrafted $\gamma$ -Al <sub>2</sub> O <sub>3</sub> membranes	Grafted $\gamma$ -Al <sub>2</sub> O <sub>3</sub> membranes
Water Contact Angle (°)	0	37.7 ± 0.7

For the unmodified gamma-alumina membrane, the water droplet immediately wetted the membrane surface. A corresponding water contact angle of 0° is therefore assumed, which is attributed to the hydrophilic characteristic of the  $\gamma$ -Al<sub>2</sub>O<sub>3</sub> membrane due to natural presence of hydroxyl (OH-) groups on the ceramic surface as well as the presence of the meso pores. After grafting, a relatively higher contact angle was observed. The higher contact angle observed might be attributed to the less polarity of the ethylene glycol groups causing a weaker interaction of the membrane surface with the water molecules. This observation is in agreement with the BET analysis on inorganic particles in which less hydrophilicity was observed after grafting with PEG (see Table 6.5). It is also worthwhile to mention that there are many other factors that can contribute to the higher contact angle observed, such as the nanotextures of the grafted moieties, the molecular orientation and/or the grafting density of the grafted moieties. The relative change in the water contact angle of the grafted membranes compared to that of native membranes may suggest that the surface characteristics of the  $\gamma$ -Al<sub>2</sub>O<sub>3</sub> has changed after grafting.

The permeability tests using pure ethanol and hexane were conducted on the grafted  $\gamma$ -Al<sub>2</sub>O<sub>3</sub> membranes. Ethanol and hexane were chosen as probe solvents since their sorption tendency with regard to PEG differ dramatically (34). First of all, the permeability of grafted membranes was investigated as a function of the applied pressure. Figure 6.9 shows the permeability test results of hexane and ethanol through the grafted membranes at 20°C as a function of Trans Membrane Pressure (TMP).

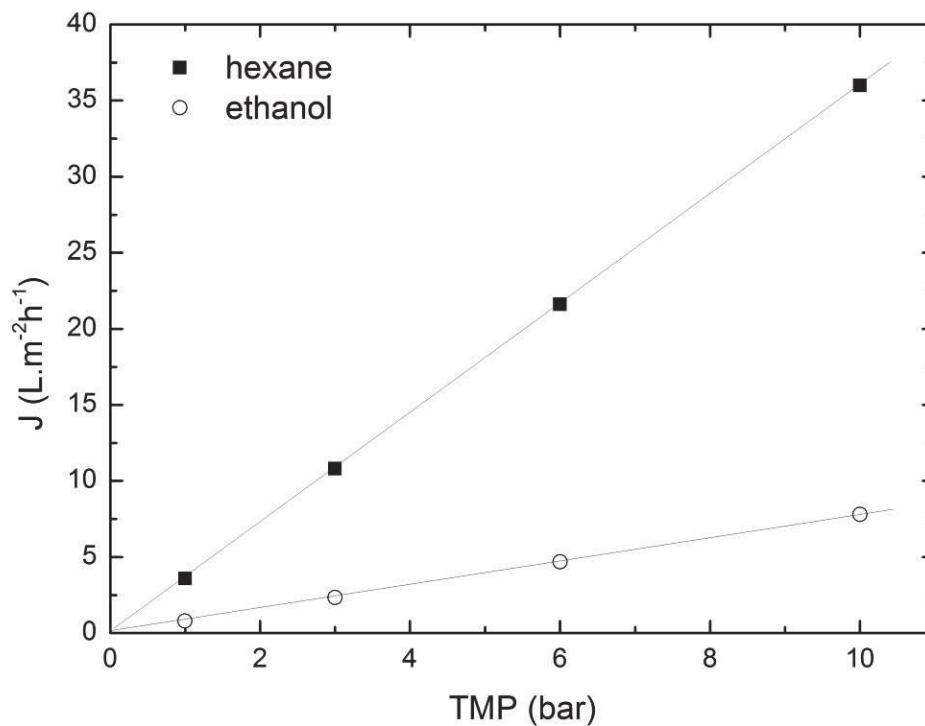


Figure 6.9. Fluxes ( $J$ ) of pure ethanol and pure hexane at 20°C through the grafted  $\gamma$ -Al<sub>2</sub>O<sub>3</sub> membranes grafted by the grafting agent E as a function of Trans Membrane Pressure ( $TMP$ )

A linear relationship between flux and TMP was observed showing no sign of compaction. This indicates the absence of shear-flow induced behaviour in the applied pressure range studied as was also observed in (8-9, 11) for PDMS grafted  $\gamma$ -Al<sub>2</sub>O<sub>3</sub> membranes.

Table 6.7 shows the pure solvent flux of hexane and ethanol at 10 bars and 20°C through the ungrafted and grafted  $\gamma$ -Al<sub>2</sub>O<sub>3</sub> membranes. The values shown are the average of three membrane samples and two measurements for each sample. The low standard deviation demonstrated that this method of grafting results in membranes with a high reproducibility.

Table 6.7. Pure solvent fluxes at 10 bars and 20°C through the ungrafted and grafted  $\gamma$ -Al<sub>2</sub>O<sub>3</sub> membranes

Solvent	Flux (L.m <sup>-2</sup> h <sup>-1</sup> )	
	Ethanol	Hexane
Ungrafted	36.0 ± 1.1	84.4 ± 2.4
Grafted	7.8 ± 0.1	37.3 ± 1.2

The flux of hexane as well as of ethanol decreased significantly after grafting (Table 6.7) due to the occupation of the membrane pores by the grafted PEG resulting in a more closed membrane structure after grafting.

The plot of pure solvent flux versus TMP/  $\mu$  (according to Hagen-Poiseuille relation) is given in Figure 6.10.

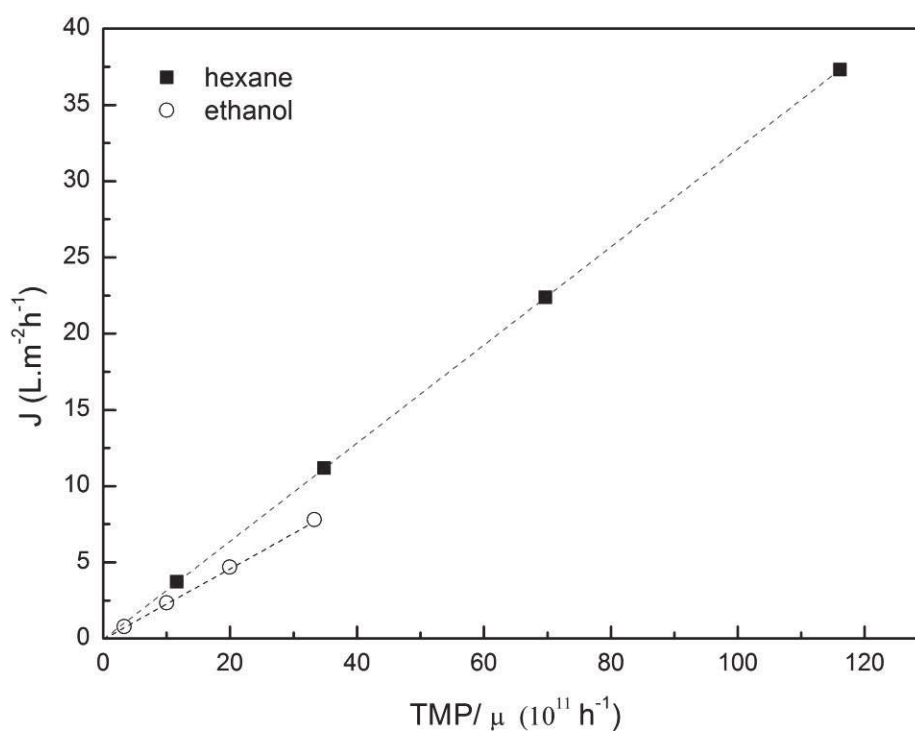


Figure 6.10. Fluxes ( $J$ ) versus the  $\text{TMP}/\mu$  (according to Hagen-Poiseuille relation) of pure ethanol and pure hexane at 20°C through the grafted  $\gamma$ -Al<sub>2</sub>O<sub>3</sub> membranes grafted by the grafting agent E

For the PEG grafted ceramic membranes, the viscosity corrected flux for ethanol is lower than that for hexane (Figure 6.10). This is in contrast with the result of the hydrophobic PDMS grafted ceramic membranes, in which a higher viscosity corrected flux was found

for polar solvents like isopropanol than for nonpolar solvents such as hexane [13]. This opposite behavior can be explained by the different sorption behavior of the grafted PDMS versus that of the grafted PEG. In contrast to PDMS, a more dramatic swelling occurs for PEG in the presence of ethanol than for hexane(34), instead of the other way around. A higher sorption of ethanol in PEG for the PEG grafted  $\gamma$ -Al<sub>2</sub>O<sub>3</sub> membranes causes a stronger reduction of the membrane permeable volume for the permeation of ethanol, while the reduction is less for the permeation of hexane. As a result, a more closed membrane structure is realized for the PEG grafted membranes in the presence of ethanol than that of hexane. The more closed structure of the PEG grafted membranes in the presence of ethanol is further investigated by performing Sudan Black rejection tests. Table 6.8 shows the rejection results of Sudan Black in ethanol and in hexane through the grafted  $\gamma$ -Al<sub>2</sub>O<sub>3</sub> membranes at 20°C and 10 bars at 50% recovery.

Table 6.8. Rejection data of Sudan Black in pure hexane and ethanol through grafted  $\gamma$ -Al<sub>2</sub>O<sub>3</sub> membranes at 20°C and 10 bars

Solvent Types	Flux (lmh)	Rejection (%)
Hexane	37.3 ± 1.5	54 ± 1
Ethanol	7.8 ± 0.3	89 ± 1

No significant differences between the flux of pure solvent and solvent with 8000 ppm of Sudan Black was observed. This indicated that concentration polarization does not occur. From the results as given in Table 6.8 it can be seen that the rejection of Sudan Black in ethanol is higher than that in hexane. The solute rejection results are in agreement with the results of the permeability tests, meaning a trade-off between membrane permeability and rejection was observed. The higher rejection of Sudan Black in the presence of a polar solvent than that of nonpolar solvent is in contrast with the rejection behavior when using PDMS grafted  $\gamma$ -Al<sub>2</sub>O<sub>3</sub> membranes (12). The differences in viscosity corrected flux (Figure 6.10) and solute rejection (Table 6.8) of the PEG grafted ceramic membranes in the presence of ethanol compared to hexane can be explained by the different sorption tendency of the grafted PEG in different types of solvent affecting the membrane effective pore size.

#### 6.4. Conclusion

A grafting method of a mesoporous  $\gamma$ -alumina layer, supported on macro porous  $\alpha$ -alumina, by polyethylene glycol (PEG) is presented. The grafting nature of  $\gamma$ -alumina with different grafting agents, having different molecular weights, numbers of alkoxy groups and numbers of ureido groups were investigated by means of FTIR, TGA,  $^{29}\text{Si}$ -NMR and BET using inorganic particles as surrogate surfaces. FTIR analysis indicated that the grafting reaction has occurred for the grafted  $\gamma\text{-Al}_2\text{O}_3$  powder. The degree of self-condensation is about the same for most of the grafting agents as analyzed from FTIR spectra.  $^{29}\text{Si}$ -NMR analysis showed that for the ureido PEG, the chain length of the grafting agents influences the structural configuration of the grafted moiety, i.e. the number of the Si-O-Al bond per PEG molecules. For PEG without ureido functionality, no significant influence of the chain length of the grafting agents on the structural configuration of the grafted moiety was observed. The chemical structure of the grafting agents such as the number of hydrolyzable groups also influences the structural configuration of the grafted moiety. TGA analysis showed that an increased grafting density was observed with a decreasing chain length of the grafting agents for grafting agents having similar numbers of alkoxy and ureido groups. Contact angle measurements and solvent permeability tests of the ungrafted and grafted  $\gamma\text{-Al}_2\text{O}_3$  membranes show that the membrane properties changed after grafting. A higher contact angle, but still in the hydrophilic region, was observed after grafting. A lower solvent permeation of both ethanol and hexane was observed due to the presence of the grafted moiety inside the membranes, reducing the membrane pore diameter. The permeability behavior with respect to different types of permeating solvent (polar and nonpolar) show a lower permeability of ethanol than hexane, accompanied by a higher selectivity of Sudan Black in ethanol than in hexane. This effect is explained by the difference in solvent sorption in the grafted moiety for different types of the permeating solvents.

## Acknowledgement

The authors acknowledge the financial support from the European Union – The Education, Audiovisual and Culture Executive Agency (EACEA) under the Program “Erasmus Mundus Doctorate in Membrane Engineering” – EUDIME (FPA 2011-2014).

## References

1. Vandezande, P., Gevers, L. E. M., and Vankelecom, I. F. J. (2008) Solvent resistant nanofiltration: Separating on a molecular level, *Chemical Society Reviews* 37, 365-405.
2. Mulder, M. (1996) *Basic principles of membrane technology*, 2nd ed., Kluwer Academic Publisher, Netherlands.
3. Faibish, R. S., and Cohen, Y. (2001) Fouling-resistant ceramic-supported polymer membranes for ultrafiltration of oil-in-water microemulsions, *Journal of Membrane Science* 185, 129-143.
4. Koonaphapdeelert, S., and Li, K. (2007) Preparation and characterization of hydrophobic ceramic hollow fibre membrane, *Journal of Membrane Science* 291, 70-76.
5. Yoshida, W., and Cohen, Y. (2004) Removal of methyl tert-butyl ether from water by pervaporation using ceramic-supported polymer membranes, *Journal of Membrane Science* 229, 27-32.
6. Popat, K. C., Mor, G., Grimes, C. A., and Desai, T. A. (2004) Surface Modification of Nanoporous Alumina Surfaces with Poly(ethylene glycol), *Langmuir* 20, 8035-8041.
7. Lee, S. W., Shang, H., Haasch, R. T., Petrova, V., and Lee, G. U. (2005) Transport and functional behaviour of poly(ethylene glycol)-modified nanoporous alumina membranes, *Nanotechnology* 16, 1335-1340.
8. Pinheiro, A. F. M., Hoogendoorn, D., Nijmeijer, A., and Winnubst, L. (2014) Development of a PDMS-grafted alumina membrane and its evaluation as solvent resistant nanofiltration membrane, *Journal of Membrane Science* 463, 24-32.
9. Tanardi, C. R., Pinheiro, A. F. M., Nijmeijer, A., and Winnubst, L. (2014) PDMS grafting of mesoporous  $\gamma$ -alumina membranes for nanofiltration of organic solvents, *Journal of Membrane Science* 469, 471-477.
10. Yoshida, W., and Cohen, Y. (2003) Ceramic-supported polymer membranes for pervaporation of binary organic/organic mixtures, *Journal of Membrane Science* 213, 145-157.

11. Tanardi, C. R., Vankelecom, I. F. J., Pinheiro, A. F. M., Tetala, K. K. R., Nijmeijer, A., and Winnubst, L. (2015) Solvent Permeation Behavior of PDMS Grafted  $\gamma$ -Alumina Membranes.
12. Tanardi, C. R., Vankelecom, I. F. J., Nijmeijer, A., and Winnubst, L. (2015) Solute Rejection in SRNF using PDMS Grafted  $\gamma$ -Alumina Membranes.
13. Nijmeijer, A., Bladergroen, B. J., and Verweij, H. (1998) Low-temperature CVI modification of  $\gamma$ -alumina membranes, *Microporous and Mesoporous Materials* 25, 179-184.
14. Cuperus, F. P., Bargeman, D., and Smolders, C. A. (1992) Permporometry: the determination of the size distribution of active pores in UF membranes, *Journal of Membrane Science* 71, 57-67.
15. Six, C., and Richter, F. (2000) Isocyanates, Organic, In *Ullmann's Encyclopedia of Industrial Chemistry*, Wiley-VCH Verlag GmbH & Co. KGaA.
16. Compton, R., Bamford, C., and Tipper, C. (1976) *Non-radical polymerisation*, Vol. 15, Elsevier.
17. Yoshida, W., Castro, R. P., Jou, J.-D., and Cohen, Y. (2001) Multilayer Alkoxysilane Silylation of Oxide Surfaces, *Langmuir* 17, 5882-5888.
18. Pinheiro, A. F. M. (2013) Development and Characterization of Polymer-grafted Ceramic Membranes for Solvent Nanofiltration, In *PhD Thesis*, University of Twente, Enschede.
19. Sah, A., Castricum, H. L., Bliet, A., Blank, D. H. A., and Ten Elshof, J. E. (2004) Hydrophobic modification of  $\gamma$ -alumina membranes with organochlorosilanes, *Journal of Membrane Science* 243, 125-132.
20. Picard, C., Larbot, A., Guida-Pietrasanta, F., Boutevin, B., and Ratsimihety, A. (2001) Grafting of ceramic membranes by fluorinated silanes: Hydrophobic features, *Separation and Purification Technology* 25, 65-69.
21. Alami Younssi, S., Iraqi, A., Rafiq, M., Persin, M., Larbot, A., and Sarrazin, J. (2003)  $\gamma$  Alumina membranes grafting by organosilanes and its application to the separation of solvent mixtures by pervaporation, *Separation and Purification Technology* 32, 175-179.
22. Van Gestel, T., Van der Bruggen, B., Buekenhoudt, A., Dotremont, C., Luyten, J., Vandecasteele, C., and Maes, G. (2003) Surface modification of  $\gamma$ -Al<sub>2</sub>O<sub>3</sub>/TiO<sub>2</sub> multilayer membranes for applications in non-polar organic solvents, *Journal of Membrane Science* 224, 3-10.
23. Leger, C., Lira, H. L., and Paterson, R. (1996) Preparation and properties of surface modified ceramic membranes. Part III. Gas permeation of 5 nm alumina membranes modified by trichloro-octadecylsilane, *Journal of Membrane Science* 120, 187-195.



24. Belyavskii, S. G., Mingalev, P. G., and Lisichkin, G. V. (2004) Chemical modification of  $\gamma$ -Al<sub>2</sub>O<sub>3</sub> surface with aryl silanes, *Colloid Journal* 66, 128-136.
25. Fadeev, A. Y., and McCarthy, T. J. (2000) Self-assembly is not the only reaction possible between alkyltrichlorosilanes and surfaces: monomolecular and oligomeric covalently attached layers of dichloro- and trichloroalkylsilanes on silicon, *Langmuir* 16, 7268-7274.
26. Pretsch, E., Buhlmann, P., and Badertscher, M. (2009) Structure Determination of Organic Compounds, 4th ed., Springer, Heidelberg.
27. Jakobsson, S. (2002) Determination of Si/Al Ratios in Semicrystalline Aluminosilicates by FT-IR Spectroscopy, *Spectroscopy Techniques* 56, 797-799.
28. Sinko K., M. R., Rohonczy, J., Frazl P. (1999) Gel Structures Containing Al(III), *Langmuir* 15, 6631-6636.
29. Anderson, D. R. (1974) *Analysis of Silicones*, Wiley-Interscience, New York.
30. Harris, R. K., and Robins, M. L. (1978) <sup>29</sup>Si nuclear magnetic resonance studies of oligomeric and polymeric siloxanes: 4. Chemical shift effects of end-groups, *Polymer* 19, 1123-1132.
31. Sugahara, Y., Okada, S., Kuroda, K., and Kato, C. (1992) <sup>29</sup>Si-NMR study of hydrolysis and initial polycondensation processes of organoalkoxysilanes. I. Dimethyldiethoxysilane, *Journal of Non-Crystalline Solids* 139, 25-34.
32. Bauer, F., Gläsel, H.-J., Decker, U., Ernst, H., Freyer, A., Hartmann, E., Sauerland, V., and Mehnert, R. (2003) Trialkoxysilane grafting onto nanoparticles for the preparation of clear coat polyacrylate systems with excellent scratch performance, *Progress in Organic Coatings* 47, 147-153.
33. Lecloux, A., and Pirard, J. P. (1979) The importance of standard isotherms in the analysis of adsorption isotherms for determining the porous texture of solids, *Journal of Colloid and Interface Science* 70, 265-281.
34. Mark, J. E. (1999) *Polymer Data Handbook*, Oxford University Press, Oxford.

## Supporting Information for Chapter 6

The preparations of the ureido PEG grafting agents (compounds **E** to **H**) were as follows:

*Compound E.* To a stirred solution of 75 mg (0.15 mmol) of amine terminated poly ethylene glycol dissolved in 5.0 mL of acetonitrile, 39.4  $\mu$ L (39 mg, 0.15 mmol) of isocyanate triethoxysilane was added. The mixture was stirred and refluxed for 24 hours at 76°C (the boiling point of acetonitrile). The product (112.9 mg, 0.15 mmol) was recovered by rotary evaporator in the form of yellowish gel.  $^1\text{H}$  NMR (300 MHz, DMSO- $d_6$ ) :  $\delta$  (ppm) = 0,542-0,478 (t, 2H, SiCH<sub>2</sub>); 1,438 (m, 2H, CH<sub>2</sub>); 2,956 (q, 2H, CH<sub>2</sub>); 3,155-3,122 (t, 2H, CH<sub>2</sub>); 3,237 (s, 3H, OCH<sub>3</sub>); 3,320 (q, 6H, CH<sub>2</sub>); 3,510 (s, 30H, CH<sub>2</sub> PEG); 3,740 (t, 2H, CH<sub>2</sub>); 5,881 (s, 1H, urea); 6,024 (s, 1H, urea).

*Compound F.* To a stirred solution of 112.5 mg (0.15 mmol) of amine terminated poly ethylene glycol dissolved in 5.0 mL of acetonitrile, 39.4  $\mu$ L (39 mg, 0.15 mmol) of isocyanate triethoxysilane was added. The mixture was heated to reflux for 24 hours. The product (150 mg, 0.15 mmol) was recovered by rotary evaporator in the form of yellowish gel.  $^1\text{H}$  NMR (300 MHz, DMSO- $d_6$ ):  $\delta$  (ppm) = 0,628-0,573 (t, 2H, SiCH<sub>2</sub>); 1,176-1,119 (m, 2H, CH<sub>2</sub>); 2,961-2,896 (q, 2H, CH<sub>2</sub>); 3,241 (s, 3H, OCH<sub>3</sub>); 3,310 (q, 6H, CH<sub>2</sub>); 3,446-3,413 (t, 2H, CH<sub>2</sub>); 3,511 (s, 60H, CH<sub>2</sub> PEG); 4,566-4.530 (t, 2H, CH<sub>2</sub>); 5,763 (t, 2H, urea).

*Compound G.* To a stirred solution of 300 mg (0.15 mmol) of amine terminated poly ethylene glycol dissolved in 5.0 mL of acetonitrile, 39.4  $\mu$ L (39 mg, 0.15 mmol) of isocyanate triethoxysilane was added. The mixture was heated to reflux for 24 hours. The product (335.61 mg, 0.15 mmol) was recovered by rotary evaporator in the form of yellowish gel.  $^1\text{H}$  NMR (300 MHz, DMSO- $d_6$ ):  $\delta$  (ppm) = 0,501 (t, 2H, SiCH<sub>2</sub>); 1,172-1,120 (m, 2H, CH<sub>2</sub>); 2,968 (q, 2H, CH<sub>2</sub>); 3,241 (s, 3H, OCH<sub>3</sub>); 3,315 (q, 6H, CH<sub>2</sub>); 3,446-3,413 (t, 2H, CH<sub>2</sub>); 3,501 (s, 60H, CH<sub>2</sub> PEG); 4,501 (t, 2H, CH<sub>2</sub>); 5,821 (t, 2H, urea).

*Compound H.* To a stirred solution of 225 mg (0.15 mmol) of amine terminated poly ethylene glycol dissolved in 5.0 mL of acetonitrile, 78.8  $\mu$ L (78 mg, 0.30 mmol) of isocyanate triethoxysilane was added. The mixture was heated to reflux for 24 hours. The product (299.81 mg, 0.15 mmol) was recovered by rotary evaporator in the form of yellowish gel.  $^1\text{H}$  NMR (300 MHz, DMSO- $d_6$ ):  $\delta$  (ppm) = 0,542-0,486 (t, 4H, SiCH<sub>2</sub>); 1,173-1,127 (t, 18H, CH<sub>2</sub>);

1,632-1,543 (q, 4H, CH<sub>2</sub>); 3,519 (s, 69H, CH<sub>2</sub> PEG); 3,780-3,710 (quin, 8H, CH<sub>2</sub>); 5,802-5,703 (2t, 4H, urea).



# **Chapter 7**

## **Reflections and Outlook**

## 7.1. Reflections

Organic Solvent Nanofiltration (OSN) is a potential technology to perform solvent recovery. Solvent nanofiltration consumes less energy than evaporation and distillation, enabling it as a potential economic and energy-efficient solution for solvent recovery in various industries (1). For this application, a chemically stable membrane that can endure continuous exposure towards organic solvents is required. This thesis deals with the grafting of ceramic membranes with organic moieties for solvent resistant nanofiltration and studying of their solvent and solute transport. Different grafting methods were employed in Chapter 2, 5, and 6 and its effect on the membrane performance were assessed. Moreover, in Chapter 6 a more detailed investigation of the effect of different properties of grafting agents on the grafting performance was presented. The transport of these membranes for SRNF application were studied in Chapter 3 and 4, 5 and 6, and a model was deduced from the observed permeability and selectivity to describe the membrane transport behavior.

### 7.1.1. Grafting as a method to prepare a robust chemically stable SRNF membrane

In Chapter 2, a method of grafting a mesoporous  $\gamma$ -alumina layer, supported on macro porous  $\alpha$ -alumina, with 3-mercaptopropyltriethoxysilane (MPTES) as linking agent and subsequently with Monovinyl terminated polydimethylsiloxane (PDMS) as polymer grafted to this linker was presented. A two-step grafting was employed in which organosilanes were grafted first to the pore wall of the  $\gamma$ -alumina and then PDMS was grafted to the silanes. This method results in stable covalent bonds between the PDMS, MPTES, and  $\gamma$ -alumina as analyzed by FTIR and chemical stability tests. The resulting membranes have a rejection of 64% in toluene using Sudan Black as the probe solutes.

In Chapter 2, PDMS was grafted to the ceramic mesoporous substrate without additional covalent coupling for growing of the organic chain from the pore wall, while in Chapter 5 a reaction between PDMS molecules and a coupling agent was used in order to result in grafted organic network inside the pores. In Chapter 5, the grafting of mesoporous  $\gamma$ -alumina membranes with hydride terminated polydimethylsiloxanes is described. Vinyltriethoxysilane is used as linking agent and tetrakis (vinyl dimethylsiloxy)silane as

coupling agent, in order to generate a membrane for solvent nanofiltration. The use of coupling agent during grafting promotes formation of grafted organic network which results in a smaller membrane pores after grafting if compared to the results given in (2) and Chapter 2. This is proven by the fact PDMS-grafted membranes as described in Chapter 5 resulted in a rejection of 95% for Sudan Black in toluene as the probe solutes, while for the non-cross-linked system a Sudan Black in toluene rejection of only 65 % was observed.

In Chapters 2 and 5, chemical grafting was carried out in two consecutive steps, where a silane linking agent was first grafted onto the pore wall, using a vapour phase deposition method and then reacted with oligomers. In Chapter 6, a different strategy was utilized, in which the organics were silylated first and then grafted to the ceramic pore wall using solution phase deposition method. The latter method was used for the grafting of a mesoporous  $\gamma$ -alumina layer, supported on a macro porous  $\alpha$ -alumina, with several types of silane terminated polyethylene glycol as to result in a hydrophilic chemically and thermally stable membrane for SRNF. The membranes resulted have a rejection of 89% for Sudan Black in ethanol as the probe solutes.

All methods result in permanent modification of  $\gamma$ -alumina membranes. A summary of SRNF results of grafted membranes, described in this thesis, are presented in Table 7.1.

Table 7.1. Summary of OSN results of grafted membranes, described in this thesis

$\gamma$ -Alumina Membranes grafted with:	Ch. no.	Contact Angle (°)	Toluene		Isopropanol		Ethanol		Hexane	
			F *	R **	F *	R **	F *	R **	F *	R **
PDMS	3,4	95 ± 1	23.7 ± 1.0	65 ± 1	7.6 ± 0.2	35 ± 1			87.1 ± 2.7	88 ± 1
Coupled PDMS	5	108 ± 1	12.7 ± 0.3	95 ± 1	4.0 ± 0.1	80 ± 1				
PEG	6	38 ± 1					7.8 ± 0.3	89 ± 1	37.3 ± 1.5	54 ± 1

\* F: Flux ( $L \cdot m^{-2} \cdot h^{-1}$ ) at trans-membrane pressure of 10 bar

\*\* R: Retention (in %) of Sudan Black at 50% recovery

The transport behavior of grafted membranes was studied in Chapter 3 and 4 for PDMS grafted ceramic membranes and Chapter 6 for PEG grafted ceramic membranes. From the transport study, it is found that the PDMS grafting of  $\gamma$ -alumina membranes is more

suitable for nonpolar solvent application, while the PEG grafting of  $\gamma$ -alumina membranes is rather appropriate for polar solvent application.

### **7.1.2. Grafting as a method to alter the membrane surface polarity**

Each type of grafted membranes exhibit a certain water contact angle that can be used as an indication of the membrane surface properties (see Table 7.1). As shown in Chapters 2 and 5, grafting of  $\gamma$ -alumina by PDMS results in a water contact angle value of 95 and 108 degrees respectively, while the grafting of  $\gamma$ -alumina by PDMS as described in (2) results in water contact angle values in range from 91 to 97 degrees. This shows that the water contact angle for membranes grafted by PDMS falls in the same range, while a significantly different water contact angle was found for PEG grafted membranes. This may indicate that the membrane surface character is heavily affected by the wettability of the grafted material.

In Chapter 6, BET is a simple tool to obtain an indication of surface polarity. BET analysis on several types of PEG grafted  $\gamma$ -alumina powders showed a change in the BET constant (c) for the grafted powder if compared to the value of an unmodified  $\gamma$ -alumina powder. Another important point to be mentioned is that the BET constant (c) does not differ significantly regardless of the different types of the PEG grafting agents, i.e. different number of hydrolyzable groups, different number of ureido functionality groups and different molecular weights. The BET constant (c) is related to the energy of adsorption in the first adsorbed layer and its value shows the magnitude of the adsorbent/adsorbate interactions. The more hydrophilic the material, the higher the BET constant (c) due to the stronger interaction of the powder with the adsorbed nitrogen (3). A lower BET constant (c) of the grafted powders versus that of the ungrafted were observed due to the lower polarity of the PEG as compared to that of the surface hydroxyl (OH-) groups causing a weaker interaction between the nitrogen molecules and the grafted powder.

### **7.1.3. Homogeneity of grafting**

Contact angle measurements were taken from 5 different points on the flat membrane surfaces and averaged for each grafted membrane, as described in this thesis. The



negligible standard deviation shows that grafting has occurred homogeneously over the membrane surface. From SEM-EDX analyses, it is observed that the grafting occurs throughout the  $\gamma$ -alumina layer with an observed thickness of about 3  $\mu\text{m}$ .

#### **7.1.4. Grafting as a method to increase the membrane selectivity**

Permeability and rejection tests of the ungrafted and grafted  $\gamma\text{-Al}_2\text{O}_3$  membranes show that the grafting influences the membrane selectivity. It is shown that grafting significantly resulted in a decrease in flux and an increase in the membrane selectivity compared to those of the unmodified  $\gamma$ -alumina. The lower permeability is attributed to the occupation of the membrane pores by the grafted moiety resulting in a more closed membrane structure after grafting.

#### **7.1.5. Chemical and thermal stability of grafted $\gamma\text{-Al}_2\text{O}_3$**

Chemical stability tests were performed by soaking the grafted membranes for several days in a variety of solvents at elevated temperatures, while the thermal stability of the membranes in air was studied by TGA. The results as described in Chapter 2, showed no degradation of the PDMS grafted  $\gamma$ -alumina membranes after tests in toluene for 6 days at room temperature and at elevated temperatures (up to 90 °C). The couple PDMS grafted  $\gamma\text{-Al}_2\text{O}_3$  systems, as described in Chapter 5 were studied by TGA. It was shown that these materials are stable up to 300°C, after which the degradation of organic component takes place. The results in Chapter 6 show that the PEG grafted  $\gamma$ -alumina membranes are thermally stable up to 250-300°C. This showed that the grafting methods, described in this thesis, result in thermally and chemically stable membranes for potential use as chemical and thermal stable organic solvent nanofiltration membranes.

#### **7.1.6. Influences of the types of the grafting agents on the grafting results**

The nature of the grafting agents such as the number of the hydrolyzable groups can affect the grafting results. Self-condensation has occurred for all types of grafting agents and in most cases a comparable degree of self-condensation was observed. For the PEG with ureido functionality, as described in Chapter 6, the chain length of the grafting agent influences the number of alkoxy groups per PEG molecule that reacted with the surface

hydroxyls. The larger the chain length, the more alkoxy groups per PEG molecules that react with the surface hydroxyls of the membrane. For non-ureido PEG, the chain length of the grafting agents does not affect the number of alkoxy groups per PEG molecule that reacted with the surface hydroxyls. For all types of grafting agents, the grafting density decreases with increasing chain length of the grafting agents. This can be explained by the difference in steric hindrance, as present during grafting, for grafting agents with different chain lengths.

### **7.1.7. Transport behavior of organically grafted ceramic membranes**

Detailed knowledge of major parameters influencing the solvent and solute transport of grafted ceramic membranes is very important in order to predict their permeation behavior for various solvent-solute systems.

In Chapter 3, the solvent permeation behavior of PDMS grafted  $\gamma$ -Al<sub>2</sub>O<sub>3</sub> membranes were studied. A positive linear relationship between membrane permeability and applied pressure is found. No compaction or shear flow-induced behavior was observed during solvent transport through the grafted membranes at trans-membrane pressures up to 20 bars. Shear-rate induced behavior was described as a condition in which the membrane is experiencing a more open membrane structure due to the movement of the grafted moieties in the direction of the feed flow, resulting in an exponential increase in the membrane permeability towards the trans-membrane pressure. This was not observed for the grafted membranes prepared in this thesis. The smaller pore size of the ceramic porous support (5 nm) used in this work which might provide higher confinement towards the shear rate effect than for macroporous ceramic supports (410 nm)(4). Selecting  $\gamma$ -alumina with a pore size as small as possible but sufficiently large to graft a (small) polymer on the pore walls in order to have the largest benefit of the rigid character of a ceramic membrane system is necessary to prevent the shear-rate induced behavior.

The solvent permeability in polymer grafted ceramic membranes is described by incorporating solvent sorption terms into the Hagen-Poiseuille equation. Two grafted alumina membranes were examined, using PDMS molecules with different chain lengths.

The results show that the flux differences can be described by incorporating sorption and viscosity differences between the solvents. This provides an initial way to predict the performance of grafted porous membranes for solvent filtration.

In Chapter 4 the solute rejection of PDMS grafted  $\gamma$ -alumina membranes was described for different solvent-solute pairs. In contrary to what is observed for pure PDMS SRNF membranes, higher rejections were found for PDMS grafted membranes in the presence of nonpolar solvents like toluene than those in polar solvents such as isopropanol. This signifies that the solvent transport of PDMS grafted in a confined (ceramic) matrix is different than that of unconfined PDMS membranes. The rejection data were compared with the calculated values from three rejection models based on the size-exclusion mechanism, namely the Ferry, the Verniory, and the steric hindrance pore model using pore diameter information from the  $N_2$  physisorption measurement when no solvent is present. A dependency of the membrane rejection rate with the solute diameter versus pore diameter ratio suggests that the solute transport is following the size based exclusion mechanism. By comparing the experimental data with the calculated rejection value by using rejection models, it can be deduced that the membrane pore geometry changes as a result of the membrane-solvent interaction. Moreover, the ability of one component to create a hydrogen bond with others are important in determining the nanofiltration performance of the grafted membranes. Finally the effect of the applied pressure on the membrane rejection behavior was studied as well for Sudan Black in different solvents showing an increase rejection with increasing trans-membrane pressures.

In Chapter 6, the permeability behavior was described of PEG grafted  $\gamma$ -alumina membranes with respect to different types of permeating solvent (polar and nonpolar). A linear relationship between flux and TMP was observed showing no sign of compaction. This indicates the absence of shear-flow induced behaviour in the applied pressure range studied, as was also observed for PDMS grafted  $\gamma$ - $Al_2O_3$  membranes. The permeability with respect to different types of permeating solvent (polar and nonpolar) show a lower permeability of ethanol than hexane, accompanied by a higher selectivity of Sudan Black in ethanol than in hexane. Here also this effect is explained by the difference in solvent

sorption of the grafted moiety for different types of permeating solvents. In contrast to PDMS, a more dramatic solvent sorption occurs for PEG in the presence of ethanol than for hexane (5). Thus, a stronger reduction in the membrane permeable volume is realized in the presence of ethanol than hexane, causing a more closed membrane structure in the presence of ethanol for PEG grafted  $\gamma$ -alumina membranes. While for PDMS grafted  $\gamma$ -alumina membranes, a more closed membrane structure occurs in the presence of hexane than ethanol.

## **7.2. Future Perspectives on Grafting Methods**

It has been shown that grafting can be used to modify the membrane surface properties as well as the membrane performance with regard to permeability and selectivity. From the membrane preparation point of view, the selection of grafting agents can still be optimized in order to reach a desired selectivity range for targeted applications. Proper selection of grafting agents should consider factors like the size of the grafting agents in relation with the pore diameter of the inorganic porous substrate, the grafting density that can be achieved with the selected grafting agents, as well as the sorption behavior of the grafted moiety in the targeted solvent.

In Chapter 6, it is reported that the number of the alkoxy groups, the chain length of the grafting agent, and the number of ureido functionality can influence the grafting nature. This type of information can be used by making the selection of grafting agents in order to result in tailor-made membranes for a desired application. The use of grafting agents with larger chain length can result in a smaller membrane pore diameter of the grafted membranes. However, the chain length of the grafting agents is not the only factor affecting the pore size of the grafted membranes. Grafting density also influences the membrane pore diameter of the grafted membranes. Large chain lengths of grafting agents often result in a lower grafting density.

The membrane selectivity will be reduced when the permeating solvent is less strongly sorbed in the grafted moiety. Thus, it is important to match the grafted material with the targeted applications. This made grafted ceramic membranes powerful for tailor-made applications.

In Chapter 5, an interesting method was presented to increase the membrane selectivity by creating a grafted PDMS network inside the membrane pores. However, optimization of the selection of coupling agent and chain length of the grafting agent is still missing. Optimization in this field can be useful for creating a grafted ceramic membrane with a targeted selectivity range.

All membranes in this thesis were prepared by a “grafting to” mechanism. In order to improve the membrane selectivity, a “grafting-from” mechanism, in which polymerization was initiated in-situ from a reactive sites on the silylated  $\gamma$ -alumina, can be an interesting method as well. Another way to graft organic moiety to inorganic substrates other than by organosilanes can be further investigated, e.g. via Grignard reaction between the surface hydroxyls and grafting agents to form a covalent Si-P-Al bond(6).

### **7.3. Future perspectives for transport study of grafted membranes**

#### **7.3.1. Theoretical calculations of sorption value**

In Chapter 2 sorption experiments were carried out in order to determine the sorption value of a grafted material in different types of solvents. Theoretical calculation of the sorption value is one of the strategies that can be implemented to establish an online system for prediction of fluxes and reduces the number of experiments needed for prediction of fluxes. To date, theories for prediction of sorption value have not been found in the scientific literature.

#### **7.3.2. Membrane-solute interaction**

In Chapter 4 the study of solute rejection is emphasized on the role of membrane-solvent interaction in the rejection of solutes. The role of solvent-solute and solute-solute interaction was discussed from the aspect of hydrogen bonding that can occur between these components. The role of the membrane-solute interaction was assumed to be negligible between the dye and the grafted material. Further investigation on the role of the membrane-solute interaction, can lead to a better understanding of the role of membrane-solute interaction in the solute rejection behavior of grafted ceramic membranes.

## References

1. Vandezande, P., Gevers, L. E. M., and Vankelecom, I. F. J. (2008) Solvent resistant nanofiltration: Separating on a molecular level, *Chemical Society Reviews* 37, 365-405.
2. Pinheiro, A. F. M., Hoogendoorn, D., Nijmeijer, A., and Winnubst, L. (2014) Development of a PDMS-grafted alumina membrane and its evaluation as solvent resistant nanofiltration membrane, *Journal of Membrane Science* 463, 24-32.
3. Lecloux, A., and Pirard, J. P. (1979) The importance of standard isotherms in the analysis of adsorption isotherms for determining the porous texture of solids, *Journal of Colloid and Interface Science* 70, 265-281.
4. Castro, R. P., Monbouquette, H. G., and Cohen, Y. (2000) Shear-induced permeability changes in a polymer grafted silica membrane, *Journal of Membrane Science* 179, 207-220.
5. Mark, J. E. (1999) *Polymer Data Handbook*, Oxford University Press, Oxford.
6. Hosseinabadi, S. R., Wyns, K., Meynen, V., Carleer, R., Adriaensens, P., Buekenhoudt, A., & Van der Bruggen, B. (2014) Organic solvent nanofiltration with Grignard functionalised ceramic nanofiltration membranes, *Journal of Membrane Science* 454, 496-504.

# SUMMARY

Solvent Resistant Nanofiltration (SRNF) is a potential technology to recover organic solvents in chemical processes. For this application, a chemically stable membrane that can endure continuous exposure towards organic solvents is required. This thesis deals with the preparation of chemically stable nanofiltration (NF) membranes through grafting of porous ceramic substrates with organic molecules and the study of their solvent and solute transport properties.

In **Chapter 1**, a literature review is given on grafting techniques as well as studies on solvent and solute transport in SRNF .

In **Chapter 2**, grafting of mesoporous  $\gamma$ -alumina membranes with monovinyl terminated polydimethylsiloxane (PDMS), using 3-mercaptopropyltriethoxysilane (MPTES) as a linking agent, was described. The grafting performance of the organic moieties on  $\gamma$ -alumina powders was studied by FTIR. The results indicated that grafting reactions were successfully carried out. Contact angle measurements and solvent permeability tests were used to characterize the membrane properties. A water contact angle of  $95^\circ$  was observed after grafting, demonstrating the presence of a hydrophobic membrane surface. The toluene permeability of the membrane was reduced after grafting due to the presence of the grafted moiety inside the membranes, reducing the membrane pore diameter. No degradation of the membrane material was observed after chemical stability tests in toluene for 6 days at room temperature and at elevated temperatures (up to  $90^\circ\text{C}$ ).

In **Chapter 3**, permeability studies of several polar and apolar solvents are given for ceramic membranes grafted with a relative short or long PDMS chain ( $n=10$  and  $n=39$ ). The solvent transport through these membranes could be described using a pore-flow model by incorporating solvent sorption terms into the Hagen-Poiseuille equation. Solvent sorption was measured "ex situ" using a pure PDMS phase. It is found that the membrane permeable volume reduces if a solvent is strongly swelling. This provides an initial way to predict the performance of grafted ceramic membranes for solvent nanofiltration.

In **Chapter 4**, the solute rejection of PDMS grafted  $\gamma$ -alumina membranes were described for different solvent-solute pairs. In contrast to the behavior of pure PDMS polymeric

membranes, higher rejections were found for apolar solvents, like toluene, than for polar solvents, such as isopropanol. It is suggested that the transport of solute is following a size-based exclusion mechanism as the solute rejection is related to the ratio solute diameter/pore diameter ( $d_c/d_p$ ). The Ferry, Verniory and Steric Hindrance Pore (SHP) size-exclusion models were applied to predict the membrane rejection using, as first approximation, the pore diameter of a grafted membrane when no solvent was present. Rejections were studied of polystyrene (PS), polyethylene glycol (PEG) and dyes with different molecular sizes. For the dye solutes in isopropanol, the experimental rejection data are in the range of the predicted rejection as based on all three models, by applying a pore diameter of the membranes, determined when no solvent was present. This is an indication that polar solvents, like isopropanol, do not significantly swell the PDMS in its confined, ceramic environment. No further conclusion can be drawn as the interactions between the dyes and the grafted moiety as well as between the dyes and isopropanol must be investigated further, as these effects may mask eventual contributions of membrane-solvent interactions on membrane selectivity.

The calculated rejections of the dyes in toluene, by using the three solute transport models were much lower than experimentally observed if the membrane pore diameter was used as determined when no solvent is present. This is an indication of a more closed pore structure for the membranes in toluene than in isopropanol, caused by a strong swelling of PDMS in the apolar solvent, toluene.

For solutes with identical size, the rejection in toluene of PS is lower than that of the dyes. A solvent-solute interaction may increase the flexibility of PS, resulting in a decrease in solute rejection. Based on the experimental rejection data, the diameter of the PS is calculated to be 0.7-0.9 of its hydrodynamic diameter, assuming that the rejection of PS as well as the dyes are following the Ferry model and that for the dyes no solvent-solute interaction exists.

The rejection of PEG in isopropanol as a function of  $d_c/d_p$  is lower than that of dyes with identical solute size  $d_c$ . This lower rejection of PEG in isopropanol can be attributed to a solute-solvent interaction. The formation of hydrogen bridges between the PEG solutes and isopropanol may increase the flexibility of PEG, resulting in a decrease in solute rejection.



Based on the experimental rejection data the diameter of the PEG is calculated to be 0.3-0.4 its hydrodynamic diameter, assuming that the rejection of PEG is following the Ferry model.

At a given  $d_c/d_p$  value, the rejection of PEG in toluene is higher than that of the dyes. A strong solute-solute interaction of the hydrophilic PEG solutes in the presence of apolar solvents like toluene may cause the formation of large PEG clusters resulting in actual PEG solute sizes larger than that of a calculated single PEG solute. Based on the experimental rejection data the diameter of the PEG clusters in toluene may reach 1.6-2 times that of a single PEG solute, assuming that the rejection of PEG follows the same size-exclusion mechanism as that of the dyes.

In **Chapter 5**, grafting of mesoporous  $\gamma$ -alumina membranes with hydride terminated polydimethylsiloxane is described. Vinyltriethoxysilane is used as linking agent and tetrakis(vinyl dimethylsiloxy)silane as a coupling agent, to couple the grafted moiety forming a polymer network inside the ceramic pores during grafting. Grafting performance of the organic moieties on  $\gamma$ -alumina powders was analyzed by FTIR and TGA. The results indicate that grafting reactions were successfully carried out. SEM-EDX and contact angle analysis on the grafted membranes showed that grafting occurs throughout the  $\gamma$ -alumina layer and that the resulting membrane surface had a water contact angle of  $108^\circ$ . The use of coupling agents results in a higher selectivity for nanofiltration of solvents, but at the cost of solvent permeability, when compared with PDMS-grafted alumina membranes where no coupling was applied.

In **Chapter 6**, a grafting method of a mesoporous  $\gamma$ -alumina layer, supported on macro porous  $\alpha$ -alumina, by polyethylene glycol (PEG) is presented. The grafting nature of  $\gamma$ -alumina with PEG grafting agents, having different molecular weights, numbers of alkoxy groups and numbers of ureido groups were investigated by means of FTIR, TGA,  $^{29}\text{Si}$ -NMR and BET using  $\gamma$ -alumina inorganic particles as surrogate membrane surfaces. FTIR analysis indicated that the grafting reaction has occurred on the  $\gamma$ -alumina powders. The degree of self-condensation is about the same for most of the grafting agents as analyzed from FTIR.  $^{29}\text{Si}$ -NMR analysis showed that for the ureido PEG, the chain length of the grafting agents influences the number of the Si-O-Al bonds per PEG molecule. For PEG without ureido functionality, no significant influence of the chain length of the grafting agents on the

structural configuration of the grafted moiety was observed. The number of hydrolyzable groups influences the structural configuration of the grafted moiety. TGA analysis showed that an increased grafting density was observed with a decreasing chain length of the grafting agents for grafting agents having similar numbers of alkoxy and ureido groups. After grafting the ceramic membranes, a higher water contact angle, but still in the hydrophilic region, was observed. A lower solvent permeation of both ethanol and hexane after grafting was observed due to the presence of the grafted moiety inside the membranes, reducing the membrane pore diameter. The permeability with respect to different types of permeating solvents (polar and anpolar) show a lower permeability for ethanol than for hexane, accompanied by a higher selectivity of Sudan Black in ethanol than in hexane. This effect is explained by the difference in solvent sorption in the grafted moiety for different types of permeating solvents.

Finally, in **Chapter 7** the main results and conclusions as reported in this thesis are summarized, while suggestions are given for future research in the field organically-modified ceramic membranes to be applied in SRNF, such as theoretical study of sorption phenomenon and study of interaction between membrane and solutes.

# SAMENVATTING

De ontwikkelingen in oplosmiddel resistente nanofiltratie (ORNF) bieden interessante mogelijkheden voor het terugwinnen van organische oplosmiddelen in o.a. de chemische en farmaceutische industrie. Voor het toepassen van deze technologie zijn chemisch stabiele membranen noodzakelijk, die bestand zijn tegen continue blootstelling aan oplosmiddelen. Het onderzoek, zoals beschreven in dit proefschrift, behandelt de fabricage van chemisch stabiele nanofiltratie membranen door het functionaliseren of “graften” van poreuze keramische materialen met organische moleculen. Daarnaast wordt ingegaan op het transport van verschillende oplosmiddelen door deze membranen en het filtratie gedrag van vaste deeltjes, waarbij transportmodellen worden geëvalueerd.

In **Hoofdstuk 1** wordt een literatuuroverzicht gegeven van verschillende graft technieken en transportmodellen, die toegepast worden in ORNF

**Hoofdstuk 2** beschrijft het graften van meso-poreuze (5 nm)  $\gamma$ -alumina membranen met PDMS met een monovinyl eindgroep, waarbij 3-mercaptopropyltriethoxysilaan (MPTES) gebruikt wordt als ‘verbindingsstuk’ tussen  $\gamma$ -alumina en PDMS. De mate van graften van deze organische moleculen aan  $\gamma$ -alumina poeders is bestudeerd met FTIR. De resultaten tonen aan dat de graft reacties succesvol zijn uitgevoerd. Contacthoek en permeabiliteit metingen zijn uitgevoerd om de membraan eigenschappen vast te leggen. Een water contacthoek van 95 ° is gemeten, wat een aanwijzing is dat we te maken hebben met een hydrofoob membraan oppervlak. De permeabiliteit van toluen door dit membraan neemt af nadat het is gegraft met een organische groep, wat aantoont dat de poriegrootte van het membraan is afgenomen. Dit membraan vertoont een goede (chemische) stabiliteit na filtratie testen in toluen van 6 dagen en behandelingen in toluen bij verhoogde temperaturen (tot 90 °C)

In **Hoofdstuk 3** worden studies beschreven van de permeabiliteit van verschillende polaire en apolaire oplosmiddelen voor keramische membranen die gegraft zijn met PDMS met een relatieve korte of lange ketenlengte ( $n=10$  en  $n=39$ ). Het transport van oplosmiddelen door deze membranen kan beschreven worden door gebruik te maken van het porie-doorstroom (“pore-flow”) model door een sorptie term van het gebruikte oplosmiddel in te voeren in de

Hagen-Poiseuille vergelijking. Aangetoond is dat het beschikbare porie volume voor oplosmiddel transport sterk afneemt als het oplosmiddel een sterke sorptie met het PDMS vertoont, waardoor het PDMS een grote zwelling vertoont. Door gebruik te maken van deze vinding kan een eerste indicatie gegeven worden om het gedrag van gegrafte keramische membranen te voorspellen bij nanofiltratie van organische oplosmiddelen.

In **Hoofdstuk 4** wordt het filtratie gedrag beschreven van PDMS-gegrafte  $\gamma$ -alumina van verschillende oplosmiddel-deeltjes mengsels. In tegenstelling tot 100 % polymere PDMS membranen wordt een hogere retentie voor vaste deeltjes gevonden in apolarie oplosmiddelen, zoals toluen, dan in polaire oplosmiddelen als isopropanol. Er wordt aangenomen dat het transport van vaste deeltjes door deze membranen bepaald wordt door de grootte van de deeltjes en is daarom gerelateerd met de deeltjes/porie diameter verhouding ( $d_c/d_p$ ). De Ferry, Verniory en "Steric Hindrance Pore" (SHP) modellen worden toegepast om een uitspraak te doen over het retentie gedrag van de membranen. Voor de poriediameter is als eerste benadering aangenomen, dat deze gelijk is aan de poriediameter van een gegrapt poreus  $\gamma$ -alumina systeem indien geen oplosmiddel aanwezig is. Als vaste stof deeltje zijn polystyreen (PS), polyethyleen glycol (PEG) en kleurstoffen (dyes) met verschillende molecuul groottes gebruikt. Voor de dyes in isopropanol komen de experimenteel gevonden retentie waarden overeen met waarden, zoals voorspeld door de drie retentie modellen, met gebruik making van de membraan porie diameter, bepaald in het geval dat er geen oplosmiddel aanwezig is. Dit is een aanwijzing dat bij polaire oplosmiddelen, zoals isopropanol, het PDMS niet significant zwelt als het ingesloten is in een star, keramisch, systeem. Op het ogenblik kunnen nog geen verdere conclusies uit deze resultaten getrokken worden omdat bij de analyse geen rekening is gehouden met interacties tussen deeltjes en oplosmiddel en tussen deeltjes en het gegrafte organisch molecuul. Deze interacties kunnen een eventuele bijdrage van membraan-oplosmiddel interacties aan de selectiviteit maskeren.

De volgens de transportmodellen berekende retenties van dyes in toluen zijn veel lager dan de experimenteel gevonden waarden, bij gebruik making van de membraan porie diameter, zoals bepaald bij afwezigheid van oplosmiddel. Dit is een aanwijzing dat hetzelfde membraan een kleinere (effectieve) poriediameter heeft in toluen dan in isopropanol, wat veroorzaakt wordt door het sterker zwellen van PDMS in het apolaire oplosmiddel toluen.

Voor PS deeltjes met dezelfde grootte als de dyes is de retentie in toluen veel lager. Een interactie tussen de PS deeltjes en het oplosmiddel (toluën) kan leiden tot een verhoogde flexibiliteit, wat resulteert in een afname van de retentie. Een PS deeltjesgrootte, welke gelijk is aan 0.7-0.9 van de hydrodynamische diameter is berekend, aannemende dat de retenties van de PS en dye deeltjes het Ferry model volgen en dat er bij de dyes geen aantoonbare interactie is met het oplosmiddel.

De retentie van PEG in isopropanol als functie van  $d_c/d_p$  is lager dan die van dyes met identieke deeltjesgrootte  $d_c$ . Dit kan verklaard worden door uit te gaan van een interactie tussen het oplosmiddel en het deeltje. De vorming van waterstof bruggen tussen de PEG deeltjes en isopropanol kan het PEG flexibeler maken. De berekende diameter van PEG, uitgaande van de experimentele retentie waardes, is 0.3-0.4 van de hydrodynamische diameter, aannemende dat de PEG retentie volgens het Ferry model verloopt.

Bij een gegeven  $d_c/d_p$  waarde, is de retentie van PEG in toluen hoger dan voor de dyes. Een sterke interactie tussen het apolaire oplosmiddel en de hydrofiele PEG deeltjes kunnen de oorzaak zijn voor de vorming van PEG clusters. De berekende diameter van deze PEG clusters is 1.6-2 maal die van een enkel PEG deeltje, aannemende dat de retentie van de PEG deeltjes volgens hetzelfde mechanisme verloopt als die van de dyes.

In **Hoofdstuk 5** wordt het graften van meso-poreuze  $\gamma$ -alumina membranen beschreven met een polydimethylsiloxaan (PDMS), welke een hydride als eindgroep heeft. Als 'linker' met het keramisch membraan wordt vinyltriethoxysilaan gebruikt. In enkele gevallen wordt tetrakis(vinyldimethylsiloxy)silaan als "coupling agent" gebruikt om de PDMS moleculen aan elkaar te binden. De mate van graften van deze organische moleculen aan  $\gamma$ -alumina poeders is bestudeerd met FTIR en TGA, waarbij is aangetoond dat het graften succesvol is verlopen. SEM-EDX en contacthoek bepalingen laten zien dat het graften in de gehele  $\gamma$ -alumina laag heeft plaatsgevonden en dat het membraan oppervlak hydrofoob is met een water contacthoek van  $108^\circ$ . Door gebruik te maken van "coupling agents" wordt een membraan verkregen met een hogere selectiviteit voor nanofiltratie, maar dit gaat ten koste van de permeabiliteit van het oplosmiddel.

In **Hoofdstuk 6** wordt het graften van meso-poreuze  $\gamma$ -alumina membranen beschreven met polyethyleen glycol (PEG). Het graften van verschillende PEG moleculen is bestudeerd,

waarbij het molecuulgewicht zowel als het aantal alkoxide groepen en ureido groepen zijn gevarieerd. Met behulp van FTIR, TGA,  $^{29}\text{Si}$ -NMR and BET analyses aan gegrachte  $\gamma$ -alumina deeltjes is aangetoond dat de mate van zelf-condensatie voor de meeste systemen identiek is en dat voor de ureido PEG moleculen het aantal Si-O-Al bindingen per PEG molecuul bepaal wordt door de ketenlengte. TGA toont aan dat een dichtere grafting structuur wordt verkregen bij een kleinere lengte van het te graften molecuul. Na het graften van het keramisch membraan heeft deze een hogere water contacthoek, maar het membraan is nog steeds hydrofiel. De permeabiliteit van het polaire ethanol is lager dan voor het apolaire hexaan, wat gecombineerd wordt met een hogere selectiviteit van het Sudan Black dye in ethanol dan in hexaan. Dit effect kan verklaard worden door verschillen in sorptie gedrag van de oplosmiddelen met het gegrachte PEG

Tenslotte worden in het afsluitende **hoofdstuk 7** de belangrijkste resultaten uit dit proefschrift samengevat en worden suggesties gegeven voor verder onderzoek op het gebied van keramische membranen, gemodificeerd met organische moleculen, welke toepassing kunnen vinden in oplosmiddel resistente nanofiltratie ORNF (Solvent Resistant Nanofiltration: SRNF).

# RÉSUMÉ

La nanofiltration (NF) est un procédé applicable à la récupération des solvants organiques. Une membrane chimiquement stable est alors requise pour résister aux solvants organiques. Cette thèse traite de la préparation de membranes NF chimiquement stables par greffage de substrats céramiques mésoporeux et de l'étude de leurs propriétés de transport des solvants et des solutés.

Dans le chapitre 1, l'état de l'art sur les techniques de greffage est présenté ainsi que celui sur le comportement au transport des membranes NF résistantes aux solvants.

Dans les chapitres 2 et 6, des membranes d'ultrafiltration en alumine mésoporeuse sont greffées avec des groupements organiques hydrophobes ou hydrophiles. La diminution du diamètre des pores permet ainsi d'accéder à la nanofiltration. Au chapitre 5, un agent couplant est utilisé pour améliorer l'ancrage de ces groupements dans les pores. Ceci réduit cependant la perméabilité aux solvants, en comparaison aux mêmes membranes modifiées avec du polydiméthylsilane (PDMS) mais sans agent couplant. Dans le chapitre 6, la capacité de greffage de poudres d'alumine est mesurée pour des agents de greffage différant par : la masse moléculaire des chaînes polyéthylène glycol (PEG), la nature et le nombre de groupements alcoxy terminaux et la présence ou non de fonctions urée. Ces poudres sont analysés par thermogravimétrie, spectrométrie RMN du  $^{29}\text{Si}$ , spectroscopie FTIR, et mesures de surface spécifique. Les densités de greffage estimées varient avec la masse des greffons, la présence de fonctions urée, et le nombre de groupements alcoxy hydrolysables.

Le comportement au transport de membranes greffées est étudié dans les chapitres 3, 4 et 6. Dans le chapitre 3, pour des membranes greffées avec du PDMS, ce comportement est décrit en incorporant des termes relatifs à la sorption des solvants dans l'équation Hagen-Poiseuille. Une membrane plus fermée est obtenue lorsque le solvant est fortement adsorbé dans la couche greffée. Dans le chapitre 4, la validité des modèles de rejet de soluté basés sur l'exclusion par la taille est discutée. Une forte influence du diamètre moléculaire du soluté et du rapport de ce diamètre avec celui des pores est observée, indiquant que le mécanisme d'exclusion par la taille est ici vérifié. Trois modèles de rejet sur la base

d'exclusion par la taille, à savoir Ferry, Verniory et SHP, sont testés pour prédire, en l'absence de solvant, le rejet des solutés à partir des diamètres de pore mesurés par physisorption de diazote. Pour des colorants et des solutés de type PEG dans du toluène, les données expérimentales sont bien au-dessus des valeurs prédites par ces modèles. Les résultats suggèrent que le diamètre de pore effectif en présence de solvant fortement adsorbé tel que le toluène est inférieur à celui en l'absence de solvant, une hypothèse étant qu'il n'y a pas d'interactions importantes entre solvant et soluté ou entre le soluté et la surface des pores. Cela peut expliquer un rejet plus élevé des solutés dans des solvants non polaires comme le toluène que dans des solvants polaires tels que l'isopropanol pour les membranes greffées avec du PDMS. Dans le chapitre 6, la perméabilité de membranes greffées avec des PEG est étudiée pour différents solvants (polaires ou non polaires). Une relation linéaire entre le flux et la pression transmembranaire est observée, comme pour les membranes greffées avec du PDMS. Cela indique l'absence de processus induit par des effets de cisaillement dans le fluide en écoulement et variant avec la pression transmembranaire appliquée. Pour le colorant Noir Soudan, une sélectivité supérieure est observée dans l'éthanol que dans l'hexane alors que pour la perméabilité inférieure de l'éthanol est inférieure à celle de l'hexane. Ici aussi, ces phénomènes sont expliqués par la différence de sorption des solvants dans la couche greffée.

Les conclusions générales et perspectives de cette étude sont présentées dans le chapitre 7.



## RÉSUMÉ GÉNÉRAL

La nanofiltration (NF), procédé baromembranaire, est applicable pour la récupération des solvants. Pour cette application, une membrane chimiquement stable est nécessaire. Cette thèse traite de la préparation de membranes NF par greffage organique de substrats céramiques poreuses et de l'étude du transport dans ces membranes de solvants et de solutés. Une membrane céramique d'ultrafiltration en alumine gamma mésoporeuse est greffée avec des groupements organiques hydrophobes ou hydrophiles à de diminuer le diamètre des pores de la membrane et d'accéder ainsi à la nanofiltration. L'utilisation d'un agent couplant permet d'améliorer l'ancrage des groupements modificateurs de surface à l'intérieur des pores de la membrane céramique au détriment d'une perméabilité aux solvants inférieure. Le comportement du transport des solvants dans les membranes céramiques greffées peut être décrit en incorporant des termes de sorption du solvant dans l'équation de Hagen- Poiseuille. Une membrane plus fermée est obtenue lorsque le solvant est fortement adsorbé dans la couche greffée.



# ACKNOWLEDGEMENT

I would like to thank each and everyone for their contributions to this project. My deepest appreciation and gratitude to my research supervisors: Arian Nijmeijer, Louis Winnubst, Ivo Vankelecom, Andre Ayrat, and Mihai Barboiu, for their patient guidance, scientific discussions, enthusiastic encouragement and useful critiques of this research work. I learnt a great deal from each of you and it has been a great experience so far. I also would like to thank Henny Bouwmeester and Nieck Benes for their valuable feedback during Thursday lectures.

I am particularly grateful for the assistance given by Mieke, Cindy, and Frank in the laboratory of the Inorganic Groups Department in the University of Twente. My sincere gratitude to Maarten Bastin for his help in the laboratory of the Catalytic Groups Department in KU Leuven. I would also like to thank Nathalie Masquelez, Eddy Petit, and Mansouri in the laboratory of Institut Europeen des Membranes, Montpellier for their invaluable help during experiments. My great appreciation for Mark Smithers for technical help in the EDX measurement. I am grateful for Susanne van Rijn, Elena Vallejo, Ines Jossa, Annemie Schellens, and Leen Cuypers for their enormous help in administrative matters. My sincere thanks to Harmen Zwijnenberg for various technical discussions.

I would like to thank Ana and Kishore for their support in the beginning of this project. My great appreciation for the current and previous IM members, Martin, Wei, Chung Yul, Emiel, Saim, Marcel, Michiel, Bas, Patrick, Giri, Evelien, Tan, Joanna, Kristianne, Hammad, Can, Rian, Roland, Ying Wu, and Wojtech, for their help in many kinds and being very supportive throughout these years. I would also like to thank Harmen, Salman, Shazia, Beata, Kah Peng, Nungky, Susilo, Vio, Alessio, Yusuf, Elif, Charu, Fei and the rest of the MTO and SFI members for nice talks during breaks.

I am grateful for my officemates in COK, Agnieszka, Chalida, Nithya, Katrien, Waqas, Elke, Roil, Lila, Warunee, Parimal, Aby, Aylin and Izabela for making my stay in Leuven very memorable and fun. Special thanks to NSA members, Yves-Marie, Sophie, Meron, Florina, Alina, Romina, Dan, Erol, Zhanhu, Yahia, Nicholas, Istvan and Florin for a very warm welcome and tons of contagious humour. Thanks for making my time in Montpellier extremely enjoyable and exciting. Romina, I am glad for our collaboration in the project. I found it very interesting and fruitful. I would also like to thank my Eudime mates: Sushumna, Ming and Laksmeesha for their help in Montpellier.

Mention should also be given to Caecil, Nden, Avissa, Yosia, Jenny, Donna, Mba Arin, Kinski, Mba Dwi, Mba Eta, Mba Tia, Febri, Aldi, Muthia, Nyak Hasti, Riswan, Yoppy, Diana, Karen, Dissa, Tiffany, Mark, Pia, Mba Ratna and all of the PPI-Enschede members (mentioning all of your names is just

impossible, but I do thank for the opportunity to meet each of you here in Enschede). I also thank my friends in Leuven and Montpellier: Dorothy, Riza, Inong, Mba Rini, Ratna, Della, Pak Aunur, Bu Ummy, Mutia, Sera, Mba Pipit, Deri, Bayu, Bu Retno, Mak Neli. Special thanks to Rindia, Citra, and Tania for being the most helpful person in the world! Finally, I would like to thank my parents, Iratius Radiman and Cynthia Linaya, for their support throughout my study. For my siblings, Catherine and Claudia, thank you for your continuous encouragement.

I also place on record, my sense of gratitude to each and every ones, who directly or indirectly, have lent their hand in this venture.

Cheryl

## About the author



Cheryl Raditya Tanardi was born on the 3<sup>rd</sup> of December 1984 in Surabaya, Indonesia. She obtained her Bachelor of Science from Institut Teknologi Bandung in June 2006 majoring in chemical engineering. As a part of an internship, she worked at the Dow Chemical Company in the division of process technology. She also spent a semester as an exchange student at the Beijing Union University, Beijing, China.

In 2007, she first started her entrepreneurial work as a CEO at the Flotech Water Management, Indonesia. She then obtained her master degree in the Department of Civil and Environmental Engineering, Stanford University, California, USA and the Civil Department of Nanyang Technological University, Singapore and joined the Environmental Resources Management providing environmental consultancy for chemical industries.

In November 2011, Cheryl started her PhD research as an Erasmus Mundus awardee, performing research at 3 different groups in 3 different universities. The research project was a joint effort among the Inorganic Membranes group, Department of Science and Technology, University of Twente, The Netherlands, the Centre of Surface Chemistry and Catalysis in KU Leuven, Belgium, and the Institute of European Membranes in the University of Montpellier, France. During this project, she worked under the supervision of Arian Nijmeijer, Louis Winnubst, Ivo Vankelecom, Andre Ayrál, and Mihai Barboiu. Cheryl presented her work at numerous events, including the International Conference on Membranes (ICOM 2014) in Suzhou, China.



# List of Publications

## Published

1. Tanardi, C. R., Vankelecom, I. F., Pinheiro, A. F., Tetala, K. K., Nijmeijer, A., & Winnubst, L. (2015). *Solvent permeation behavior of PDMS grafted  $\gamma$ -alumina membranes*. Journal of Membrane Science, 495, 216-225.
2. Tanardi, C. R., Pinheiro, A. F., Nijmeijer, A., & Winnubst, L. (2014). *PDMS grafting of mesoporous  $\gamma$ -alumina membranes for nanofiltration of organic solvents*. Journal of Membrane Science, 469, 471-477.

## Submitted

1. Tanardi, C.R., Vankelecom, I. F., Nijmeijer, A., Winnubst, L. (2015). *Solute Rejection in SRNF using PDMS Grafted  $\gamma$ -Alumina Membranes*.
2. Tanardi, C. R., Nijmeijer, A., and Winnubst, L. (2015). *Coupled-PDMS Grafted Mesoporous  $\gamma$ -Alumina Membranes for Solvent Nanofiltration*.
3. Tanardi, C. R., Catana, R., Barboiu, M., Ayrat, A., Vankelecom, I.F., Nijmeijer, A., and Winnubst, L. (2015). *Polyethyleneglycol Grafting of  $\gamma$ -Alumina Membranes for Solvent Resistant Nanofiltration*.





ISBN 978-94-6233-135-8



9 789462 331358